

Stable Minima of ReLU Neural Networks Suffer from the Curse of Dimensionality: The Neural Shattering Phenomenon

Tongtong Liang
Mathematics, UCSD
ttliang@ucsd.edu

Dan Qiao
CSE, UCSD
d2qiao@ucsd.edu

Yu-Xiang Wang
HDSI, UCSD
yuxiangw@ucsd.edu

Rahul Parhi
ECE, UCSD
rahul@ucsd.edu

Abstract

We study the implicit bias of flatness / low (loss) curvature and its effects on generalization in two-layer overparameterized ReLU networks with multivariate inputs—a problem well motivated by the minima stability and edge-of-stability phenomena in gradient-descent training. Existing work either requires interpolation or focuses only on univariate inputs. This paper presents new and somewhat surprising theoretical results for multivariate inputs. On two natural settings (1) generalization gap for flat solutions, and (2) mean-squared error (MSE) in nonparametric function estimation by stable minima, we prove upper and lower bounds, which establish that while flatness does imply generalization, the resulting rates of convergence necessarily deteriorate exponentially as the input dimension grows. This gives an exponential separation between the flat solutions vis-à-vis low-norm solutions (i.e., weight decay), which knowingly do not suffer from the curse of dimensionality. In particular, our minimax lower bound construction, based on a novel packing argument with boundary-localized ReLU neurons, reveals how flat solutions can exploit a kind of “neural shattering” where neurons rarely activate, but with high weight magnitudes. This leads to poor performance in high dimensions. We corroborate these theoretical findings with extensive numerical simulations. To the best of our knowledge, our analysis provides the first systematic explanation for why flat minima may fail to generalize in high dimensions.

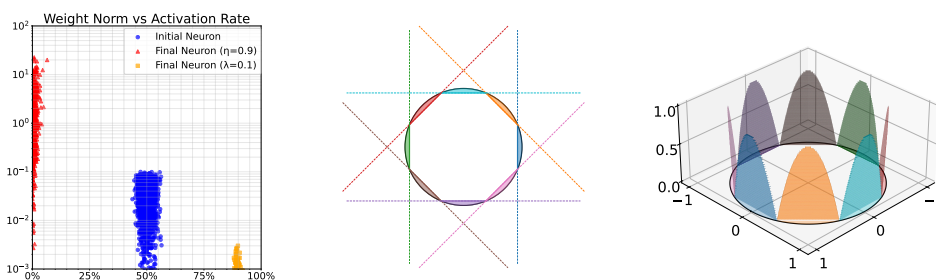


Figure 1: The “neural shattering” phenomenon: From empirical observations to its geometric origin and theoretical consequences. **Left panel:** Training with a large learning rate and gradient descent empirically results in “neural shattering”: Neurons develop large weights despite activating on very few inputs, leading to a high MSE of ≈ 1.105 (red points). In contrast, explicit ℓ^2 -regularization prevents this, achieving a much lower MSE of ≈ 0.055 (orange points). **Middle panel:** The number of distinct directions, or “caps”, on a high-dimensional sphere grows exponentially. Consequently, the data sites are spread thinly across these caps. This makes it trivial for a ReLU neuron to find a direction that isolates only a few data points. This sparse activation pattern allows neurons to use large weight magnitudes for this local fitting without impacting the global loss curvature, thus “tricking” the flatness criterion. **Right panel:** Visualization of “hard-to-learn” function from our minimax lower bound construction, built from localized ReLU neurons described in the middle panel.

Contents

1	Introduction	4
1.1	Contributions	5
1.2	Related Work	6
2	Preliminaries, Notation, and Problem Setup	7
3	Main Results	8
3.1	Stable Solutions Generalize But Suffer the Curse of Dimensionality	10
3.2	Nonparametric Function Estimation With Stable Minima	11
4	Experiments	12
5	Discussion and Conclusion	13
6	Acknowledgments	14
A	Additional Experiments	18
A.1	Empirical Evidence: High Dimensionality Yields Neural Shattering	18
A.2	Neural Shattering and Learning Rate (dim=5)	19
A.3	Empirical Analysis of the Curse of Dimensionality (I)	20
A.4	Empirical Analysis of the Curse of Dimensionality (II)	20
B	Overview of the Proofs	23
B.1	Proof Overview of Theorem 3.2.	23
B.2	Proof Overview of Theorem 3.5	24
B.3	Proof Overview of Theorem 3.6	25
B.4	Proof Overview of Theorem 3.7	25
B.5	Discussion of the Proofs	27
C	Proof of Theorem 3.2: Stable Minima Regularity	27
D	Proof of Theorem 3.4: Radon-Domain Characterization of Stable Minima	30
E	Characterization of the Weight Function for the Uniform Distribution	30
E.1	The Computation of the Population Weight Function	30
E.2	Empirical Process for the Regularity Weight Function	35
F	Proof of Theorem 3.5: Generalization Gap of Stable Minima	36
F.1	Definition of the Variation Space of ReLU Neural Networks	37
F.2	Metric Entropy and Variation Spaces	37
F.3	Generalization Gap of Unweighted Variation Function Class	38
F.4	Concentration Property of Ball-Uniform Distribution	39
F.5	Upper Bound of Generalization Gap of Stable Minima	40
G	Proof of Theorem 3.6: Estimation Error Rate for Stable Minima	43
G.1	Computation of Local Gaussian Complexity	43
G.2	Proof of the Estimation Error Upper Bound	45
H	Proof of Theorem 3.7: Minimax Lower Bound	47
H.1	Preliminaries: Minimax Risk and Fano’s Lemma	47
H.2	The Multivariate Case	47
H.3	Why Classical Bump-Type Constructions Are Ineffective	52
H.4	The Univariate Case	53
I	Lower Bound on Generalization Gap	55

1 Introduction

Modern deep learning is inherently overparameterized. In this regime, there are typically infinitely many global (i.e., zero-loss or interpolating) minima to the training objective, yet gradient-descent (GD) training seems to successfully avoid “bad” minima, finding those that generalize well. Understanding this phenomenon boils down to understanding the *implicit biases* of training algorithms [Zhang et al., 2021]. A large body of work has focused on understanding this phenomenon in the interpolation regime [Du et al., 2018, Liu et al., 2022], and the related concept of “benign overfitting” [Belkin et al., 2019, Bartlett et al., 2020, Frei et al., 2022].

While these directions have been fruitful, there is increasing evidence that rectified linear unit (ReLU) neural networks do not benignly overfit [Mallinar et al., 2022, Haas et al., 2023], particularly in the case of learning problems with noisy data [Joshi et al., 2023, Qiao et al., 2024]. Furthermore, for noisy labels, it takes many iterations of GD to actually interpolate the labels [Zhang et al., 2021]. This discounts theories based on interpolation to explain the generalization performance of *practical* neural networks, which would have entered the so-called *edge-of-stability* regime [Cohen et al., 2020], or stopped long before interpolating the training data.

To that end, it has been observed that an important factor that affects/characterizes the implicit bias of GD training is the notion of *dynamical stability* [Wu et al., 2018]. Intuitively, the (dynamical) stability of a particular minimum refers to the ability of the training algorithm to “stably converge” to that minimum. The stability of a minimum is intimately related to the flatness of the loss landscape about the minima [Mulayoff et al., 2021]. A number of recent works have focused on understanding *linear stability*, i.e., the stability of an algorithm’s linearized dynamics about a minima, in order to characterize the implicit biases of training algorithms [Wu et al., 2018, Nar and Sastry, 2018, Mulayoff et al., 2021, Ma and Ying, 2021, Nacson et al., 2023]. Minima that exhibit linear stability are often referred to as stable minima. In particular, Mulayoff et al. [2021] and Nacson et al. [2023] focus on the interpolation regime of two-layer overparameterized ReLU neural networks in the univariate input and multivariate input settings, respectively. Roughly speaking, the main takeaway from their work is that stability / flatness in parameter space implies a bounded-variation-type of smoothness in function space.

Moving beyond the interpolation regime, Qiao et al. [2024] extend the framework of Mulayoff et al. [2021] and provide generalization and risk bounds for stable minima in the non-interpolation regime for univariate inputs. They show that for univariate nonparametric regression, the functions realized by stable minima cannot overfit in the sense that the generalization gap vanishes as the number of training examples grows. Furthermore, they show that the learned functions achieve near-optimal estimation error rates for functions of second-order bounded variation on an interval strictly inside the data support. While this work is a good start, it begs the questions of (i) what happens in the multivariate / high-dimensional case and (ii) what happens off of this interval (i.e., how does the network *extrapolate*). Indeed, these are key to understanding the implicit bias of GD trained neural networks, especially since learning high dimensions seems to always amount to extrapolation [Balestriero et al., 2021]. These two questions motivate the present paper in which we provide a precise answer to the following fundamental question.

How well do stable minima of two-layer overparameterized ReLU neural networks perform in the high-dimensional and non-interpolation regime?

We provide several new theoretical results for stable minima in this scenario, which are corroborated by numerical simulations. Some of our findings are surprising given the current state of understanding of stable minima. Notably, we show that, while flatness does imply generalization, the resulting sample complexity grows exponentially with the input dimension. This gives an exponential separation

between flat solutions and low-norm solutions (weight decay) which knowingly do not suffer from the curse of dimensionality [Bach, 2017, Parhi and Nowak, 2023].

1.1 Contributions

In this paper, we provide new theoretical results for stable minima of two-layer ReLU neural networks, particularly in the high-dimensional and non-interpolation regime. Our primary contributions lie in the rigorous analysis of the generalization and statistical properties of stable minima and the resulting insights into their high-dimensional behavior. In particular, our contributions include the following.

1. We establish that the functions realized by stable minima are regular in the sense of a weighted variation norm (Theorem 3.2 and Corollary 3.3). This norm defines a *data-dependent* function class that captures the inductive bias of stable minima.¹ Furthermore, this regularity admits an analytic description as a form of weighted total variation in the domain of the Radon transform. These results synthesize and extend previous work [cf., Nacson et al., 2023, Qiao et al., 2024] by removing interpolation assumptions and generalizing them to multivariate inputs.
2. We formally analyzed the generalization properties of stable minima in both a statistical learning setting and a nonparametric regression setting defined using the smoothness class above.
 - We establish that stable minima provably cannot overfit in the sense that their generalization gap (i.e., a uniform convergence bound) tends to 0 as the number of training examples $n \rightarrow \infty$ at a rate $n^{-\frac{1}{2d+4}}$ up to logarithmic factors (Theorem 3.5).
 - For high-dimensional ($d > 1$) nonparametric regression, we show that stable minima (up to logarithmic factors) achieve an estimation error rate, in mean-squared error (MSE), upper bounded by $n^{-\frac{1}{2d+4}}$ (Theorem 3.6).
 - We prove a minimax lower bound of rate $n^{-\frac{2}{d+1}}$ up to a constant (Theorem 3.7) on both the MSE and the generalization gap, which certifies that stable minima are not immune to the curse of dimensionality. This gives an exponential separation between flat solutions and low-norm solutions (weight decay) [Bach, 2017, Parhi and Nowak, 2023].
 - By specializing the MSE upper bound to the univariate case ($d = 1$), we show that stable minima (up to logarithmic factors) achieve an upper bound of $n^{-\frac{4}{11}}$. Furthermore, by a construction specific to the univariate case, we have a sharper lower bound of $n^{-\frac{1}{2}}$ when $d = 1$. These results should be contrasted to those of Qiao et al. [2024], who derive matching upper and lower bounds of $n^{-\frac{4}{5}}$ on an interval strictly inside the data support. Note that our results hold over the full domain, therefore capturing how the networks extrapolate. Thus, our results provide a more realistic characterization of the statistical properties of stable minima in the univariate case than in prior work.
3. In Section 4, we corroborate our theoretical results with extensive numerical simulations. As a by-product, we uncover and characterize a phenomenon we refer to as “neural shattering” that is inherent to stable minima in high dimensions. This refers to the observation that each neuron in a flat solution has very few activated data points, which means that the activation boundaries of the ReLU neurons in the solutions shatter the dataset into small pieces. This leads to poor performance in high dimensions. We also highlight that this observation exactly matches the construction of “hard-to-learn” functions for our minimax lower bound. Thus,

¹More specifically, this quantity defines a *seminorm* which correspondingly defines a kind of Banach space of functions called a *weighted variation space* [DeVore et al., 2025].

our empirical validation combined with our theoretical analysis offers fresh insights into how high-dimensionality impacts neural network optimization and generalization, and reveals a subtle mechanism that can lead to overfitting.

These results are based on two novel technical innovations in the analysis of minima stability in comparison to prior works, which we summarize below.

Statistical bounds on the full input domain. The data-dependent nature of the stable minima function class implies that there are regions of the input domain where neuron activations are sparse for stable minima. This is because the functions in this class have local smoothness that can become arbitrarily irregular near the boundary of the data support. This makes it challenging to study the statistical performance of stable minima in the irregular regions. This was bypassed in the univariate case by Qiao et al. [2024] by restricting their attention to an interval strictly inside the data support, completely ignoring these hard-to-handle regions. Our analysis overcomes this via a novel technique that balances the error strictly inside the data support with the error close to the boundary. This allows us to establish meaningful statistical bounds on the full input domain.

ReLU-specific minimax lower bound construction. We develop a novel minimax lower bound construction (see proof of Theorem 3.7) using functions built from sums of ReLU neurons. These neurons are strategically chosen to have activation regions near the boundary of the input domain. This exploits the “on/off” nature of ReLUs and high-dimensional geometry to create “hard-to-learn” functions. The data-dependent weighting allows these sparsely active, high-magnitude neurons to exist within the stable minima function class. This construction is fundamentally different from classical nonparametric techniques and is tightly linked to our experimental findings on neural shattering (see Figure 1).

1.2 Related Work

Stable minima and function spaces. Many works have investigated characterizations of the implicit bias of GD training from the perspective of dynamical stability [Wu et al., 2018, Nar and Sastry, 2018, Mulayoff et al., 2021, Ma and Ying, 2021, Nacson et al., 2023, Qiao et al., 2024]. In particular, Mulayoff et al. [2021] characterized the function-space implicit bias of minima stability for two-layer overparameterized univariate ReLU networks in the interpolation regime. This was extended to the multivariate case by Nacson et al. [2023] and, in the univariate case, this was extended to the non-interpolation regime by Qiao et al. [2024] with the addition of generalization guarantees. In this paper, we extend these works to the high-dimensional and non-interpolation regime and characterize the generalization and statistical properties of stable minima.

Nonparametric function estimation with neural networks. It is well known that neural networks are minimax optimal estimators for a wide variety of functions [Suzuki, 2018, Schmidt-Hieber, 2020, Kohler and Langer, 2021, Parhi and Nowak, 2023, Zhang and Wang, 2023, Yang and Zhou, 2024, Qiao et al., 2024]. Outside of the univariate work of Qiao et al. [2024], all prior works construct their estimators via empirical risk minimization problems. Thus, they do not incorporate the training dynamics that arise when training neural networks in practice. Thus, the results of this paper provide more practically relevant results on nonparametric function estimation, providing estimation error rates achieved by local minima that GD training can stably converge to.

Loss curvature and generalization. A long-standing theory to explain why overparameterized neural networks generalize well is that the flat minima found by GD training generalize well [Hochreiter and Schmidhuber, 1997, Keskar et al., 2017]. Although there is increasing theoretical evidence for

this phenomenon in various settings [Ding et al., 2024, Qiao et al., 2024], there is also evidence that sharp minima can also generalize [Dinh et al., 2017]. Thus, this paper adds complementary results to this list where we establish that, while flatness does imply generalization for two-layer ReLU networks, the resulting sample complexity grows exponentially with the input dimension.

2 Preliminaries, Notation, and Problem Setup

We investigate learning with two-layer ReLU neural networks. Our focus is on understanding the generalization and statistical performance of solutions obtained through GD training, particularly those that are stable.

Neural networks. We consider two-layer ReLU neural networks with K neurons. Such a network implements a function $f_{\boldsymbol{\theta}} : \mathbb{R}^d \rightarrow \mathbb{R}$ of the form

$$f_{\boldsymbol{\theta}}(\mathbf{x}) = \sum_{k=1}^K v_k \phi(\mathbf{w}_k^\top \mathbf{x} - b_k) + \beta, \quad (1)$$

where $\boldsymbol{\theta} = \{v_k, \mathbf{w}_k, b_k\}_{k=1}^K \cup \{\beta\}$ denotes the collection of all neural network parameters. Here, $v_k \in \mathbb{R}$ denotes the output-layer weights, $\mathbf{w}_k \in \mathbb{R}^d$ denotes the input-layer weights, $b_k \in \mathbb{R}$ denotes the input-layer biases, and $\beta \in \mathbb{R}$ denotes the output-layer bias.

Data fitting and loss function. We consider the problem of fitting the data $\mathcal{D} = \{(\mathbf{x}_i, y_i)\}_{i=1}^n$, where $\mathbf{x}_i \in \mathbb{R}^d$ and $y_i \in \mathbb{R}$. We consider the empirical risk minimization problem with squared-error loss $\mathcal{L}(\boldsymbol{\theta}) = \frac{1}{2n} \sum_{i=1}^n (y_i - f_{\boldsymbol{\theta}}(\mathbf{x}_i))^2$.

Gradient descent and minima stability. We aim to minimize $\mathcal{L}(\cdot)$ via GD training, i.e., we consider the iteration $\boldsymbol{\theta}_{t+1} = \boldsymbol{\theta}_t - \eta \nabla_{\boldsymbol{\theta}} \mathcal{L}(\boldsymbol{\theta}_t)$, for $t = 0, 1, 2, \dots$, where $\eta > 0$ is the step size / learning rate, $\nabla_{\boldsymbol{\theta}}$ denotes the gradient operator with respect to $\boldsymbol{\theta}$, $\nabla_{\boldsymbol{\theta}}^2$ denotes the Hessian operator with respect to $\boldsymbol{\theta}$, and the iteration is initialized with some initial condition $\boldsymbol{\theta}_0$. The analysis of these dynamics in generality is intractable in most cases. Thus, following the work of Wu et al. [2018], many works [e.g., Nar and Sastry, 2018, Mulayoff et al., 2021, Ma and Ying, 2021, Nacson et al., 2023, Qiao et al., 2024] have considered the behavior of this iteration using *linearized dynamics* about a minimum. Following Mulayoff et al. [2021], we consider the Taylor series expansion of the loss function about a minimum $\boldsymbol{\theta}^*$.² That is,

$$\mathcal{L}(\boldsymbol{\theta}) \approx \mathcal{L}(\boldsymbol{\theta}^*) + (\boldsymbol{\theta} - \boldsymbol{\theta}^*)^\top \nabla_{\boldsymbol{\theta}} \mathcal{L}(\boldsymbol{\theta}^*) + \frac{1}{2} (\boldsymbol{\theta} - \boldsymbol{\theta}^*)^\top \nabla_{\boldsymbol{\theta}}^2 \mathcal{L}(\boldsymbol{\theta}^*) (\boldsymbol{\theta} - \boldsymbol{\theta}^*). \quad (2)$$

As the GD iteration approaches a minimum $\boldsymbol{\theta}^*$, it is well approximated by the *linearized dynamics*

$$\boldsymbol{\theta}_{t+1} = \boldsymbol{\theta}_t - \eta \left[\nabla_{\boldsymbol{\theta}} \mathcal{L}(\boldsymbol{\theta}^*) + \nabla_{\boldsymbol{\theta}}^2 \mathcal{L}(\boldsymbol{\theta}^*) (\boldsymbol{\theta}_t - \boldsymbol{\theta}^*) \right], \quad t = 0, 1, 2, \dots \quad (3)$$

This motivates the following definition of *linear stability* which we adopt from Mulayoff et al. [2021], Nacson et al. [2023], Qiao et al. [2024].

²Technically, we require that the loss is twice differentiable at $\boldsymbol{\theta}^*$. Due to the ReLU activation, there is a measure 0 set in the parameter space where this is not true. However, if we randomly initialize the weights with a density and use gradient descent with non-vanishing learning rate, then with probability 1 the GD iterations do not visit such non-differentiable points. For the interest of generalization bounds, the behaviors of non-differentiable points are identical to their infinitesimally perturbed neighbor, which is differentiable. For these reasons, this assumption will be implicitly assumed at each candidate $\boldsymbol{\theta}$ in the remainder of the paper.

Definition 2.1. Consider the iterates in (3). Let θ^* be a minimum (local or global) of $\mathcal{L}(\cdot)$. Given $\varepsilon > 0$, the minimum θ^* is said to be ε -linearly stable if, for any θ_0 in the Euclidean-norm ball of radius ε , denoted by $B_\varepsilon(\theta^*)$, it holds that $\limsup_{t \rightarrow \infty} \|\theta_t - \theta^*\| \leq \varepsilon$.

This definition defines a minimum to be stable if the GD iterates are “trapped” once they enter a neighborhood of the minimum. It turns out that stability is connected to the flatness of the minimum. Indeed, the following result is due to Qiao et al. [2024, Lemma 2.2], which is an adaptation of a result of Mulayoff et al. [2021, Lemma 1].

Proposition 2.2. Consider the iterates in (3). For any $\varepsilon > 0$, a minimum (local or global) θ^* is ε -linearly stable if and only if $\lambda_{\max}(\nabla_{\theta}^2 \mathcal{L}(\theta^*)) \leq 2/\eta$.

Thus, we see that the stability of a minimum is exactly related to the flatness of the minimum, measured by the maximum eigenvalue of the Hessian. We use this as the rigorous definition of stable minima and the generalization and statistical performance of such minima. Given a data set \mathcal{D} , we refer to the class of neural networks $\mathcal{F}_{\text{stable}}(\eta) := \left\{ f_{\theta} : \lambda_{\max}(\nabla_{\theta}^2 \mathcal{L}(\theta)) \leq \frac{2}{\eta} \right\}$, where we recall that $\eta > 0$ is the step size of GD for the empirical risk minimization problem, as the collection of stable minima or stable solutions, and analyze their performance. Empirically, it has been observed that GD often operates in the edge-of-stability regime, where $\lambda_{\max}(\nabla_{\theta}^2 \mathcal{L}(\theta_t))$ hovers around $2/\eta$ [Cohen et al., 2020, Damian et al., 2024]. This further motivates our study of solutions that lie in $\mathcal{F}_{\text{stable}}(\eta)$. In particular, we see that larger step sizes correspond to flatter minima.

3 Main Results

In this section, we characterize the implicit bias of stable solutions. It turns out that every $f \in \mathcal{F}_{\text{stable}}(\eta)$ is regular in the sense of a weighted variation norm. In particular, the weight function is a data-dependent quantity. This weight function reveals that neural networks can learn features that are intrinsic within the structure of the training data. To that end, given a dataset $\mathcal{D} = \{(\mathbf{x}_i, y_i)\}_{i=1}^n \subset \mathbb{R}^d \times \mathbb{R}$, we consider a weight function $g : \mathbb{S}^{d-1} \times \mathbb{R} \rightarrow \mathbb{R}$, where $\mathbb{S}^{d-1} := \{\mathbf{u} \in \mathbb{R}^d : \|\mathbf{u}\| = 1\}$ denotes the unit sphere. This weight is defined by $g(\mathbf{u}, t) := \min\{\tilde{g}(\mathbf{u}, t), \tilde{g}(-\mathbf{u}, -t)\}$, where

$$\tilde{g}(\mathbf{u}, t) := \mathbb{P}(\mathbf{X}^\top \mathbf{u} > t)^2 \cdot \mathbb{E}[\mathbf{X}^\top \mathbf{u} - t \mid \mathbf{X}^\top \mathbf{u} > t] \cdot \sqrt{1 + \|\mathbb{E}[\mathbf{X} \mid \mathbf{X}^\top \mathbf{u} > t]\|^2}. \quad (4)$$

Here, \mathbf{X} is a random vector drawn uniformly at random from the training examples $\{\mathbf{x}_i\}_{i=1}^n$. Note that the distribution \mathbb{P}_X from which $\{\mathbf{x}_i\}_{i=1}^n$ are drawn i.i.d. controls the regularity of g .

With this weight function in hand, we define a (semi)norm on functions of the form

$$f_{\nu, \mathbf{c}, c_0}(\mathbf{x}) = \int_{\mathbb{S}^{d-1} \times [-R, R]} \phi(\mathbf{u}^\top \mathbf{x} - t) d\nu(\mathbf{u}, t) + \mathbf{c}^\top \mathbf{x} + c_0, \quad \mathbf{x} \in \mathbb{R}^d, \quad (5)$$

where $R > 0$, $\mathbf{c} \in \mathbb{R}^d$, and $c_0 \in \mathbb{R}$. Functions of this form are “infinite-width” neural networks. We define the *weighted variation (semi)norm* as

$$|f|_{V_g} := \inf_{\substack{\nu \in \mathcal{M}(\mathbb{S}^{d-1} \times [-R, R]) \\ \mathbf{c} \in \mathbb{R}^d, c_0 \in \mathbb{R}}} \|g \cdot \nu\|_{\mathcal{M}} \quad \text{s.t.} \quad f = f_{\nu, \mathbf{c}, c_0}, \quad (6)$$

where, if there does not exist a representation of f in the form of (5), then the seminorm³ is understood to take the value $+\infty$. Here, $\mathcal{M}(\mathbb{S}^{d-1} \times [-R, R])$ denotes the Banach space of (Radon)

³We use the notation $|\cdot|$ instead of $\|\cdot\|$ to highlight that this quantity is a seminorm. This quantity is a seminorm since affine functions are in its null space. See Kůrková and Sanguinetti [2001, 2002], Mhaskar [2004], Bach [2017], Siegel and Xu [2023], Shenouda et al. [2024] for more details about variation spaces.

measures and, for $\mu \in \mathcal{M}(\mathbb{S}^{d-1} \times [-R, R])$, $\|\mu\|_{\mathcal{M}} := \int_{\mathbb{S}^{d-1} \times [-R, R]} d|\mu|(\mathbf{u}, t)$ is the measure-theoretic total-variation norm.

With this seminorm, we define the Banach space of functions $V_g(\mathbb{B}_R^d)$ on the ball $\mathbb{B}_R^d := \{\mathbf{x} \in \mathbb{R}^d : \|\mathbf{x}\|_2 \leq R\}$ as the set of all functions f such that $|f|_{V_g}$ is finite. When $g \equiv 1$, $|\cdot|_{V_g}$ and $V_g(\mathbb{B}_R^d)$ coincide with the variation (semi)norm and variation norm space of Bach [2017].

Example 3.1. *Since we are interested in functions defined on \mathbb{B}_R^d , for a finite-width neural network $f_{\boldsymbol{\theta}}(\mathbf{x}) = \sum_{k=1}^K v_k \phi(\mathbf{w}_k^\top \mathbf{x} - b_k) + \beta$, we observe that it has the equivalent implementation as $f_{\boldsymbol{\theta}}(\mathbf{x}) = \sum_{j=1}^J a_j \phi(\mathbf{u}_j^\top \mathbf{x} - t_j) + \mathbf{c}^\top \mathbf{x} + c_0$, where $a_j \in \mathbb{R}$, $\mathbf{u}_j \in \mathbb{S}^{d-1}$, $t_j \in \mathbb{R}$, $\mathbf{c} \in \mathbb{R}^d$, and $c_0 \in \mathbb{R}$. Indeed, this is due to the fact that the ReLU is homogeneous, which allows us to absorb the magnitude of the input weights into the output weights (i.e., each $a_j = |v_{k_j}| \|\mathbf{w}_{k_j}\|_2$ for some $k_j \in \{1, \dots, K\}$). Furthermore, any ReLUs in the original parameterization whose activation threshold⁴ is outside \mathbb{B}_R^d can be implemented by an affine function on \mathbb{B}_R^d , which gives rise to the $\mathbf{c}^\top \mathbf{x} + c_0$ term in the implementation. If this new implementation is in “reduced form”, i.e., the collection $\{(\mathbf{u}_j, t_j)\}_{j=1}^J$ are distinct, then we have that $|f_{\boldsymbol{\theta}}|_{V_g} = \sum_{j=1}^J |a_j| g(\mathbf{u}_j, t_j)$.*

This example reveals that this seminorm is a weighted path norm of a neural network and, in fact, coincides with the path norm when $g \equiv 1$ [Neyshabur et al., 2015]. It also turns out that the data-dependent regularity induced by this seminorm is tightly linked to the flatness of a neural network minimum. We summarize this fact in the next theorem.

Theorem 3.2. *Suppose that $f_{\boldsymbol{\theta}}$ is a two-layer neural network such that the loss $\mathcal{L}(\cdot)$ is twice differentiable at $\boldsymbol{\theta}$. Then, $|f_{\boldsymbol{\theta}}|_{V_g} \leq \frac{\lambda_{\max}(\nabla_{\boldsymbol{\theta}}^2 \mathcal{L}(\boldsymbol{\theta}))}{2} - \frac{1}{2} + (R+1)\sqrt{2\mathcal{L}(\boldsymbol{\theta})}$.*

The proof of this theorem appears in Appendix C. This theorem reveals that flatness implies regularity in the sense of the variation space $V_g(\mathbb{B}_R^d)$. In particular, we also have an immediate corollary for stable minima thanks to Proposition 2.2.

Corollary 3.3. *For any $f_{\boldsymbol{\theta}} \in \mathcal{F}_{\text{stable}}(\eta)$, $|f_{\boldsymbol{\theta}}|_{V_g} \leq \frac{1}{\eta} - \frac{1}{2} + (R+1)\sqrt{2\mathcal{L}(\boldsymbol{\theta})}$.*

The main takeaway messages from Theorem 3.2 and Corollary 3.3 are that flat / stable solutions are smooth in the sense of $V_g(\mathbb{B}_R^d)$. In particular, we see that the Banach space $V_g(\mathbb{B}_R^d)$ is the natural function space to study stable minima. This framework provides the mathematical foundation and sets the stage to investigate the generalization and statistical performance of stable minima.

We also note that, from Corollary 3.3 and Example 3.1, for stable solutions $f_{\boldsymbol{\theta}}$, as the step size η grows, the function $f_{\boldsymbol{\theta}}$ becomes smoother, eventually approaching an affine function as $\eta \rightarrow \infty$. This can be viewed as an example of the *simplicity bias* phenomenon of GD training [Arpit et al., 2017, Kalimeris et al., 2019, Valle-Perez et al., 2019].

Finally, we note that the function-space regularity induced by $V_g(\mathbb{B}_R^d)$ has an equivalent analytic description via a weighted norm in the domain of the Radon transform of the function. This analytic description is based on the \mathcal{R} -(semi)norm/second-order Radon-domain total variation inductive bias of infinite-width two-layer neural networks [Ongie et al., 2020, Parhi and Nowak, 2021, Bartolucci et al., 2023]. Before stating our theorem, we first recall the definition of the Radon transform. The Radon transform of a function $f \in L^1(\mathbb{R}^d)$ is given by

$$\mathcal{R}\{f\}(\mathbf{u}, t) = \int_{\mathbf{u}^\top \mathbf{x} = t} f(\mathbf{x}) d\mathbf{x}, \quad (\mathbf{u}, t) \in \mathbb{S}^{d-1} \times \mathbb{R}, \quad (7)$$

where the integration is against the $(d-1)$ -dimensional Lebesgue measure on the hyperplane $\mathbf{u}^\top \mathbf{x} = t$. Thus, we see that the Radon transform integrates functions along hyperplanes.

⁴The activation threshold of a neuron $\phi(\mathbf{w}^\top \mathbf{x} - b)$ is the hyperplane $\{\mathbf{x} \in \mathbb{R}^d : \mathbf{w}^\top \mathbf{x} = b\}$.

Theorem 3.4. For every $f \in V_g(\mathbb{B}_R^d)$, consider the canonical extension⁵ $f_{\text{ext}} : \mathbb{R}^d \rightarrow \mathbb{R}$ via its integral representation (5). It holds that $|f|_{V_g} = \|g \cdot \mathcal{R}(-\Delta)^{\frac{d+1}{2}} f_{\text{ext}}\|_{\mathcal{M}}$, where fractional powers of the Laplacian are understood via the Fourier transform.

The proof of this theorem appears in Appendix D. We remark that the operators that appear in the theorem must be understood in the distributional sense (i.e., by duality). We refer the reader to Parhi and Unser [2024] for rigorous details about the distributional extension of the Radon transform. We also remark that a version of this theorem also appeared in Nacson et al. [2023, Theorem 1], but we note that their problem setting was the implicit bias of minima stability in the interpolation regime.

3.1 Stable Solutions Generalize But Suffer the Curse of Dimensionality

In the remainder of this paper, we focus on the scenario where inputs $\{\mathbf{x}_i\}_{i=1}^n$ are drawn i.i.d. uniformly from the unit ball \mathbb{B}_1^d (i.e., $R = 1$). Under this assumption, the *population version* of the weight function, which we denote as g_P , has a well-defined asymptotic behavior. As detailed in Appendix E, for $|t| \geq 1$, $g_P(\mathbf{u}, t) = 0$, and as $|t| \rightarrow 1^-$, $g_P(\mathbf{u}, t) \asymp (1 - |t|)^{d+2}$. While the actual weight function g in our analysis remains the empirical one derived from the data, this population behavior serves as a crucial analytical guide. Our proofs will show that the empirical g concentrates around this population version (Appendix E.2). For clarity in expressing our main results and their dependence on dimensionality, we will characterize the function space of stable minima with respect to a canonical weight function $g(\mathbf{u}, t) := (1 - |t|)^{d+2}$, which captures this essential asymptotic property.

With this in hand, we can now characterize the *generalization gap* of stable minima, which is defined to be the absolute difference between the training loss and the population risk. We are able to characterize the generalization gap under mild conditions on the joint distribution of the training examples and the labels.

Theorem 3.5. Let \mathcal{P} denote the joint distribution of (\mathbf{x}, y) . Assume that \mathcal{P} is supported on $\mathbb{B}_1^d \times [-D, D]$ for some $D > 0$ and that the marginal distribution of \mathbf{x} is $\text{Uniform}(\mathbb{B}_1^d)$. Fix a dataset $\mathcal{D} = \{(\mathbf{x}_i, y_i)\}_{i=1}^n$, where each (\mathbf{x}_i, y_i) is drawn i.i.d. from \mathcal{P} . Then, with probability $\geq 1 - \delta$ we have that for the plug-in risk estimator $\hat{R}(f) := \frac{1}{n} \sum_{i=1}^n (f(\mathbf{x}_i) - y_i)^2$

$$\begin{aligned} \sup_{f_{\boldsymbol{\theta}} \in \mathcal{F}_{\text{stable}}(\eta)} \text{GeneralizationGap}(f_{\boldsymbol{\theta}}; \hat{R}) &:= \left| \mathbb{E}_{(\mathbf{x}, y) \sim \mathcal{P}} \left[(f_{\boldsymbol{\theta}}(\mathbf{x}) - y)^2 \right] - \hat{R}(f_{\boldsymbol{\theta}}) \right| \\ &\lesssim_d \left(\frac{1}{\eta} - \frac{1}{2} + 4M \right)^{\frac{d}{d^2+4d+3}} M^2 n^{-\frac{1}{2d+4}}, \end{aligned} \quad (8)$$

where $M := \max\{D, \|f_{\boldsymbol{\theta}}\|_{L^\infty(\mathbb{B}_1^d)}\}$ and \lesssim_d hides constants (which could depend on d) and logarithmic factors in n and $(1/\delta)$. Furthermore, if the network have more than $O(n)$ neurons, it holds that for any risk estimator $\tilde{R} : \mathcal{D} \rightarrow \mathbb{R}^{\mathcal{F}_{\text{stable}}(\eta)}$,

$$\sup_{\mathcal{P}} \mathbb{E}_{\mathcal{D} \sim \mathcal{P}^{\otimes n}} \left[\sup_{f_{\boldsymbol{\theta}} \in \mathcal{F}_{\text{stable}}(\eta)} \text{GeneralizationGap}(f_{\boldsymbol{\theta}}; \tilde{R}) \right] \gtrsim_d \min \left\{ M, \frac{1}{\eta} - \frac{1}{2} + 4M \right\}^2 n^{-\frac{2}{d+1}}, \quad (9)$$

where \gtrsim_d hides constants (which could depend on d) and the sup is over all distributions that satisfy the above hypotheses.

⁵Since functions in $V_g(\mathbb{B}_R^d)$ are only defined on \mathbb{B}_R^d , we must consider their extension to \mathbb{R}^d when working with the Radon transform. See Parhi and Nowak [2023, Section IV] for more details.

The proof of this theorem appears in Appendix F. While this theorem does show that as $n \rightarrow \infty$, the generalization gap vanishes, it reveals that the sample complexity grows exponentially with the input dimension (as seen by the $n^{-\frac{1}{2d+4}}$ term in the upper bound and the $n^{-\frac{2}{d+1}}$ term in the lower bound). This suggests that the curse-of-dimensionality is intrinsic to the stable minima set $\mathcal{F}_{\text{stable}}(\eta)$ —not an artifact of our mathematical analysis nor the naive plug-in empirical risk estimator being suboptimal. On the other hand, for low-norm solutions (in the sense that they minimize the weight-decay objective), it can be shown that the generalization gap decays at a rate of $\tilde{O}(n^{-\frac{1}{4}})$, where $\tilde{O}(\cdot)$ hides logarithmic factors [cf., Bach, 2017, Parhi and Nowak, 2023]. This uncovers an exponential gap between flat and low-norm solutions, and, in particular, that stable solutions suffer the curse of dimensionality. When $d = 1$, this result also provides a strict generalization of Qiao et al. [2024, Theorem 4.3], as they measure the error strictly inside the input domain, rather than on the full input domain. Thus, our result also characterizes how stable solutions *extrapolate*.

3.2 Nonparametric Function Estimation With Stable Minima

We now turn to the problem of nonparametric function estimation. As we have seen that $V_g(\mathbb{B}_1^d)$ is a natural model class for stable minima, this raises two fundamental questions: (i) How well do stable minima estimate functions in $V_g(\mathbb{B}_1^d)$ from noisy data? and (ii) What is the best performance any estimation method could hope to achieve for functions in $V_g(\mathbb{B}_1^d)$. In this section we provide answers to both these questions by deriving a mean-squared error upper bound for stable minima and a minimax lower bound for this function class.

Theorem 3.6. *Fix a step size $\eta > 0$ and noise level $\sigma > 0$. Given a ground truth function $f_0 \in V_g(\mathbb{B}_1^d)$ such that $\|f_0\|_{L^\infty} \leq B$ and $|f_0|_{V_g} \leq \tilde{O}\left(\frac{1}{\eta} - \frac{1}{2} + 2\sigma\right)$, suppose that we are given a data set $y_i = f_0(\mathbf{x}_i) + \varepsilon_i$, where \mathbf{x}_i are i.i.d. $\text{Uniform}(\mathbb{B}_1^d)$ and ε_i are i.i.d. $\mathcal{N}(0, \sigma^2)$. Then, with probability $\geq 1 - \delta$, we have that*

$$\frac{1}{n} \sum_{i=1}^n (f_\theta(\mathbf{x}_i) - f_0(\mathbf{x}_i))^2 \lesssim_d \left(\frac{1}{\eta} - \frac{1}{2} + 2\sigma\right)^{\frac{d}{(2d^2+6d+3)(d+2)}} B^2 \left(\frac{\sigma^2}{n}\right)^{\frac{1}{2d+4}}, \quad (10)$$

for any $f_\theta \in \mathcal{F}_{\text{stable}}(\eta)$ that is optimized, i.e., $(f_\theta(\mathbf{x}_i) - y_i)^2 \leq (f_0(\mathbf{x}_i) - y_i)^2$, for $i = 1, \dots, n$.

The proof of this theorem appears in Appendix G. This theorem shows that *optimized* stable minima incur an estimation error rate that decays as $\tilde{O}(n^{-\frac{1}{2d+4}})$, which suffers the curse of dimensionality. The optimized assumption is mild as it only asks that the error for each data point is smaller than the label noise σ^2 , which is easy to achieve in practice with GD training, especially in the overparameterized regime. The next theorem shows that the curse of dimensionality is actually necessary for this function class.

Theorem 3.7. *Consider the same data-generating process as in Theorem 3.6. We have the following minimax lower bounds.*

$$\inf_{\hat{f}} \sup_{\substack{f \in V_g(\mathbb{B}_1^d) \\ \|f\|_{L^\infty} \leq B, |f|_{V_g} \leq C}} \mathbb{E} \|\hat{f} - f\|_{L^2}^2 \gtrsim_d \begin{cases} \min(B, C)^2 \left(\frac{\sigma^2}{n}\right)^{\frac{2}{d+1}}, & d > 1, \\ \min(B, C)^2 \left(\frac{\sigma^2}{n}\right)^{\frac{1}{2}}, & d = 1. \end{cases} \quad (11)$$

where \gtrsim_d hides constants (that could depend on d).

The proof of this theorem appears in Appendix H. Our proof relies on two high-dimensional constructions. The first construction is to pack the unit sphere \mathbb{S}^{d-1} with $M = \exp(\Omega(d))$ pairwise-disjoint spherical caps, each specified by a unit vector \mathbf{u}_i as its center. Then, for every center \mathbf{u}_i the

ReLU neuron $\varphi_i(\mathbf{x}) = c\phi(\mathbf{u}_i^\top \mathbf{x} - t)$ is active only on its outward-facing cap, and attains its peak value $\min\{B, C\}$ by choosing a suitable t . The second construction is to observe that since the weight function $g(\mathbf{u}, t)$ decreases exponentially fast as $|t| \rightarrow 1$ (see Appendix E), the regularity constraint $|\cdot|_{V_g} \leq C$ allows us to combine an exponential number of such atoms to construct a family of “hard-to-learn” functions. Traditional lower-bound constructions satisfy regularity by shrinking bump amplitudes (vertical changes), whereas our approach fundamentally differs by shifting and resizing bump supports (horizontal changes). Our experiments reveal that stable minima actually favor these kinds of hard-to-learn functions and we refer to this as the *neural shattering* phenomenon.

4 Experiments

In this section, we empirically validate our claims that (i) stable minima are not immune to the curse of dimensionality and (ii) the “neural shattering” phenomenon occurs. All synthetic data points are generated by uniformly sampling \mathbf{x} from \mathbb{B}_1^d and $y_i = f_0(\mathbf{x}_i) + \mathcal{N}(0, \sigma^2)$, where the ground-truth function $f_0(\mathbf{x}) = \mathbf{w}^\top \mathbf{x}$ for some fixed vector \mathbf{w} with $\|\mathbf{w}\| = 1$. All the models are two-layer ReLU neural networks with width four times the training data size. The networks are randomly initialized by the standard Kaiming initialization [He et al., 2015]. We also use gradient clipping with threshold 50 to avoid divergence for large learning rates.⁶

Curse of dimensionality. In this experiment, we train neural networks with GD and vary the dataset sizes in $\{32, 64, 128, 256, 512\}$ and dimensions in $\{1, 2, 3, 4, 5\}$, with noise level $\sigma = 1$. For each dataset size, dimension, and training parameters ($\eta = 0.2$ without weight decay and $\eta = 0.01$ with weight-decay 0.1), we conduct 5 experiments and take the median. The log-log curves are displayed in Figure 2.

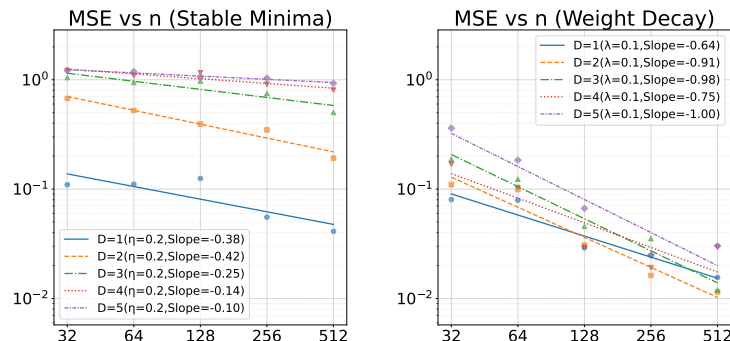


Figure 2: Empirical validation of the curse of dimensionality. **Left panel:** The slope of log MSE versus log n for training with vanilla gradient descent rapidly decreases with dimension, falling to about 0.1 at $d = 5$. **Right panel:** Training with ℓ^2 (weight decay) results in slopes above 0.5 in the log-log scale.

Neural shattering. As briefly illustrated in the right panel of Figure 1, Figure 3 presents more detailed experiments. We train a two-layer ReLU network of width 2048 on 512 noisy samples ($\sigma = 1$) of a 10-dimensional linear target. Under a large stepsize $\eta = 0.9$ (no weight decay), gradient descent enters a flat / stable minimum ($\lambda_{\max}(\nabla_{\theta}^2 \mathcal{L}(\theta))$ oscillates around $2/\eta \approx 2.2$, signaling edge-of-stability dynamics). This drastically reduces each neuron’s data-activation rate to $\leq 10\%$, rather than reducing their weight norms. The network overfits (train MSE ≈ 1.105 , matching the noise level).

⁶We monitor clipping during the training, and the clipping only occurs in the first 10 epochs. Gradient clipping does not prevent the training dynamics from entering edge-of-stability regime.

In contrast, with $\eta = 0.01$ plus ℓ^2 -weight-decay $\lambda = 0.1$, all neurons remain active and weight norms stay tightly bounded, so the model avoids overfitting (train MSE ≈ 0.055).

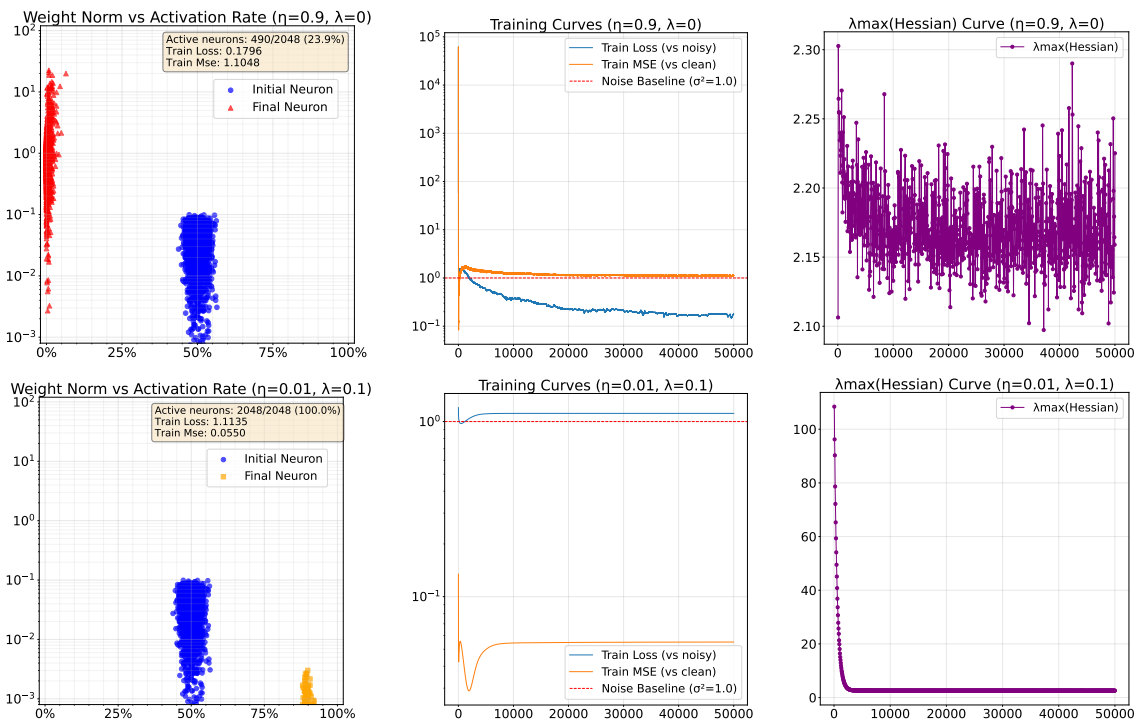


Figure 3: The top-left plot illustrates the *neural shattering* phenomenon: after large-step training each ReLU neuron (orange) is active on only a tiny fraction of the data (small horizontal support) yet its weight norm remains large, exactly as in our sphere-packing lower-bound construction where each outward-facing ReLU atom fires on very few inputs but retains full peak amplitude.

5 Discussion and Conclusion

This paper presents a nuanced conclusion on the link between minima stability and generalization: Stable solutions do generalize, but when data is distributed uniformly on a ball, this generalization ability is severely weakened by the Curse of Dimensionality (CoD). Our analysis pinpoints the mechanism behind this failure. The implicit regularization from GD is not uniform across the input domain. While it imposes strong regularity in the strict interior of the data support, this guarantee collapses at the boundary. This localized failure of regularization is precisely what enables “neural shattering”, a phenomenon where neurons satisfy the stability condition not by shrinking their weights, but by minimizing their activation frequency. This causes the CoD: The intrinsic geometry of a high-dimensional ball provides an exponential increase in available directions for shattering to occur, while the boundary regularization simultaneously weakens exponentially as the input dimension d grows. This mechanism, confirmed by both our lower bounds and experiments, explains why stable solutions exhibit poor generalization in high dimensions.

Several simplifications limit the scope of these results. The theory treats only two-layer ReLU networks and relies on the idealized assumption that samples are drawn uniformly from the unit ball. For more general distributions, the induced weight function g inherits the full geometry of the data and becomes harder to describe and interpret. Understanding this effect, together with extending the analysis to deeper architectures and adaptive algorithms, will take substantial effort, which we

leave as future work.

6 Acknowledgments

The research was partially supported by NSF Award # 2134214. The authors acknowledge early discussion with Peter Bartlett at the Simons Foundation that motivated us to consider the problem. Tongtong Liang thanks Zihan Shao for providing helpful suggestions on the implementation of the experiments.

References

- Devansh Arpit, Stanisław Jastrzębski, Nicolas Ballas, David Krueger, Emmanuel Bengio, Maxinder S Kanwal, Tegan Maharaj, Asja Fischer, Aaron Courville, Yoshua Bengio, et al. A closer look at memorization in deep networks. In *International Conference on Machine Learning*, pages 233–242. PMLR, 2017.
- Francis Bach. Breaking the curse of dimensionality with convex neural networks. *Journal of Machine Learning Research*, 18(1):629–681, 2017.
- Randall Balestriero, Jerome Pesenti, and Yann LeCun. Learning in high dimension always amounts to extrapolation. *arXiv preprint arXiv:2110.09485*, 2021.
- Peter L Bartlett, Philip M Long, Gábor Lugosi, and Alexander Tsigler. Benign overfitting in linear regression. *Proceedings of the National Academy of Sciences*, 117(48):30063–30070, 2020.
- Francesca Bartolucci, Ernesto De Vito, Lorenzo Rosasco, and Stefano Vigogna. Understanding neural networks with reproducing kernel Banach spaces. *Applied and Computational Harmonic Analysis*, 62:194–236, 2023.
- Mikhail Belkin, Alexander Rakhlin, and Alexandre B Tsybakov. Does data interpolation contradict statistical optimality? In *The 22nd International Conference on Artificial Intelligence and Statistics*, pages 1611–1619. PMLR, 2019.
- Jeremy Cohen, Simran Kaur, Yuanzhi Li, J Zico Kolter, and Ameet Talwalkar. Gradient descent on neural networks typically occurs at the edge of stability. In *International Conference on Learning Representations*, 2020.
- Alex Damian, Eshaan Nichani, and Jason D Lee. Self-stabilization: The implicit bias of gradient descent at the edge of stability. In *International Conference on Learning Representations*, 2024.
- Ronald DeVore, Robert D. Nowak, Rahul Parhi, and Jonathan W. Siegel. Weighted variation spaces and approximation by shallow ReLU networks. *Applied and Computational Harmonic Analysis*, 74:101713, 2025.
- Lijun Ding, Dmitriy Drusvyatskiy, Maryam Fazel, and Zaid Harchaoui. Flat minima generalize for low-rank matrix recovery. *Information and Inference: A Journal of the IMA*, 13(2):iaae009, 2024.
- Laurent Dinh, Razvan Pascanu, Samy Bengio, and Yoshua Bengio. Sharp minima can generalize for deep nets. In *International Conference on Machine Learning*, pages 1019–1028. PMLR, 2017.
- Simon S Du, Xiyu Zhai, Barnabas Poczos, and Aarti Singh. Gradient descent provably optimizes over-parameterized neural networks. In *International Conference on Learning Representations*, 2018.

- Spencer Frei, Niladri S Chatterji, and Peter Bartlett. Benign overfitting without linearity: Neural network classifiers trained by gradient descent for noisy linear data. In *Conference on Learning Theory*, pages 2668–2703. PMLR, 2022.
- Moritz Haas, David Holzmüller, Ulrike Luxburg, and Ingo Steinwart. Mind the spikes: Benign overfitting of kernels and neural networks in fixed dimension. *Advances in Neural Information Processing Systems*, 36, 2023.
- David Haussler. Decision-theoretic generalizations of the pac model for neural net and other learning applications. *Information and Computation*, 100(1):78–150, 1992.
- Kaiming He, Xiangyu Zhang, Shaoqing Ren, and Jian Sun. Delving deep into rectifiers: Surpassing human-level performance on imagenet classification. In *Proceedings of the IEEE international conference on computer vision (ICCV)*, pages 1026–1034, 2015.
- Sepp Hochreiter and Jürgen Schmidhuber. Flat minima. *Neural computation*, 9(1):1–42, 1997.
- Nirmit Joshi, Gal Vardi, and Nathan Srebro. Noisy interpolation learning with shallow univariate ReLU networks. In *International Conference on Learning Representations*, 2023.
- Dimitris Kalimeris, Gal Kaplun, Preetum Nakkiran, Benjamin Edelman, Tristan Yang, Boaz Barak, and Haofeng Zhang. SGD on neural networks learns functions of increasing complexity. *Advances in Neural Information Processing Systems*, 32, 2019.
- Nitish Shirish Keskar, Dheevatsa Mudigere, Jorge Nocedal, Mikhail Smelyanskiy, and Ping Tak Peter Tang. On large-batch training for deep learning: Generalization gap and sharp minima. In *International Conference on Learning Representations*, 2017.
- Michael Kohler and Sophie Langer. On the rate of convergence of fully connected deep neural network regression estimates. *Annals of Statistics*, 49(4):2231–2249, 2021.
- Věra Kůrková and Marcello Sanguineti. Bounds on rates of variable-basis and neural-network approximation. *IEEE Transactions on Information Theory*, 47(6):2659–2665, 2001.
- Věra Kůrková and Marcello Sanguineti. Comparison of worst case errors in linear and neural network approximation. *IEEE Transactions on Information Theory*, 48(1):264–275, 2002.
- Chaoyue Liu, Libin Zhu, and Mikhail Belkin. Loss landscapes and optimization in over-parameterized non-linear systems and neural networks. *Applied and Computational Harmonic Analysis*, 59:85–116, 2022.
- Chao Ma and Lexing Ying. On linear stability of sgd and input-smoothness of neural networks. *Advances in Neural Information Processing Systems*, 34:16805–16817, 2021.
- Neil Mallinar, James Simon, Amirhesam Abedsoltan, Parthe Pandit, Misha Belkin, and Preetum Nakkiran. Benign, tempered, or catastrophic: Toward a refined taxonomy of overfitting. *Advances in Neural Information Processing Systems*, 35:1182–1195, 2022.
- Hrushikesh N. Mhaskar. On the tractability of multivariate integration and approximation by neural networks. *Journal of Complexity*, 20(4):561–590, 2004.
- Rotem Mulayoff, Tomer Michaeli, and Daniel Soudry. The implicit bias of minima stability: A view from function space. *Advances in Neural Information Processing Systems*, 34:17749–17761, 2021.
- Mor Shpigel Nacson, Rotem Mulayoff, Greg Ongie, Tomer Michaeli, and Daniel Soudry. The implicit bias of minima stability in multivariate shallow ReLU networks. In *International Conference on Learning Representations*, 2023.

- Kamil Nar and Shankar Sastry. Step size matters in deep learning. *Advances in Neural Information Processing Systems*, 31, 2018.
- Behnam Neyshabur, Russ R. Salakhutdinov, and Nati Srebro. Path-SGD: Path-normalized optimization in deep neural networks. *Advances in Neural Information Processing Systems*, 28, 2015.
- Greg Ongie, Rebecca Willett, Daniel Soudry, and Nathan Srebro. A function space view of bounded norm infinite width relu nets: The multivariate case. In *International Conference on Learning Representations*, 2020.
- Rahul Parhi and Robert D. Nowak. Banach space representer theorems for neural networks and ridge splines. *Journal of Machine Learning Research*, 22(43):1–40, 2021.
- Rahul Parhi and Robert D. Nowak. Near-minimax optimal estimation with shallow ReLU neural networks. *IEEE Transactions on Information Theory*, 69(2):1125–1139, 2023.
- Rahul Parhi and Michael Unser. Distributional extension and invertibility of the k -plane transform and its dual. *SIAM Journal on Mathematical Analysis*, 56(4):4662–4686, 2024.
- Dan Qiao, Kaiqi Zhang, Esha Singh, Daniel Soudry, and Yu-Xiang Wang. Stable minima cannot overfit in univariate ReLU networks: Generalization by large step sizes. In *Advances in Neural Information Processing Systems*, volume 37, pages 94163–94208, 2024.
- Johannes Schmidt-Hieber. Nonparametric regression using deep neural networks with ReLU activation function. *Annals of Statistics*, 48(4):1875–1897, 2020.
- Joseph Shenouda, Rahul Parhi, Kangwook Lee, and Robert D. Nowak. Variation spaces for multi-output neural networks: Insights on multi-task learning and network compression. *Journal of Machine Learning Research*, 25(231):1–40, 2024.
- Jonathan W. Siegel and Jinchao Xu. Characterization of the variation spaces corresponding to shallow neural networks. *Constructive Approximation*, pages 1–24, 2023.
- Taiji Suzuki. Adaptivity of deep relu network for learning in besov and mixed smooth besov spaces: optimal rate and curse of dimensionality. *arXiv preprint arXiv:1810.08033*, 2018.
- Alexandre B. Tsybakov. *Introduction to Nonparametric Estimation*. Springer Series in Statistics. Springer, New York, 1st edition, 2009. ISBN 9780387790511.
- Guillermo Valle-Perez, Chico Q. Camargo, and Ard A. Louis. Deep learning generalizes because the parameter-function map is biased towards simple functions. In *International Conference on Learning Representations*, 2019.
- Vladimir N. Vapnik. *Statistical Learning Theory*. Wiley, 1998.
- Roman Vershynin. *High-Dimensional Probability: An Introduction with Applications in Data Science*. Cambridge Series in Statistical and Probabilistic Mathematics. Cambridge University Press, 2018. ISBN 978-1108415194. doi: 10.1017/9781108231596.
- Martin J Wainwright. *High-dimensional statistics: A non-asymptotic viewpoint*, volume 48. Cambridge university press, 2019.
- Larry Wasserman. Minimax theory lecture notes. <https://www.stat.cmu.edu/~larry/=sml/minimax.pdf>, 2020. Accessed: 2025-05-21.

- Lei Wu, Chao Ma, and Weinan E. How SGD selects the global minima in over-parameterized learning: A dynamical stability perspective. *Advances in Neural Information Processing Systems*, 31, 2018.
- Yunfei Yang and Ding-Xuan Zhou. Optimal rates of approximation by shallow ReLU^k neural networks and applications to nonparametric regression. *Constructive Approximation*, pages 1–32, 2024.
- Chiyuan Zhang, Samy Bengio, Moritz Hardt, Benjamin Recht, and Oriol Vinyals. Understanding deep learning (still) requires rethinking generalization. *Communications of the ACM*, 64(3): 107–115, 2021.
- Kaiqi Zhang and Yu-Xiang Wang. Deep learning meets nonparametric regression: Are weight-decayed DNNs locally adaptive? In *International Conference on Learning Representations*, 2023.

A Additional Experiments

A.1 Empirical Evidence: High Dimensionality Yields Neural Shattering

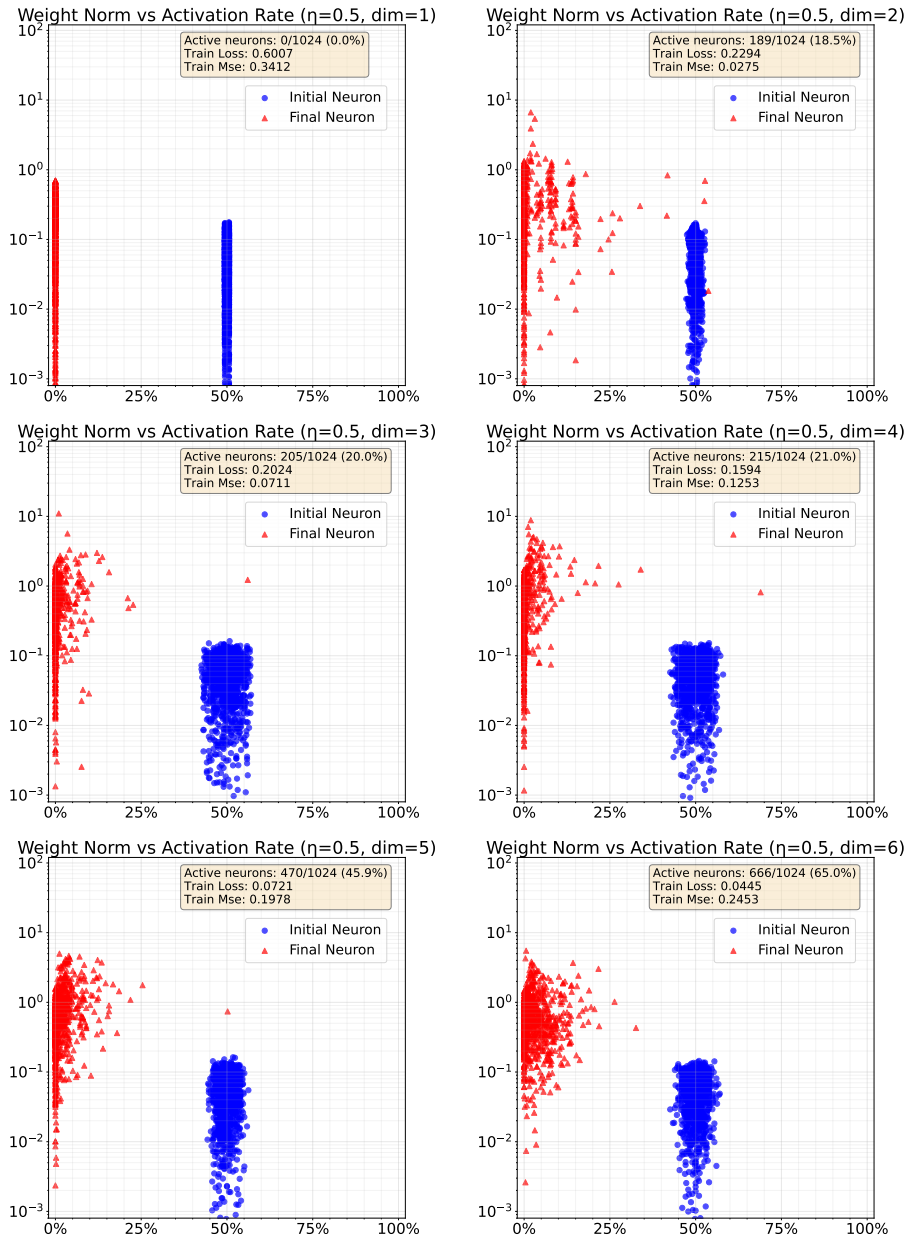


Figure 4: Comparison across input dimension d for a two-layer ReLU network of width 1024 trained on 512 samples for 20000 epochs with learning rate $\eta = 0.5$. At $d = 1$, all neurons extrapolate (0% active), while as d increases the fraction of neurons surviving training rises dramatically (up to 65% at $d = 6$). Simultaneously, the training loss monotonically decreases whereas the training MSE increases with d , demonstrating that neural shattering under large learning rates may be the key driver of the curse of dimensionality in stable minima.

A.2 Neural Shattering and Learning Rate (dim=5)

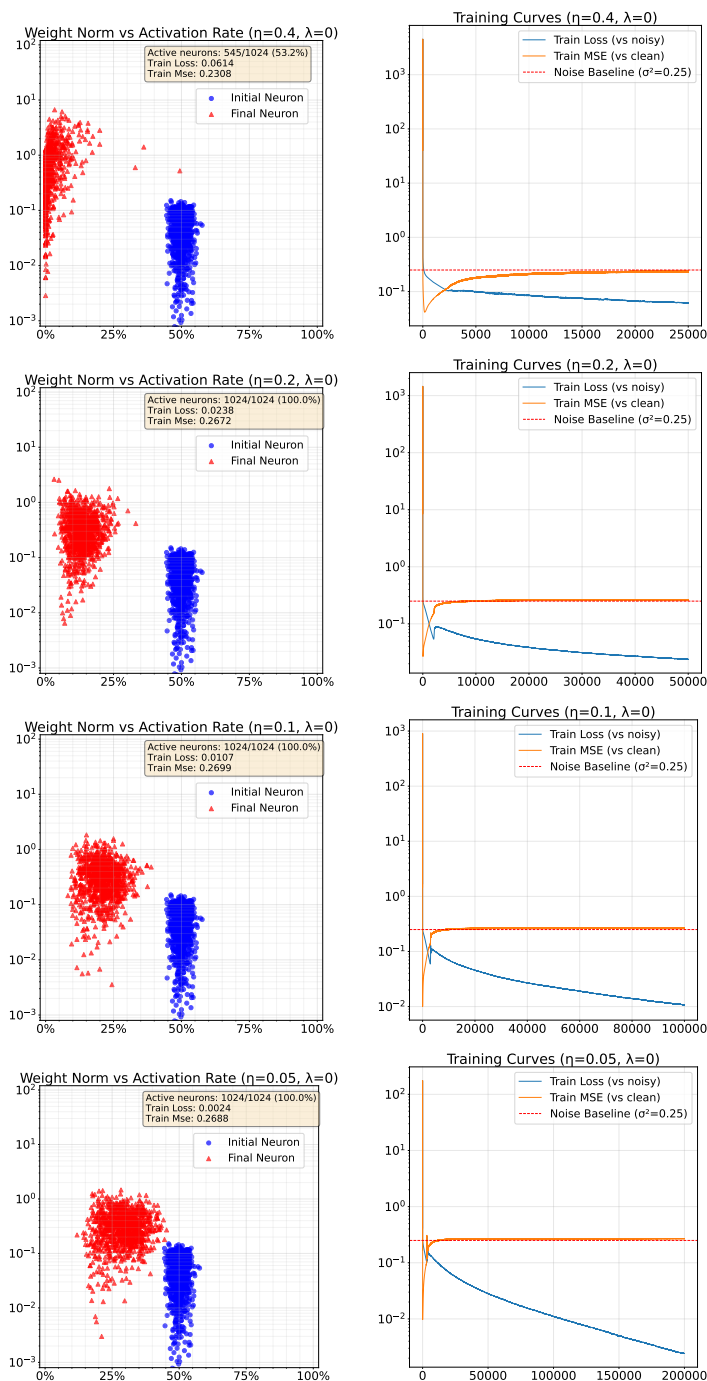


Figure 5: Effect of increasing learning rate η on shattering ($\eta \times \text{epochs} = 10000$): as η grows, the stability/flatness constraint forces an ever larger fraction of neurons to activate only on a small subset of the data (neural shattering). To further decrease the training loss, gradient descent correspondingly increases the weight norms of the remaining active neurons.

A.3 Empirical Analysis of the Curse of Dimensionality (I)

We conduct the following experiments in the setting where the ground-truth function is linear with Gaussian noise $\sigma^2 = 1$. The width of neural network is 4 times of the number of samples.

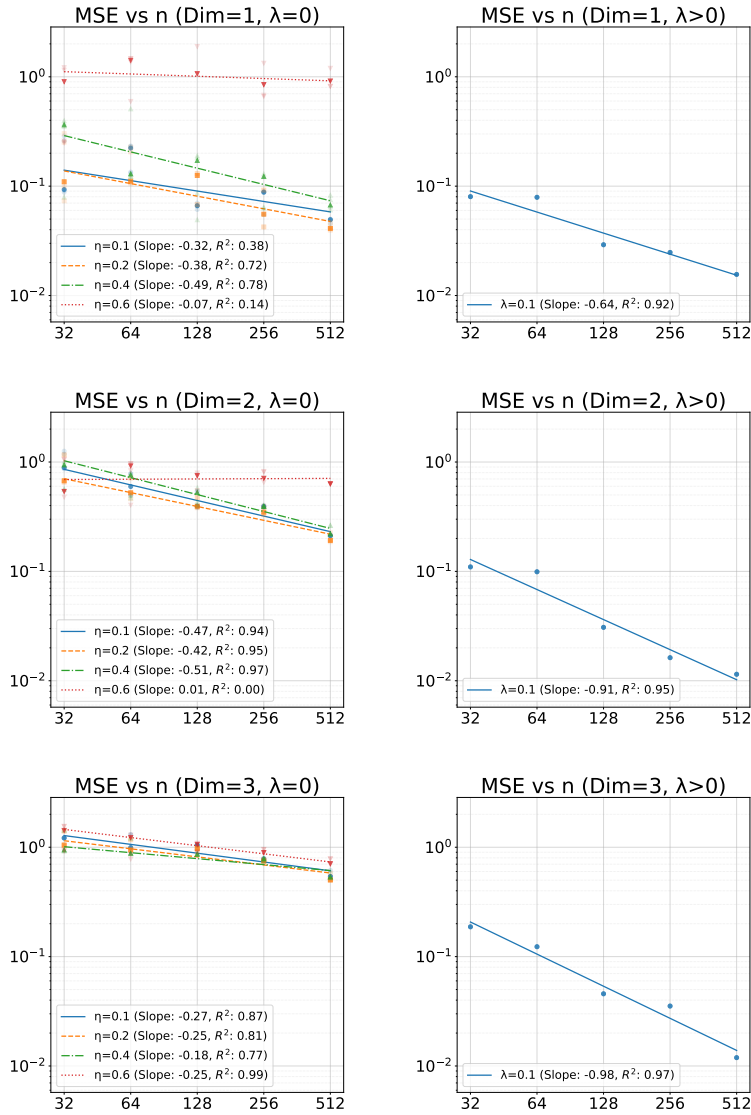


Figure 6: Log-log plots of the mean squared error (MSE) versus sample size n (Part I). Each curve is regressed by the median result over five random initializations (lighter markers), while the shallow markers denote the other runs. As the input dimension increases, the slope of the fitted regression line becomes progressively shallower, indicating slower error decay.

A.4 Empirical Analysis of the Curse of Dimensionality (II)

We conduct the following experiments in the setting where the ground-truth function is linear with Gaussian noise $\sigma^2 = 0.25$. The width of neural network is 2 times of the number of samples.

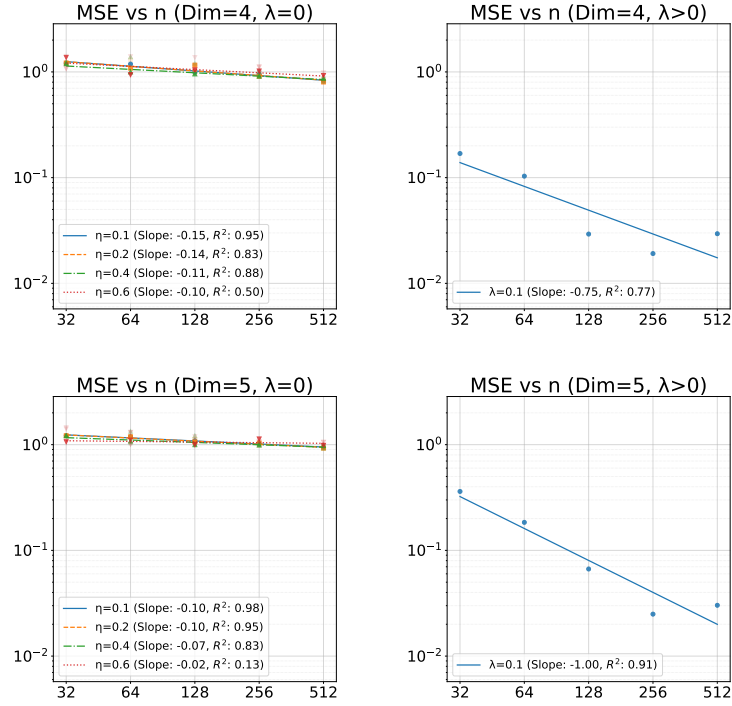


Figure 7: Log-log plots of the mean squared error (MSE) versus sample size n , illustrating the curse of dimensionality in stable minima (Part II). We can see in dimension 5, the slope is almost flat and even the large-step size cannot save the results (even worse than small step-size).

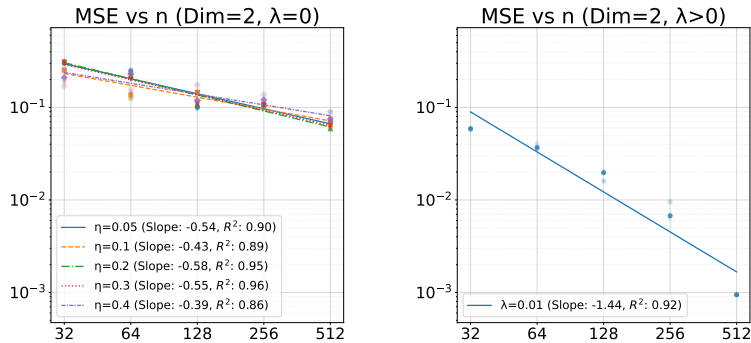


Figure 8: Log-log plots of the mean squared error (MSE) versus sample size n (Part III). Compared to the previous experiments, this setup reduces the noise level to $\sigma = 0.5$, applies weight decay $\lambda = 0.01$, and constrains the model width to $2n$.

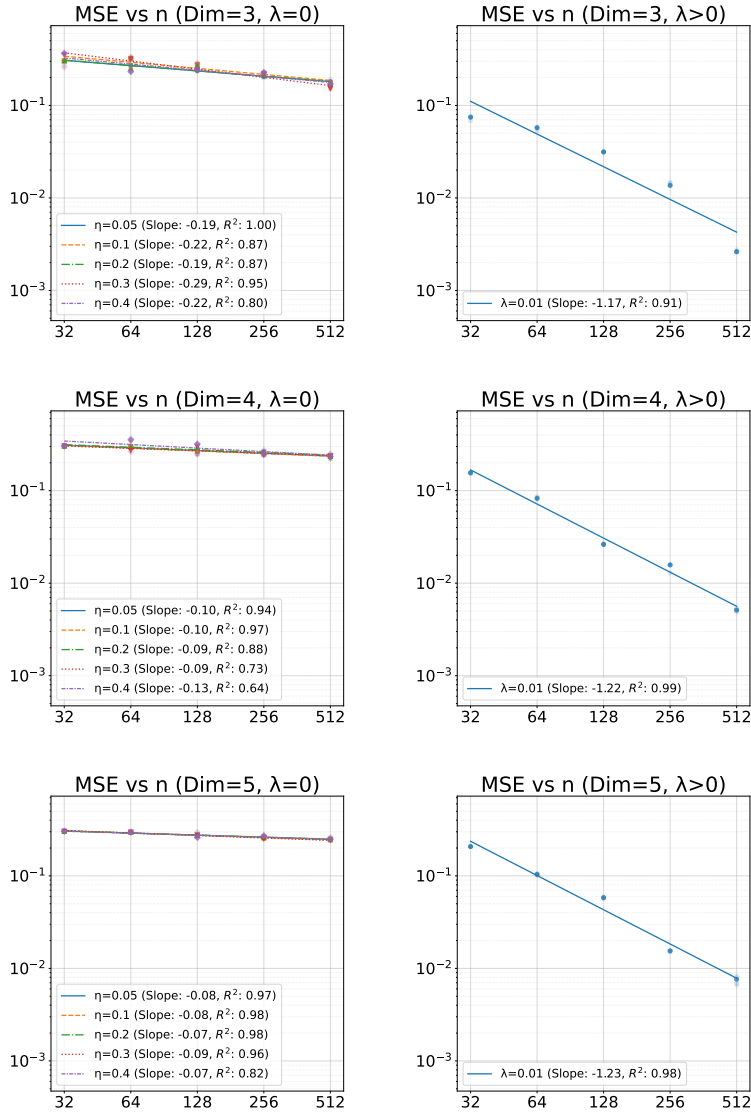


Figure 9: Log-log plots of the mean squared error (MSE) versus sample size n (Part IV). The log-log MSE vs. n curves still exhibit progressively flattening slopes as the input dimension grows, demonstrating the enduring curse of dimensionality in stable minima.

B Overview of the Proofs

In this section, we provide an overview for the proofs of the claims in the paper. The full proofs are deferred to later appendices. We introduce the following notations we use in our proofs and their overviews.

- Let $\varphi(\varepsilon)$ and $\psi(\varepsilon)$ be two functions in variable of ε . For constants $a, b \in \mathbb{R}$ (independent of ε), the notation

$$\varphi(\varepsilon) \stackrel{a}{\asymp} \psi(\varepsilon)$$

means that $\varphi(\varepsilon) \leq a\psi(\varepsilon)$ and $b\psi(\varepsilon) \leq \varphi(\varepsilon)$. We may directly use the notation \asymp if the constants are hidden (we may use the simplified version when the constants are justified).

- $f(x) = O(g(x))$ means there exist constants $c > 0$ and $x_0 > 0$ such that

$$0 \leq f(x) \leq cg(x), \quad \forall x \geq x_0.$$

Intuitively, for sufficiently large x , $f(x)$ grows at most as fast as $g(x)$, up to a constant factor. We may also use $f(x) \lesssim g(x)$.

- $f(x) = \Omega(g(x))$ means there exist constants $c' > 0$ and $x_1 > 0$ such that

$$0 \leq c'g(x) \leq f(x), \quad \forall x \geq x_1.$$

Intuitively, for sufficiently large x , $f(x)$ grows at least as fast as $g(x)$, up to a constant factor.

- $f(x) = \Theta(g(x))$ means there exist constants $c_1, c_2 > 0$ and $x_2 > 0$ such that

$$0 \leq c_1g(x) \leq f(x) \leq c_2g(x), \quad \forall x \geq x_2.$$

Equivalently,

$$f(x) = \Theta(g(x)) \iff [f(x) = O(g(x))] \text{ and } [f(x) = \Omega(g(x))].$$

Intuitively, for sufficiently large x , $f(x)$ grows at the same rate as $g(x)$, up to constant factors.

B.1 Proof Overview of Theorem 3.2.

We consider the neural network of the form:

$$f_{\boldsymbol{\theta}}(\mathbf{x}) = \sum_{k=1}^K v_k \phi(\mathbf{w}_k^\top \mathbf{x} - b_k) + \beta. \quad (12)$$

The Hessian matrix of the loss function, obtained through direct computation, is expressed as:

$$\nabla_{\boldsymbol{\theta}}^2 \mathcal{L}(\boldsymbol{\theta}) = \frac{1}{n} \sum_{i=1}^n (\nabla_{\boldsymbol{\theta}} f_{\boldsymbol{\theta}}(\mathbf{x}_i)) (\nabla_{\boldsymbol{\theta}} f_{\boldsymbol{\theta}}(\mathbf{x}_i))^\top + \frac{1}{n} \sum_{i=1}^n (f_{\boldsymbol{\theta}}(\mathbf{x}_i) - y_n) \nabla_{\boldsymbol{\theta}}^2 f_{\boldsymbol{\theta}}(\mathbf{x}_i). \quad (13)$$

Consider \mathbf{v} to be the unit eigenvector (i.e., $\|\mathbf{v}\|_2 = 1$) corresponding to the largest eigenvalue of the matrix $\frac{1}{n} \sum_{i=1}^n (\nabla_{\boldsymbol{\theta}} f_{\boldsymbol{\theta}}(\mathbf{x}_i)) (\nabla_{\boldsymbol{\theta}} f_{\boldsymbol{\theta}}(\mathbf{x}_i))^\top$. Consequently, the maximum eigenvalue of the Hessian of

the loss can be lower-bounded as follows:

$$\begin{aligned}
\lambda_{\max}(\nabla_{\theta}^2 \mathcal{L}(\theta)) &\geq \mathbf{v}^\top \nabla_{\theta}^2 \mathcal{L}(\theta) \mathbf{v} \\
&= \lambda_{\max} \left(\underbrace{\frac{1}{n} \sum_{i=1}^n (\nabla_{\theta} f_{\theta}(\mathbf{x}_i)) (\nabla_{\theta} f_{\theta}(\mathbf{x}_i))^\top}_{\text{(Term A)}} \right) \\
&\quad + \underbrace{\frac{1}{n} \sum_{i=1}^n (f_{\theta}(\mathbf{x}_i) - y_i) \mathbf{v}^\top \nabla_{\theta}^2 f_{\theta}(\mathbf{x}_i) \mathbf{v}}_{\text{(Term B)}}.
\end{aligned} \tag{14}$$

Regarding (Term A), its maximum eigenvalue at a given θ can be related to the V_g seminorm of the associated function $f = f_{\theta}$. Letting $\Omega = \mathbb{B}^d(\mathbf{0}, R)$, [Nacson et al. \[2023, Appendix F.2\]](#) demonstrate that:

$$\text{(Term A)} = \lambda_{\max} \left(\frac{1}{n} \sum_{i=1}^n (\nabla_{\theta} f_{\theta}(\mathbf{x}_i)) (\nabla_{\theta} f_{\theta}(\mathbf{x}_i))^\top \right) \geq 1 + 2 \sum_{k=1}^K |v_k| \|\mathbf{w}_k\|_2 \tilde{g}(\bar{\mathbf{w}}_k, \bar{b}_k), \tag{15}$$

where $\bar{\mathbf{w}}_k = \mathbf{w}_k / \|\mathbf{w}_k\|_2 \in \mathbb{S}^{d-1}$, $\bar{b}_k = b_k / \|\mathbf{w}_k\|_2$ and

$$\tilde{g}(\bar{\mathbf{w}}, \bar{b}) = \mathbb{P}(\mathbf{X}^\top \bar{\mathbf{w}} > \bar{b})^2 \cdot \mathbb{E}[\mathbf{X}^\top \bar{\mathbf{w}} - \bar{b} \mid \mathbf{X}^\top \bar{\mathbf{w}} > \bar{b}] \cdot \sqrt{1 + \|\mathbb{E}[\mathbf{X} \mid \mathbf{X}^\top \bar{\mathbf{w}} > \bar{b}]\|^2}. \tag{16}$$

For (Term B), an upper bound can be established using the training loss $\mathcal{L}(\theta)$ via the Cauchy-Schwarz inequality. This also employs a notable uniform upper bound for $\mathbf{v}^\top \nabla_{\theta}^2 f_{\theta}(\mathbf{x}_n) \mathbf{v}$, as detailed in [Lemma C.1](#):

$$|\text{(Term B)}| \leq \sqrt{\frac{1}{n} \sum_{i=1}^n (f_{\theta}(\mathbf{x}_i) - y_i)^2} \cdot \sqrt{\frac{1}{n} \sum_{i=1}^n (\mathbf{v}^\top \nabla_{\theta}^2 f_{\theta}(\mathbf{x}_i) \mathbf{v})^2} \leq 2(R+1) \sqrt{2\mathcal{L}(\theta)}. \tag{17}$$

B.2 Proof Overview of Theorem 3.5

This proof establishes an upper bound on the generalization gap for stable minima in $\mathcal{F}_{\text{stable}}(\eta)$. The strategy leverages the structural properties of these solutions, which are captured by a data-dependent weighted variation norm.

First, we recall from [Corollary 3.3](#) that any stable solution f_{θ} has a bounded norm, $|f_{\theta}|_{V_g} \leq A$. The weight function g is determined by the training data. This data-dependent nature is central to our analysis. To bound the generalization gap, we must translate the constraint on the weighted norm $|f|_{V_g}$ into a bound on the standard, unweighted norm $|f|_V$. This is possible only in regions where the weight function g is bounded away from zero. This naturally suggests a decomposition of the input domain into two parts: a “well-behaved” region where g has a positive lower bound, and the remaining region where g may be arbitrarily close to zero.

To facilitate a tractable analysis, we introduce the deterministic population weight function g_P as a reference. We then bridge the two using empirical process theory. As established in [Appendix E.2](#) ([Theorem E.5](#)), the uniform deviation between g and its population counterpart is bounded by a statistical error term $\epsilon_n = \tilde{O}(\sqrt{d/n})$ with high probability. This allows us to leverage the well-behaved properties of g_P to characterize the behavior of the empirical function g .

For inputs from $\text{Uniform}(\mathbb{B}_1^d)$, this population function behaves like $(1 - |t|)^{d+2}$ (see [Appendix E](#)), where $|t|$ is the distance of a neuron’s activation boundary from the origin. This behavior motivates

a specific geometric decomposition: an inner core $\mathbb{B}_{1-\varepsilon}^d$ (where $|t| < 1 - \varepsilon$) and an outer annulus \mathbb{A}_ε^d .

For the inner core $\mathbb{B}_{1-\varepsilon}^d$, the key step is to translate the bound on $|f|_{V_g}$ to a bound on the standard (unweighted) norm $|f|_V$. To do this, we need a lower bound on the empirical weight g within the core. Using g_P as our analytical proxy, we establish that $g_{\min} \geq g_{P,\min} - \varepsilon_n \approx \varepsilon^{d+2} - \varepsilon_n$. This step requires a validity condition: ε must be large enough such that the geometric term ε^{d+2} dominates the statistical error ε_n . With the unweighted norm now bounded, we utilize metric entropy arguments (e.g., Proposition F.4 and results from Parhi and Nowak [2023]) to bound the generalization error in the core that scales with $O\left(\varepsilon^{-\frac{d(d+2)}{2d+3}} n^{-\frac{d+3}{4d+6}}\right)$. In the annulus \mathbb{A}_ε^d , the contribution is small, scaling with $O(\varepsilon)$.

B.3 Proof Overview of Theorem 3.6

The proof for Theorem 3.6 establishes an upper bound on the mean squared error (MSE) for estimating a true function f_0 using a stable minimum f_θ . The overall strategy shares similarities with the proof of the generalization gap, particularly in its treatment of the data-dependent function class.

The argument begins by leveraging the property that a stable minimum $f_\theta \in \mathcal{F}_{\text{stable}}(\eta)$ has a bounded weighted variation norm $|f_\theta|_{V_g}$, where g is the empirical weight function. The theorem also assumes the ground truth f_0 lies in a similar space. A key condition is that f_θ is “optimized” such that its empirical loss is no worse than that of f_0 . This is crucial as it allows us to bound the empirical MSE primarily by an empirical process term involving the noise terms ε_i .

To bound this empirical process, the proof again decomposes the input domain \mathbb{B}_1^d into a strict interior ball $\mathbb{B}_{1-\varepsilon}^d$ and an annulus \mathbb{A}_ε^d . In the outer shell, the contribution to the MSE is controlled by the function’s L^∞ bound. For the strict interior $\mathbb{B}_{1-\varepsilon}^d$, we analyze the difference function $f_\Delta = f_\theta - f_0$. Consistent with our generalization analysis, we use the results from Appendix E.2 to ensure the empirical weight function g can be reliably analyzed via its population counterpart. This allows us to bound the unweighted variation norm of f_Δ over the core, which is then used to bound the empirical process via local Gaussian complexities (as detailed in Appendix G).

The bounds from the annulus and the core are then summed. The resulting expression for the total MSE is minimized by choosing an optimal ε . This balancing yields the final estimation error rate presented in Theorem 3.6, connecting the stability-induced regularity and the “optimized” nature of the solution to its statistical performance.

B.4 Proof Overview of Theorem 3.7

The proof establishes the minimax lower bound by constructing a packing set of functions within the specified function class $V_g(\mathbb{B}_1^d)$ and then applying Fano’s Lemma. The construction differs for multivariate ($d > 1$) and univariate ($d = 1$) cases.

Multivariate Case ($d > 1$) The core idea is to use highly localized ReLU atoms that have a small V_g norm due to the weighting $g(\mathbf{u}, t)$ vanishing near the boundary ($|t| \rightarrow 1$), yet can be combined to form a sufficiently rich and separated set of functions.

1. **Atom Construction:** We utilize ReLU atoms $\Phi_{\mathbf{u}, \varepsilon^2}(\mathbf{x}) = \varepsilon^{-2} \phi(\mathbf{u}^\top \mathbf{x} - (1 - \varepsilon^2))$ as defined in Construction H.5 (see Eq. (105) for the unnormalized version). These atoms are L^∞ -normalized, have an $L^2(\mathbb{B}_1^d)$ -norm $\|\Phi_{\mathbf{u}, \varepsilon^2}\|_{L^2} \asymp \varepsilon^{\frac{d+1}{2}}$ (Lemma H.2), and a weighted variation norm $|\Phi_{\mathbf{u}, \varepsilon^2}|_{V_g} = \varepsilon^{2d+2}$ (Lemma H.3, Eq. (116)). The small V_g norm is crucial.

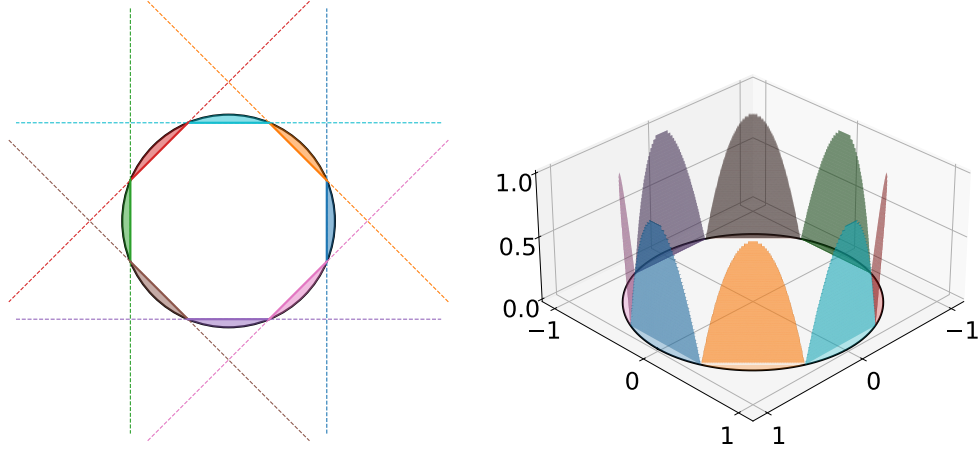


Figure 10: The ReLU atoms only activate on the localized spherical cap and with $L^\infty(\mathbb{B}_1^d)$ -norm equal to 1. As dimension increases, more data points will concentrate on the boundary region and the choice of directions increase exponentially.

2. **Packing Set:** Using a packing of $K \asymp \varepsilon^{-(d-1)}$ disjoint spherical caps on \mathbb{S}^{d-1} (Lemma H.4), we construct a family of functions $f_\xi(\mathbf{x}) = \sum_{i=1}^K \xi_i \Phi_{\mathbf{u}_i, \varepsilon^2}(\mathbf{x})$ for $\xi \in \{-1, 1\}^K$. By Varshamov-Gilbert lemma (Lemma J.2), we can find a subset $\Xi \subset \{-1, 1\}^K$ such that $\log |\Xi| \asymp K \asymp \varepsilon^{-(d-1)}$ and for any distinct $f_\xi, f_{\xi'} \in \{f_\zeta\}_{\zeta \in \Xi}$, their L^2 -distance is $\|f_\xi - f_{\xi'}\|_{L^2} \gtrsim \varepsilon$. The total variation norm $|f_\xi|_{V_g} \leq K \varepsilon^{2d+2} \asymp \varepsilon^{d+3}$, which is significantly smaller than 1 when $\varepsilon < 1$.
3. **Leveraging Fano's Lemma:** (Proposition H.6) The KL divergence between distributions induced by f_ξ and $f_{\xi'}$ is $\text{KL}(P_\xi \| P_{\xi'}) \asymp n \varepsilon^2 / \sigma^2$. To apply Fano's Lemma (see Lemma J.1), we need to satisfy the condition (140) that $n \varepsilon^2 / \sigma^2 \lesssim \log |\Xi| \asymp \varepsilon^{-(d-1)}$, which implies $\varepsilon \asymp (\sigma^2 / n)^{\frac{1}{d+1}}$ and the minimax risk is then given by $\mathbb{E} \|\hat{f} - f\|_{L^2}^2 \gtrsim \varepsilon^2 \asymp (\sigma^2 / n)^{\frac{2}{d+1}}$.

Univariate Case ($d = 1$) The high-dimensional spherical cap packing is not applicable. Instead, we use scaled bump functions and exploit the simplified 1D V_g norm.

1. **Function Class:** For $d = 1$, if we assume f is smooth, then $|f|_{V_g} = \|f'' \cdot g\|_{\mathcal{M}} = \int_{-1}^1 |f''(x)|(1 - |x|)^3 dx$ (from Theorem 3.4 and leading to the class in Eq. (120)).
2. **Atom Construction:** We construct functions $\Phi_k(x)$ as smooth bump functions, each supported on a distinct interval of width ε^2 near the boundary (e.g., $x \in [1 - \varepsilon + (k-1)\varepsilon^2, 1 - \varepsilon + k\varepsilon^2]$). These are scaled such that $\|\Phi_k\|_{L^2} \asymp \varepsilon$. Due to the $(1 - |x|)^3 \lesssim \varepsilon^3$ factor in the V_g norm and $\int_{-1}^1 |\Phi_k''(x)| dx \asymp 1/\varepsilon^2$, the weighted variation is $|\Phi_k|_{V_g} \asymp \varepsilon^3 \cdot (1/\varepsilon^2) = \varepsilon$.
3. **Packing Set:** A family $f_\xi(x) = \sum_{k=1}^K \xi_k \Phi_k(x)$ is formed with $K \asymp 1/\varepsilon$ terms. Using Varshamov-Gilbert (Lemma J.2), we find a subset Ξ with $\log |\Xi| \asymp K \asymp 1/\varepsilon$ such that for distinct $f_\xi, f_{\xi'}$, the L^2 -distance is $\|f_\xi - f_{\xi'}\|_{L^2} \gtrsim \sqrt{K} \varepsilon \asymp \sqrt{1/\varepsilon} \cdot \varepsilon = \sqrt{\varepsilon}$.
4. **Leveraging Fano's Lemma:** The KL divergence is $\text{KL}(P_\xi \| P_{\xi'}) \asymp n(\sqrt{\varepsilon})^2 / \sigma^2 = n\varepsilon / \sigma^2$. Fano's condition (140) $n\varepsilon / \sigma^2 \lesssim \log |\Xi| \asymp 1/\varepsilon$ implies $\varepsilon \asymp (\sigma^2 / n)^{1/2}$. The minimax risk is then $\mathbb{E} \|\hat{f} - f\|_{L^2}^2 \gtrsim (\sqrt{\varepsilon})^2 = \varepsilon \asymp (\sigma^2 / n)^{1/2}$.

B.5 Discussion of the Proofs

A notable feature in the proofs for the generalization gap upper bound (Theorem 3.5) and the MSE upper bound (Theorem 3.6) is the strategy of decomposing the domain \mathbb{B}_1^d into an inner core $\mathbb{B}_{1-\varepsilon}^d$ and an annulus \mathbb{A}_ε^d . This decomposition, involving a trade-off by treating the boundary region differently, is not merely a technical convenience but is fundamentally motivated by the characteristics of the function class $V_g(\mathbb{B}_1^d)$ and the nature of “hard-to-learn” functions within it.

The necessity for this approach is starkly illustrated by our minimax lower bound construction in Theorem 3.7 (see Appendix H for construction details) and Lemma I.1. The hard-to-learn functions used to establish this lower bound are specifically constructed using ReLU neurons that activate *only* near the boundary of the unit ball (i.e., for \mathbf{x} such that $\mathbf{u}^\top \mathbf{x} \approx 1$). The crucial insight here is the behavior of the weight function $g(\mathbf{u}, t) \asymp (1 - |t|)^{d+2}$ (see Appendix E). For these boundary-activating neurons, $|t|$ is close to 1, making $g(\mathbf{u}, t)$ exceptionally small. This allows for functions that are potentially complex or have large unweighted magnitudes near the boundary (the annulus) to still possess a small weighted variation norm $|f|_{V_g}$, thus qualifying them as members of the function class under consideration. Our lower bound construction focuses almost exclusively on these boundary phenomena, as they represent the primary source of difficulty for estimation within this specific weighted variation space.

The upper bound proofs implicitly acknowledge this. By isolating the annulus \mathbb{A}_ε^d , the analysis effectively concedes that this region might harbor complex behavior. The error contribution from this annulus is typically bounded by simpler means, often proportional to its small volume (controlled by ε) and the L^∞ norm of the functions. The more sophisticated analysis, involving metric entropy or Gaussian complexity arguments (which depend on an *unweighted* variation norm that becomes large as $|f|_{V_g}/\varepsilon^{d+2}$ when restricted to the strict interior $\mathbb{B}_{1-\varepsilon}^d$), is applied to the “better-behaved” interior region. The parameter ε is then chosen optimally to balance the error from the boundary (which increases with ε) against the error from the interior (where the complexity term effectively increases as ε shrinks).

This methodological alignment between our upper and lower bounds underscores a self-consistency in our analysis. Both components of the argument effectively exploit the geometric properties stemming from the uniform data distribution on a sphere and the specific decay characteristics of the data-dependent weight function g near the boundary. The strategy of “sacrificing the boundary” in the upper bounds is thus a direct and necessary consequence of where the challenging functions identified by the lower bound constructions.

C Proof of Theorem 3.2: Stable Minima Regularity

In this section, we prove the regularity constraint of stable minima. We begin by upper bounding the operator norm of the Hessian matrix. In other words, we upper bound $|\mathbf{v}^\top \nabla_{\theta}^2 f_{\theta}(\mathbf{x}) \mathbf{v}|$ under the constraint that $\|\mathbf{v}\|_2 = 1$.

Lemma C.1. *Assume $f_{\theta}(\mathbf{x}) = \sum_{k=1}^K v_k \phi(\mathbf{w}_k^\top \mathbf{x} + b_k) + \beta$ is a two-layer ReLU network with input $\mathbf{x} \in \mathbb{R}^d$ such that $\|\mathbf{x}\|_2 \leq R$. Let θ represent all parameters $\{\mathbf{w}_k, b_k, v_k, \beta\}_{k=1}^K$. Assume $f_{\theta}(\mathbf{x})$ is twice differentiable with respect to θ at \mathbf{x} . Then for any vector \mathbf{v} corresponding to a perturbation in θ such that $\|\mathbf{v}\|_2 = 1$, it holds that:*

$$|\mathbf{v}^\top \nabla_{\theta}^2 f_{\theta}(\mathbf{x}) \mathbf{v}| \leq 2(R + 1). \quad (18)$$

Proof. Let the parameters be $\theta = (\mathbf{w}_1^\top, \dots, \mathbf{w}_K^\top, b_1, \dots, b_K, v_1, \dots, v_K, \beta)^\top$. The total number of parameters is $N = K \times d + K + K + 1 = K(d + 2) + 1$. Let the corresponding perturbation vector be

$\mathbf{v} \in \mathbb{R}^N$, structured as: $\mathbf{v} = (\boldsymbol{\alpha}_1^\top, \dots, \boldsymbol{\alpha}_K^\top, \delta_1, \dots, \delta_K, \gamma_1, \dots, \gamma_K, \iota)^\top$, where $\boldsymbol{\alpha}_k \in \mathbb{R}^d$ corresponds to \mathbf{w}_k , $\delta_k \in \mathbb{R}$ corresponds to b_k , $\gamma_k \in \mathbb{R}$ corresponds to v_k , and $\iota \in \mathbb{R}$ corresponds to β . The normalization constraint is

$$\|\mathbf{v}\|_2^2 = \sum_{k=1}^K \|\boldsymbol{\alpha}_k\|_2^2 + \sum_{k=1}^K \delta_k^2 + \sum_{k=1}^K \gamma_k^2 + \iota^2 = 1 \quad (19)$$

We need to compute the Hessian matrix $\nabla_{\boldsymbol{\theta}}^2 f_{\boldsymbol{\theta}}(\mathbf{x})$. Let $z_k = \mathbf{w}_k^\top \mathbf{x} + b_k$ and $1_k = 1(z_k > 0)$. Since we assume twice differentiability, $z_k \neq 0$ for all k , the Hessian $\nabla_{\boldsymbol{\theta}}^2 f_{\boldsymbol{\theta}}(\mathbf{x})$ is block diagonal, with K blocks corresponding to each neuron. The k -th block, $\nabla_{(\boldsymbol{\theta}_k)}^2 f_{\boldsymbol{\theta}}(\mathbf{x})$, involves derivatives with respect to $\boldsymbol{\theta}_k = (\mathbf{w}_k^\top, b_k, v_k)^\top$. The relevant non-zero second partial derivatives defining this block are:

- $\frac{\partial^2 f_{\boldsymbol{\theta}}}{\partial \mathbf{w}_k \partial v_k} = \frac{\partial}{\partial v_k} (\nabla_{\mathbf{w}_k} f_{\boldsymbol{\theta}}) = \frac{\partial}{\partial v_k} (v_k \phi'(z_k) \mathbf{x}) = \phi'(z_k) \mathbf{x} = 1_k \mathbf{x}$
- $\frac{\partial^2 f_{\boldsymbol{\theta}}}{\partial b_k \partial v_k} = \frac{\partial}{\partial v_k} \left(\frac{\partial f_{\boldsymbol{\theta}}}{\partial b_k} \right) = \frac{\partial}{\partial v_k} (v_k \phi'(z_k)) = \phi'(z_k) = 1_k$

All other second derivatives within the block are zero, as are derivatives between different blocks or involving β . The k -th block of the Hessian is thus:

$$\nabla_{(\boldsymbol{\theta}_k)}^2 f_{\boldsymbol{\theta}}(\mathbf{x}) = \begin{pmatrix} \frac{\partial^2 f_{\boldsymbol{\theta}}}{(\partial \mathbf{w}_k)^2} & \frac{\partial^2 f_{\boldsymbol{\theta}}}{\partial \mathbf{w}_k \partial b_k} & \frac{\partial^2 f_{\boldsymbol{\theta}}}{\partial \mathbf{w}_k \partial v_k} \\ \frac{\partial^2 f_{\boldsymbol{\theta}}}{\partial b_k \partial \mathbf{w}_k} & \frac{\partial^2 f_{\boldsymbol{\theta}}}{(\partial b_k)^2} & \frac{\partial^2 f_{\boldsymbol{\theta}}}{\partial b_k \partial v_k} \\ \frac{\partial^2 f_{\boldsymbol{\theta}}}{\partial v_k \partial \mathbf{w}_k} & \frac{\partial^2 f_{\boldsymbol{\theta}}}{\partial v_k \partial b_k} & \frac{\partial^2 f_{\boldsymbol{\theta}}}{(\partial v_k)^2} \end{pmatrix} = \begin{pmatrix} \mathbf{0}_{d \times d} & \mathbf{0}_d & 1_k \mathbf{x} \\ \mathbf{0}_d^\top & 0 & 1_k \\ 1_k \mathbf{x}^\top & 1_k & 0 \end{pmatrix} \quad (20)$$

where $\mathbf{0}_{d \times d}$ is the $d \times d$ zero matrix and $\mathbf{0}_d$ is the d -dimensional zero vector.

The quadratic form $\mathbf{v}^\top \nabla_{\boldsymbol{\theta}}^2 f_{\boldsymbol{\theta}}(\mathbf{x}) \mathbf{v}$ becomes:

$$\begin{aligned} \mathbf{v}^\top \nabla_{\boldsymbol{\theta}}^2 f_{\boldsymbol{\theta}}(\mathbf{x}) \mathbf{v} &= \sum_{k=1}^K \begin{pmatrix} \boldsymbol{\alpha}_k^\top & \delta_k & \gamma_k \end{pmatrix} \begin{pmatrix} \mathbf{0}_{d \times d} & \mathbf{0}_d & 1_k \mathbf{x} \\ \mathbf{0}_d^\top & 0 & 1_k \\ 1_k \mathbf{x}^\top & 1_k & 0 \end{pmatrix} \begin{pmatrix} \boldsymbol{\alpha}_k \\ \delta_k \\ \gamma_k \end{pmatrix} \\ &= \sum_{k=1}^K \left(\boldsymbol{\alpha}_k^\top (1_k \mathbf{x}) \gamma_k + \delta_k (1_k) \gamma_k + \gamma_k (1_k \mathbf{x}^\top) \boldsymbol{\alpha}_k + \gamma_k (1_k) \delta_k \right) \\ &= \sum_{k=1}^K 2 \cdot 1_k \cdot \gamma_k (\boldsymbol{\alpha}_k^\top \mathbf{x} + \delta_k) \end{aligned} \quad (21)$$

Now, we bound the absolute value:

$$\begin{aligned} |\mathbf{v}^\top \nabla_{\boldsymbol{\theta}}^2 f_{\boldsymbol{\theta}}(\mathbf{x}) \mathbf{v}| &= \left| \sum_{k=1}^K 2 \cdot 1_k \cdot \gamma_k (\boldsymbol{\alpha}_k^\top \mathbf{x} + \delta_k) \right| \leq \sum_{k=1}^K 2 \cdot 1_k \cdot |\gamma_k| |\boldsymbol{\alpha}_k^\top \mathbf{x} + \delta_k| \\ &\leq \sum_{k=1}^K 2 |\gamma_k| (|\boldsymbol{\alpha}_k^\top \mathbf{x}| + |\delta_k|) \leq \sum_{k=1}^K 2 |\gamma_k| (\|\boldsymbol{\alpha}_k\|_2 \|\mathbf{x}\|_2 + |\delta_k|) \quad (\text{Cauchy-Schwarz}) \\ &= 2R \sum_{k=1}^K |\gamma_k| \|\boldsymbol{\alpha}_k\|_2 + 2 \sum_{k=1}^K |\gamma_k| |\delta_k| \\ &\leq 2R \sqrt{\sum_{k=1}^K \gamma_k^2} \sqrt{\sum_{k=1}^K \|\boldsymbol{\alpha}_k\|_2^2} + 2 \sqrt{\sum_{k=1}^K \gamma_k^2} \sqrt{\sum_{k=1}^K \delta_k^2} \quad (\text{Cauchy-Schwarz on sums}) \\ &\leq 2R \sqrt{\sum_{k=1}^K \gamma_k^2} \cdot \sqrt{1} + 2 \sqrt{\sum_{k=1}^K \gamma_k^2} \cdot \sqrt{1} \end{aligned}$$

$$= 2(R+1)\sqrt{\sum_{k=1}^K \gamma_k^2} \leq 2(R+1).$$

□

Now we are ready to prove Theorem 3.2.

Proof of Theorem 3.2. Without loss of generality, we consider neural networks of the following form:

$$f_{\boldsymbol{\theta}}(\mathbf{x}) = \sum_{k=1}^K v_k \phi(\mathbf{w}_k^\top \mathbf{x} - b_k) + \beta. \quad (22)$$

The Hessian matrix of the loss function, obtained through direct computation, is expressed as:

$$\nabla_{\boldsymbol{\theta}}^2 \mathcal{L}(\boldsymbol{\theta}) = \frac{1}{n} \sum_{i=1}^n (\nabla_{\boldsymbol{\theta}} f_{\boldsymbol{\theta}}(\mathbf{x}_i)) (\nabla_{\boldsymbol{\theta}} f_{\boldsymbol{\theta}}(\mathbf{x}_i))^\top + \frac{1}{n} \sum_{i=1}^n (f_{\boldsymbol{\theta}}(\mathbf{x}_i) - y_i) \nabla_{\boldsymbol{\theta}}^2 f_{\boldsymbol{\theta}}(\mathbf{x}_i). \quad (23)$$

Let \mathbf{v} be the unit eigenvector (i.e., $\|\mathbf{v}\|_2 = 1$) corresponding to the largest eigenvalue of the matrix $\frac{1}{n} \sum_{i=1}^n (\nabla_{\boldsymbol{\theta}} f_{\boldsymbol{\theta}}(\mathbf{x}_i)) (\nabla_{\boldsymbol{\theta}} f_{\boldsymbol{\theta}}(\mathbf{x}_i))^\top$, the maximum eigenvalue of the Hessian matrix of the loss can be lower-bounded as follows:

$$\begin{aligned} \lambda_{\max}(\nabla_{\boldsymbol{\theta}}^2 \mathcal{L}(\boldsymbol{\theta})) &\geq \mathbf{v}^\top \nabla_{\boldsymbol{\theta}}^2 \mathcal{L}(\boldsymbol{\theta}) \mathbf{v} \\ &= \underbrace{\lambda_{\max} \left(\frac{1}{n} \sum_{i=1}^n (\nabla_{\boldsymbol{\theta}} f_{\boldsymbol{\theta}}(\mathbf{x}_i)) (\nabla_{\boldsymbol{\theta}} f_{\boldsymbol{\theta}}(\mathbf{x}_i))^\top \right)}_{\text{(Term A)}} \\ &\quad + \underbrace{\frac{1}{n} \sum_{i=1}^n (f_{\boldsymbol{\theta}}(\mathbf{x}_i) - y_i) \mathbf{v}^\top \nabla_{\boldsymbol{\theta}}^2 f_{\boldsymbol{\theta}}(\mathbf{x}_i) \mathbf{v}}_{\text{(Term B)}}. \end{aligned} \quad (24)$$

Regarding (Term A), its maximum eigenvalue at a given $\boldsymbol{\theta}$ can be related to the V_g norm of the associated function $f = f_{\boldsymbol{\theta}}$. Considering the domain \mathbb{B}_R^d , [Nacson et al. \[2023, Appendix F.2\]](#) demonstrate that:

$$\text{(Term A)} = \lambda_{\max} \left(\frac{1}{n} \sum_{i=1}^n (\nabla_{\boldsymbol{\theta}} f_{\boldsymbol{\theta}}(\mathbf{x}_i)) (\nabla_{\boldsymbol{\theta}} f_{\boldsymbol{\theta}}(\mathbf{x}_i))^\top \right) \geq 1 + 2 \sum_{k=1}^K |v_k| \|\mathbf{w}_k\|_2 \tilde{g}(\bar{\mathbf{w}}_k, \bar{b}_k), \quad (25)$$

where $\bar{\mathbf{w}}_k = \mathbf{w}_k / \|\mathbf{w}_k\|_2 \in \mathbb{S}^{d-1}$, $\bar{b}_k = b_k / \|\mathbf{w}_k\|_2$ and

$$\tilde{g}(\bar{\mathbf{w}}, \bar{b}) = \mathbb{P}(\mathbf{X}^\top \bar{\mathbf{w}} > \bar{b})^2 \cdot \mathbb{E}[\mathbf{X}^\top \bar{\mathbf{w}} - \bar{b} \mid \mathbf{X}^\top \bar{\mathbf{w}} > \bar{b}] \cdot \sqrt{1 + \|\mathbb{E}[\mathbf{X} \mid \mathbf{X}^\top \bar{\mathbf{w}} > \bar{b}]\|^2}. \quad (26)$$

For (Term B), an upper bound can be established using the training loss $\mathcal{L}(\boldsymbol{\theta})$ via the Cauchy-Schwarz inequality. This also employs a notable uniform upper bound for $|\mathbf{v}^\top \nabla_{\boldsymbol{\theta}}^2 f_{\boldsymbol{\theta}}(\mathbf{x}_n) \mathbf{v}|$, as detailed in Lemma C.1:

$$|(\text{Term B})| \leq \sqrt{\frac{1}{n} \sum_{i=1}^n (f_{\boldsymbol{\theta}}(\mathbf{x}_i) - y_i)^2} \cdot \sqrt{\frac{1}{n} \sum_{i=1}^n (\mathbf{v}^\top \nabla_{\boldsymbol{\theta}}^2 f_{\boldsymbol{\theta}}(\mathbf{x}_i) \mathbf{v})^2} \leq 2(R+1) \sqrt{2\mathcal{L}(\boldsymbol{\theta})}. \quad (27)$$

Finally, the proof of Theorem 3.2 is complete by plugging (25), (27) into (24). □

D Proof of Theorem 3.4: Radon-Domain Characterization of Stable Minima

In this part, we prove Theorem 3.4 by extending the unweighted case to the weighted one.

Proof of Theorem 3.4. In the unweighted scenario, i.e., $g \equiv 1$, it was established by Parhi and Nowak [2023, Lemma 2] that if $f \in \mathcal{V}(\mathbb{B}_R^d) := \mathcal{V}_1(\mathbb{B}_R^d)$ with integral representation

$$f(\mathbf{x}) = \int_{\mathbb{S}^{d-1} \times [-R, R]} \phi(\mathbf{u}^\top \mathbf{x} - t) d\nu(\mathbf{u}, t) + \mathbf{c}^\top \mathbf{x} + c_0, \quad \mathbf{x} \in \mathbb{B}_R^d, \quad (28)$$

where ν , \mathbf{c} , and c_0 solve (6) (with $g \equiv 1$) that

$$\nu = \mathcal{R}(-\Delta)^{\frac{d+1}{2}} f_{\text{ext}}, \quad (29)$$

where we recall that f_{ext} is the canonical extension of f from \mathbb{B}_R^d to \mathbb{R}^d via the formula (28) and $\nu \in \mathcal{M}(\mathbb{S}^{d-1} \times \mathbb{R})$ with $\text{supp } \nu = \mathbb{S}^{d-1} \times [-R, R]$ (i.e., we can identify ν with a measure in $\mathcal{M}(\mathbb{S}^{d-1} \times [-R, R])$). Since the weighted variation seminorm $|\cdot|_{\mathcal{V}_g}$ is simply (cf., (6))

$$|f|_{\mathcal{V}_g} = \inf_{\substack{\nu \in \mathcal{M}(\mathbb{S}^{d-1} \times [-R, R]) \\ \mathbf{c} \in \mathbb{R}^d, c_0 \in \mathbb{R}}} \|g \cdot \nu\|_{\mathcal{M}} \quad \text{s.t.} \quad f = f_{\nu, \mathbf{c}, c_0}, \quad (30)$$

we readily see that $|f|_{\mathcal{V}_g} = \|g \cdot \mathcal{R}(-\Delta)^{\frac{d+1}{2}} f_{\text{ext}}\|_{\mathcal{M}}$. \square

Remark D.1. The unweighted variation seminorm exactly corresponds to the second-order Radon-domain total variation of the function [Ongie et al., 2020, Parhi and Nowak, 2021, 2023]. Thus, the weighted variation seminorm is a weighted variant of the second-order Radon-domain total variation.

E Characterization of the Weight Function for the Uniform Distribution

Recall that, given a dataset $\mathcal{D} = \{(\mathbf{x}_i, y_i)\}_{i=1}^n \subset \mathbb{R}^d \times \mathbb{R}$, we consider a weight function $g : \mathbb{S}^{d-1} \times \mathbb{R} \rightarrow \mathbb{R}$, where $\mathbb{S}^{d-1} := \{\mathbf{u} \in \mathbb{R}^d : \|\mathbf{u}\| = 1\}$ denotes the unit sphere. This weight is defined by $g(\mathbf{u}, t) := \min\{\tilde{g}(\mathbf{u}, t), \tilde{g}(-\mathbf{u}, -t)\}$, where

$$\tilde{g}(\mathbf{u}, t) := \mathbb{P}(\mathbf{X}^\top \mathbf{u} > t)^2 \cdot \mathbb{E}[\mathbf{X}^\top \mathbf{u} - t \mid \mathbf{X}^\top \mathbf{u} > t] \cdot \sqrt{1 + \|\mathbb{E}[\mathbf{X} \mid \mathbf{X}^\top \mathbf{u} > t]\|^2}. \quad (31)$$

Here, \mathbf{X} is a random vector drawn uniformly at random from the training examples $\{\mathbf{x}_i\}_{i=1}^n$. Note that the distribution $\mathbb{P}_{\mathbf{X}}$ for which the $\{\mathbf{x}_i\}_{i=1}^n$ are drawn i.i.d. from controls the regularity of g .

In this section, We first analyze the properties of the population version g_P by assuming that the random vector \mathbf{X} is uniformly sampled from the d -dimensional unit ball $\mathbb{B}_1^d = \{\mathbf{x} \in \mathbb{R}^d : \|\mathbf{x}\|_2 \leq 1\}$. Then we analyze the gap between the empirical g and the population g_P using the empirical process.

E.1 The Computation of the Population Weight Function

We focus on the marginal distribution of a single coordinate and related conditional expectations. Let X_1 be the first coordinate of \mathbf{X} . Due to symmetry, all coordinates have the same marginal distribution.

The following proposition calculates the marginal probability density function of the first coordinate (and also other coordinates) of the random vector \mathbf{X} .

Proposition E.1 (Marginal PDF of a Coordinate). *Let \mathbf{X} follow the uniform distribution in \mathbb{B}_1^d . The probability density function (PDF) of its first coordinate X_1 is given by:*

$$f_{X_1}(t) = c_1(d) (1 - t^2)^\alpha, \quad t \in [-1, 1] \quad (32)$$

where $\alpha = \frac{d-1}{2}$ and the normalization constant is

$$c_1(d) = \frac{\Gamma(\frac{d}{2} + 1)}{\sqrt{\pi} \Gamma(\frac{d+1}{2})}. \quad (33)$$

Proof. The volume of the unit ball is $V_d = \frac{\pi^{d/2}}{\Gamma(d/2+1)}$. The uniform density is $f_{\mathbf{X}}(\mathbf{x}) = 1/V_d$ for $\mathbf{x} \in \mathbb{B}_1^d$. The marginal PDF is found by integrating out the other coordinates:

$$f_{X_1}(t) = \int_{\{\mathbf{x}' \in \mathbb{R}^{d-1} : \|\mathbf{x}'\|^2 \leq 1-t^2\}} \frac{1}{V_d} d\mathbf{x}' = \frac{\text{Vol}_{d-1}(\sqrt{1-t^2})}{V_d}$$

where $\text{Vol}_{d-1}(R)$ is the volume of a $(d-1)$ -ball of radius R . Using $V_{d-1} = \frac{\pi^{(d-1)/2}}{\Gamma((d-1)/2+1)} = \frac{\pi^{(d-1)/2}}{\Gamma((d+1)/2)}$, we get

$$f_{X_1}(t) = \frac{V_{d-1}(1-t^2)^{(d-1)/2}}{V_d} = \frac{\pi^{(d-1)/2}}{\Gamma((d+1)/2)} \frac{\Gamma(d/2+1)}{\pi^{d/2}} (1-t^2)^{(d-1)/2}$$

which simplifies to the stated result. For $d = 2$, $\alpha = 1/2$, $c_1(2) = \frac{\Gamma(2)}{\sqrt{\pi}\Gamma(3/2)} = \frac{1}{\sqrt{\pi}(\sqrt{\pi}/2)} = \frac{2}{\pi}$. For $d = 3$, $\alpha = 1$, $c_1(3) = \frac{\Gamma(5/2)}{\sqrt{\pi}\Gamma(2)} = \frac{3\sqrt{\pi}/4}{\sqrt{\pi}} = \frac{3}{4}$. \square

Given the marginal probability density function, the tail probability follows from direct calculation.

Proposition E.2 (Tail Probability). *Let \mathbf{X} be a random vector uniformly distributed in the d -dimensional unit ball $\mathbb{B}_1^d = \{\mathbf{x} \in \mathbb{R}^d : \|\mathbf{x}\|_2 \leq 1\}$. Let X_1 be its first coordinate whose tail probability is defined as $Q(x) = \mathbb{P}(X_1 > x)$ for $x \in [-1, 1]$. Then there exists a fixed $x_0 \in [0, 1]$ (specifically, we choose $x_0 = 3/4$, which implies $(1-x) \in (0, 1/4]$) such that for all $x \in [x_0, 1]$:*

$$Q(x) \underset{c_2(d)}{\overset{c_3(d)}{\asymp}} (1-x)^{\frac{d+1}{2}}.$$

Or equivalently,

$$c_2(d)(1-x)^{\frac{d+1}{2}} \leq Q(x) \leq c_3(d)(1-x)^{\frac{d+1}{2}},$$

where the constants $c_2(d)$ and $c_3(d)$ are given by:

$$c_2(d) = \frac{c_1(d)}{d+1} \left(\frac{7}{4}\right)^{\frac{d+1}{2}}$$

$$c_3(d) = \frac{c_1(d)}{d+1} 2^{\frac{d+2}{2}}$$

and $c_1(d) = \frac{\Gamma(\frac{d}{2}+1)}{\sqrt{\pi}\Gamma(\frac{d+1}{2})}$ is the normalization constant from the marginal PDF of X_1 .

Proof. The tail probability $Q(x)$ is given by the integral of the marginal PDF $f_{X_1}(t) = c_1(d)(1-t^2)^\alpha$ for $t \in [-1, 1]$, where $\alpha = \frac{d-1}{2}$.

$$Q(x) = \int_x^1 c_1(d)(1-t^2)^\alpha dt$$

Let $s = t^2$, so $dt = ds/(2\sqrt{s})$. The limits of integration for s become x^2 to 1.

$$Q(x) = c_1(d) \int_{x^2}^1 (1-s)^\alpha \frac{ds}{2\sqrt{s}}$$

Now, let $u = 1 - s$. Then $s = 1 - u$ and $ds = -du$. Let $\delta_s = 1 - x^2$. The limits for u become δ_s to 0.

$$Q(x) = \frac{c_1(d)}{2} \int_0^{\delta_s} (1-u)^{-1/2} u^\alpha du$$

For $u \in [0, \delta_s]$, we have $1 \leq (1-u)^{-1/2} \leq (1-\delta_s)^{-1/2}$, because $(1-u)$ is decreasing and non-negative. The integral $\int_0^{\delta_s} u^\alpha du = \frac{\delta_s^{\alpha+1}}{\alpha+1}$. Substituting these bounds for the term $(1-u)^{-1/2}$:

$$\frac{c_1(d)}{2(\alpha+1)} \delta_s^{\alpha+1} \leq Q(x) \leq \frac{c_1(d)}{2(\alpha+1)} (1-\delta_s)^{-1/2} \delta_s^{\alpha+1}$$

We use $\alpha = \frac{d-1}{2}$, so $2(\alpha+1) = 2(\frac{d-1}{2} + 1) = 2(\frac{d+1}{2}) = d+1$. The exponent $\alpha+1 = \frac{d+1}{2}$. Thus,

$$\frac{c_1(d)}{d+1} \delta_s^{\frac{d+1}{2}} \leq Q(x) \leq \frac{c_1(d)}{d+1} (1-\delta_s)^{-1/2} \delta_s^{\frac{d+1}{2}}$$

We choose $x_0 = 3/4$, so we consider $x \in [3/4, 1)$, which means $(1-x) \in (0, 1/4]$. For $x \in [3/4, 1)$, we have $1+x \in [7/4, 2)$. The term $\delta_s = 1 - x^2 = (1-x)(1+x)$. Given the range for $1+x$, for $(1-x) \in (0, 1/4]$:

$$\frac{7}{4}(1-x) \leq \delta_s < 2(1-x)$$

- Lower Bound for $Q(x)$: Using $\delta_s \geq \frac{7}{4}(1-x)$ from the above range:

$$Q(x) \geq \frac{c_1(d)}{d+1} \left(\frac{7}{4}(1-x) \right)^{\frac{d+1}{2}} = \frac{c_1(d)}{d+1} \left(\frac{7}{4} \right)^{\frac{d+1}{2}} (1-x)^{\frac{d+1}{2}}$$

This establishes the lower bound with $c_2(d) = \frac{c_1(d)}{d+1} \left(\frac{7}{4} \right)^{\frac{d+1}{2}}$.

- Upper Bound for $Q(x)$: For the term $\delta_s^{\frac{d+1}{2}}$, we use $\delta_s < 2(1-x)$, so $\delta_s^{\frac{d+1}{2}} < (2(1-x))^{\frac{d+1}{2}}$. For the term $(1-\delta_s)^{-1/2}$: Since $(1-x) \in (0, 1/4]$, $\delta_s < 2(1-x) \leq 2(1/4) = 1/2$. So, $1-\delta_s > 1-1/2 = 1/2$. This implies $(1-\delta_s)^{-1/2} < (1/2)^{-1/2} = \sqrt{2}$. Combining these for the upper bound of $Q(x)$:

$$Q(x) \leq \frac{c_1(d)}{d+1} 2^{1/2} \cdot 2^{\frac{d+1}{2}} (1-x)^{\frac{d+1}{2}} = \frac{c_1(d)}{d+1} 2^{\frac{d+2}{2}} (1-x)^{\frac{d+1}{2}}$$

This establishes the upper bound with $c_3(d) = \frac{c_1(d)}{d+1} 2^{\frac{d+2}{2}}$.

Thus, for $x \in [3/4, 1)$ (i.e., $1-x \in (0, 1/4]$):

$$c_2(d)(1-x)^{\frac{d+1}{2}} \leq Q(x) \leq c_3(d)(1-x)^{\frac{d+1}{2}}$$

This corresponds to $Q(x) \asymp_{c_2(d)}^{c_3(d)} (1-x)^{\frac{d+1}{2}}$. The constants $c_2(d)$ and $c_3(d)$ depend only on the dimension d (via $c_1(d)$ and the exponents derived from d) and are valid for the specified range of x . \square

Based on the tail probability, we calculate the expectation conditional on the tail events.

Proposition E.3 (Conditional Expectation). *For $x \in [3/4, 1)$, the conditional expectation $\mathbb{E}[X_1 | X_1 > x]$ is bounded by*

$$1 - c_5(d)(1 - x) \leq \mathbb{E}[X_1 | X_1 > x] \leq 1 - c_4(d)(1 - x), \quad (34)$$

where the constants $c_4(d)$ and $c_5(d)$ are given by:

$$c_4(d) = \frac{2(d+1)}{d+3} \frac{(7/4)^{(d-1)/2}}{2^{(d+2)/2}},$$

$$c_5(d) = \frac{2(d+1)}{d+3} \frac{2^{(d-1)/2}}{(7/4)^{(d+1)/2}}.$$

Proof. We consider $1 - \mathbb{E}[X_1 | X_1 > x] = \mathbb{E}[1 - X_1 | X_1 > x]$.

$$\begin{aligned} \mathbb{E}[1 - X_1 | X_1 > x] &= \frac{1}{Q(x)} \int_x^1 (1-t) f_{X_1}(t) dt \\ &= \frac{c_1(d)}{Q(x)} \int_x^1 (1-t)(1-t^2)^\alpha dt \\ &= \frac{c_1(d)}{Q(x)} \int_x^1 (1-t)^{\alpha+1} (1+t)^\alpha dt \end{aligned}$$

Let $I_1(x) = \int_x^1 (1-t)^{\alpha+1} (1+t)^\alpha dt$. We consider $x \in [3/4, 1)$. For $t \in [x, 1]$, we have $1+t \in [1+x, 2]$. Since $x \geq 3/4$, $1+x \geq 7/4$. Thus, $(7/4)^\alpha \leq (1+t)^\alpha \leq 2^\alpha$ for $t \in [x, 1]$ (assuming $\alpha \geq 0$, which holds for $d \geq 1$). The integral $\int_x^1 (1-t)^{\alpha+1} dt = \left[-\frac{(1-t)^{\alpha+2}}{\alpha+2} \right]_x^1 = \frac{(1-x)^{\alpha+2}}{\alpha+2}$. So, $I_1(x)$ is bounded by:

$$(7/4)^\alpha \frac{(1-x)^{\alpha+2}}{\alpha+2} \leq I_1(x) \leq 2^\alpha \frac{(1-x)^{\alpha+2}}{\alpha+2}$$

Let $N_1(x) = c_1(d)I_1(x)$. Then, using $\alpha + 2 = (d + 3)/2$:

$$\frac{2c_1(d)(7/4)^{(d-1)/2}}{d+3} (1-x)^{\frac{d+3}{2}} \leq N_1(x) \leq \frac{2c_1(d)2^{(d-1)/2}}{d+3} (1-x)^{\frac{d+3}{2}}$$

From Proposition E.2, for $x \in [3/4, 1)$, $Q(x)$ is bounded by:

$$c_2(d)(1-x)^{\frac{d+1}{2}} \leq Q(x) \leq c_3(d)(1-x)^{\frac{d+1}{2}}$$

where $c_2(d) = \frac{c_1(d)}{d+1} \left(\frac{7}{4}\right)^{\frac{d+1}{2}}$ and $c_3(d) = \frac{c_1(d)}{d+1} 2^{\frac{d+2}{2}}$. Therefore, $\mathbb{E}[1 - X_1 | X_1 > x] = \frac{N_1(x)}{Q(x)}$ is bounded by:

- Lower bound:

$$\begin{aligned} \frac{\frac{2c_1(d)(7/4)^{(d-1)/2}}{d+3} (1-x)^{\frac{d+3}{2}}}{c_3(d)(1-x)^{\frac{d+1}{2}}} &= \frac{2c_1(d)(7/4)^{(d-1)/2}/(d+3)}{\frac{c_1(d)}{d+1} 2^{\frac{d+2}{2}}} (1-x) \\ &= \frac{2(d+1)}{d+3} \frac{(7/4)^{(d-1)/2}}{2^{(d+2)/2}} (1-x) = c_4(d)(1-x) \end{aligned}$$

- Upper bound:

$$\begin{aligned} \frac{\frac{2c_1(d)2^{(d-1)/2}}{d+3} (1-x)^{\frac{d+3}{2}}}{c_2(d)(1-x)^{\frac{d+1}{2}}} &= \frac{2c_1(d)2^{(d-1)/2}/(d+3)}{\frac{c_1(d)}{d+1} \left(\frac{7}{4}\right)^{\frac{d+1}{2}}} (1-x) \\ &= \frac{2(d+1)}{d+3} \frac{2^{(d-1)/2}}{(7/4)^{(d+1)/2}} (1-x) = c_5(d)(1-x) \end{aligned}$$

So, for $x \in [3/4, 1)$:

$$c_4(d)(1-x) \leq \mathbb{E}[1 - X_1 \mid X_1 > x] \leq c_5(d)(1-x)$$

This implies:

$$1 - c_5(d)(1-x) \leq \mathbb{E}[X_1 \mid X_1 > x] \leq 1 - c_4(d)(1-x)$$

This completes the proof. \square

Finally, we combine the results and characterize the asymptotic behavior of the weight function g .

Proposition E.4 (Asymptotic Behavior of $g^+(x)$). *Let the function $g^+(x)$ be defined as: for $x \in (-1, 1)$,*

$$g^+(x) = \mathbb{P}(X_1 > x)^2 \cdot \mathbb{E}[X_1 - x \mid X_1 > x] \cdot \sqrt{1 + (\mathbb{E}[X_1 \mid X_1 > x])^2}. \quad (35)$$

Then for $x \in [3/4, 1)$, we have:

$$c_L^{(g)}(d)(1-x)^{d+2} \leq g^+(x) \leq c_U^{(g)}(d)(1-x)^{d+2}, \quad (36)$$

where $c_L^{(g)}(d)$ and $c_U^{(g)}(d)$ are positive constants depending on dimension d , defined in the proof (37).

Proof. Let $Q(x) = \mathbb{P}(X_1 > x)$ and $E(x) = \mathbb{E}[X_1 \mid X_1 > x]$. The function is $g^+(x) = Q(x)^2 \cdot (E(x) - x) \cdot \sqrt{1 + E(x)^2}$. Now, we establish precise bounds for $x \in [3/4, 1)$. Let $(1-x)$ be the variable.

1. Bounds for $Q(x)^2$: From Propostion E.2, $c_2(d)(1-x)^{\frac{d+1}{2}} \leq Q(x) \leq c_3(d)(1-x)^{\frac{d+1}{2}}$. So, $A_L(d)(1-x)^{d+1} \leq Q(x)^2 \leq A_U(d)(1-x)^{d+1}$, where

$$A_L(d) = (c_2(d))^2 = \left(\frac{c_1(d)}{d+1} \left(\frac{7}{4} \right)^{\frac{d+1}{2}} \right)^2,$$

$$A_U(d) = (c_3(d))^2 = \left(\frac{c_1(d)}{d+1} 2^{\frac{d+2}{2}} \right)^2.$$

2. Bounds for $E(x) - x = \mathbb{E}[X_1 - x \mid X_1 > x]$: From Propostion E.3, we have $(1-x) - c_5(d)(1-x) \leq E(x) - x \leq (1-x) - c_4(d)(1-x)$. So, $B_L(d)(1-x) \leq E(x) - x \leq B_U(d)(1-x)$, where

$$B_L(d) = 1 - c_5(d) = 1 - \frac{2(d+1)}{d+3} \frac{2^{(d-1)/2}}{(7/4)^{(d+1)/2}},$$

$$B_U(d) = 1 - c_4(d) = 1 - \frac{2(d+1)}{d+3} \frac{(7/4)^{(d-1)/2}}{2^{(d+2)/2}}.$$

Since $E(x) - x = \mathbb{E}[X_1 - x \mid X_1 > x]$ must be positive (as $X_1 > x$), we take $B_L(d) = \max(0, 1 - c_5(d))$.

3. Bounds for $\sqrt{1 + E(x)^2}$: We know $1 - c_5(d)(1-x) \leq E(x) \leq 1 - c_4(d)(1-x)$. For $x \in [3/4, 1)$, $(1-x) \in (0, 1/4]$ and the upper bound of $E(x)$ is given by

$$E(x) \leq 1 - c_4(d)(1-x) < 1.$$

The lower bound is also given in this way

$$E(x) = \mathbb{E}[X_1 \mid X_1 > x] \geq x \geq 3/4.$$

Therefore, we deduce that

$$C_L(d) \leq \sqrt{1 + E(x)^2} \leq C_U(d),$$

where

$$C_L(d) = \frac{5}{4}, C_U(d) = \sqrt{2}.$$

Combining these bounds, for $x \in [3/4, 1)$:

$$\begin{aligned} g^+(x) &\geq A_L(d)B_L(d)C_L(d)(1-x)^{d+1}(1-x) = c_L^{(g)}(d)(1-x)^{d+2}, \\ g^+(x) &\leq A_U(d)B_U(d)C_U(d)(1-x)^{d+1}(1-x) = c_U^{(g)}(d)(1-x)^{d+2}. \end{aligned}$$

The constants are:

$$\begin{aligned} c_L^{(g)}(d) &= (c_2(d))^2 \cdot (1 - c_5(d)) \cdot 5/4, \\ c_U^{(g)}(d) &= (c_3(d))^2 \cdot (1 - c_4(d)) \cdot \sqrt{2}. \end{aligned} \tag{37}$$

□

E.2 Empirical Process for the Regularity Weight Function

In this section, we discuss the empirical process of g_P . Now we may relax the assumption by just assuming that \mathbf{X} is random variable with $\text{supp}(\mathbf{X}) \subseteq \mathbb{B}_1^d$. Fix dimension $d \in \mathbb{N}$, sample size $n \in \mathbb{N}$, and let $\mathbf{X}_1, \dots, \mathbf{X}_n$ be i.i.d. copies of X . We use the notation \hat{g}_n to denote empirical weight function g as we defined previously.

For $\mathbf{u} \in \mathbb{S}^{d-1}$ and $t \in [-1, 1]$, define

$$p(\mathbf{u}, t) := \mathbb{P}(\mathbf{X}^\top \mathbf{u} > t), \quad s(\mathbf{u}, t) := \mathbb{E}[(\mathbf{X}^\top \mathbf{u} - t)_+],$$

and recall the population weight $g_P(\mathbf{u}, t)$. By the bounds $0 \leq (\mathbf{X}^\top \mathbf{u} - t)_+ \leq 2$ and $\|\mathbb{E}[\mathbf{X} \mid \mathbf{X}^\top \mathbf{u} > t]\| \leq 1$ (valid on \mathbb{B}_1^d), we have the pointwise comparison

$$g_P(\mathbf{u}, t) \asymp p(\mathbf{u}, t) s(\mathbf{u}, t) \quad \text{with absolute constants,} \tag{38}$$

i.e., there exist universal $c, C \in (0, \infty)$ such that $c p s \leq g_P \leq C p s$ for all $(\mathbf{u}, t) \in \mathbb{S}^{d-1} \times [-1, 1]$. Consider the empirical plug-ins

$$\hat{p}_n(\mathbf{u}, t) := \frac{1}{n} \sum_{i=1}^n \mathbb{1}\{\mathbf{X}_i^\top \mathbf{u} > t\}, \quad \hat{s}_n(\mathbf{u}, t) := \frac{1}{n} \sum_{i=1}^n (\mathbf{X}_i^\top \mathbf{u} - t)_+, \quad \hat{g}_n(\mathbf{u}, t) := \hat{p}_n(\mathbf{u}, t) \hat{s}_n(\mathbf{u}, t).$$

Note that \hat{g}_n involves no division by \hat{p}_n , hence avoids any small-mass instability. We now give a self-contained proof of a sharp, distribution-free uniform deviation bound.

Theorem E.5 (Distribution-free uniform deviation for \hat{g}_n). *There exists a universal constant $C > 0$ such that, for every $\delta \in (0, 1)$,*

$$\mathbb{P} \left(\sup_{\mathbf{u} \in \mathbb{S}^{d-1}, t \in [-1, 1]} |\hat{g}_n(\mathbf{u}, t) - g_P(\mathbf{u}, t)| > C \sqrt{\frac{d + \log(2/\delta)}{n}} \right) \leq \delta.$$

Proof. Using (38), it is enough (up to absolute constants) to control $|\hat{p}_n(\mathbf{u}, t) \hat{s}_n(\mathbf{u}, t) - p(\mathbf{u}, t) s(\mathbf{u}, t)|$ uniformly over $(\mathbf{u}, t) \in \mathbb{S}^{d-1} \times [-1, 1]$. Observe that $0 \leq s, \hat{s}_n \leq 2$ and $0 \leq p, \hat{p}_n \leq 1$, so

$$|\hat{p}_n \hat{s}_n - p s| \leq |\hat{p}_n - p| s + |\hat{s}_n - s| \hat{p}_n \leq 2 |\hat{p}_n - p| + |\hat{s}_n - s|. \tag{39}$$

We thus seek uniform bounds for the two empirical processes appearing on the right-hand side. The argument proceeds in two steps:

- **Halfspaces.** The class $\{x \mapsto \mathbf{1}\{x^\top \mathbf{u} > t\} : \mathbf{u} \in \mathbb{S}^{d-1}, t \in \mathbb{R}\}$ has VC-dimension $d + 1$. Hence, by the VC uniform convergence inequality for $\{0, 1\}$ -valued classes (e.g., [Vapnik, 1998]), there exists a universal constant $C_1 > 0$ such that, for all $\delta \in (0, 1)$,

$$\mathbb{P} \left(\sup_{\mathbf{u} \in \mathbb{S}^{d-1}, t \in [-1, 1]} |\hat{p}_n(\mathbf{u}, t) - p(\mathbf{u}, t)| > C_1 \sqrt{\frac{d + \log(1/\delta)}{n}} \right) \leq \delta. \quad (40)$$

- **ReLU class.** Let $\mathcal{F} := \{f_{\mathbf{u}, t}(\mathbf{x}) = (\mathbf{u}^\top \mathbf{x} - t)_+ : \mathbf{u} \in \mathbb{S}^{d-1}, t \in [-1, 1]\}$. Since $\|\mathbf{x}\| \leq 1$ and $t \in [-1, 1]$, we have $f \in [0, 2]$. Consider the subgraph family

$$\text{subG}(\mathcal{F}) = \{(\mathbf{x}, y) \in \mathbb{R}^d \times \mathbb{R} : y \leq (\mathbf{u}^\top \mathbf{x} - t)_+\}.$$

For $y \leq 0$ membership is automatic; for $y > 0$ it is equivalent to the affine halfspace condition $\mathbf{u}^\top \mathbf{x} - t - y \geq 0$ in \mathbb{R}^{d+1} . Thus $\text{VCdim}(\text{subG}(\mathcal{F})) \leq d + 2$, whence $\text{Pdim}(\mathcal{F}) \leq d + 2$. Standard pseudo-dimension bounds (see [Haussler, 1992, Thm. 3, 6, 7]) give a universal $C_2 > 0$ with

$$\mathbb{P} \left(\sup_{\mathbf{u} \in \mathbb{S}^{d-1}, t \in [-1, 1]} |\hat{s}_n(\mathbf{u}, t) - s(\mathbf{u}, t)| > C_2 \sqrt{\frac{d + \log(1/\delta)}{n}} \right) \leq \delta. \quad (41)$$

Combining Step (I) and Step (II) with a union bound and the previous inequality yields

$$\mathbb{P} \left(\sup_{\mathbf{u}, t} |\hat{p}_n \hat{s}_n - p s| > C' \sqrt{\frac{d + \log(2/\delta)}{n}} \right) \leq \delta \quad (42)$$

for an absolute constant $C' > 0$. Finally, the equivalence (38) transfers this bound to $\sup_{\mathbf{u}, t} |\hat{g}_n - g_P|$, up to a universal multiplicative factor and the same failure probability. \square

F Proof of Theorem 3.5: Generalization Gap of Stable Minima

Let \mathcal{P} denote the joint distribution of (\mathbf{x}, y) . Assume that \mathcal{P} is supported on $\mathbb{B}_1^d \times [-D, D]$ for some $D > 0$. Let f be a function. The *population risk* or *expected risk* of f is defined to be

$$R(f) = \mathbb{E}_{(\mathbf{x}, y) \sim \mathcal{P}} \left[(f(\mathbf{x}) - y)^2 \right] \quad (43)$$

Let $\mathcal{D} = \{(\mathbf{x}_i, y_i)\}_{i=1}^n$ be a dataset where each (\mathbf{x}_i, y_i) is drawn i.i.d. from \mathcal{P} . Then the *empirical risk* is defined to be

$$\hat{R}(f) = \frac{1}{n} \sum_{i=1}^n (f(\mathbf{x}_i) - y_i)^2 \quad (44)$$

The *generalization gap* is defined to be

$$\text{GeneralizationGap}(f; \hat{R}) := |R(f) - \hat{R}(f)|. \quad (45)$$

The generalization gap measures the difference between the train loss and the expected testing error. The smaller the generalization gap, the less likely the model overfits.

F.1 Definition of the Variation Space of ReLU Neural Networks

Recall the notion in Section 3, the *weighted variation (semi)norm* is defined to be

$$|f|_{V_g} := \inf_{\substack{\nu \in \mathcal{M}(\mathbb{S}^{d-1} \times [-R, R]) \\ \mathbf{c} \in \mathbb{R}^d, c_0 \in \mathbb{R}}} \|g \cdot \nu\|_{\mathcal{M}} \quad \text{s.t.} \quad f = f_{\nu, \mathbf{c}, c_0}, \quad (46)$$

and now we define the *unweighted variation norm* or simply *variation norm* to be

$$|f|_V := \inf_{\substack{\nu \in \mathcal{M}(\mathbb{S}^{d-1} \times [-R, R]) \\ \mathbf{c} \in \mathbb{R}^d, c_0 \in \mathbb{R}}} \|\nu\|_{\mathcal{M}} \quad \text{s.t.} \quad f = f_{\nu, \mathbf{c}, c_0}. \quad (47)$$

This definition is identical to the one in [Parhi and Nowak, 2023, Section V.B]. The following example for unweighted variation norm is similar to Example 3.1.

Example F.1. *Since we are interested in functions defined on \mathbb{B}_R^d , for a finite-width neural network $f_{\boldsymbol{\theta}}(\mathbf{x}) = \sum_{k=1}^K v_k \phi(\mathbf{w}_k^\top \mathbf{x} - b_k) + \beta$, we observe that it has the equivalent implementation as $f_{\boldsymbol{\theta}}(\mathbf{x}) = \sum_{j=1}^J a_j \phi(\mathbf{u}_j^\top \mathbf{x} - t_j) + \mathbf{c}^\top \mathbf{x} + c_0$, where $a_j \in \mathbb{R}$, $\mathbf{u}_j \in \mathbb{S}^{d-1}$, $t_j \in \mathbb{R}$, $\mathbf{c} \in \mathbb{R}^d$, and $c_0 \in \mathbb{R}$. Indeed, this is due to the fact that the ReLU is homogeneous, which allows us to absorb the magnitude of the input weights into the output weights (i.e., each $a_j = |v_{k_j}| \|\mathbf{w}_{k_j}\|_2$ for some $k_j \in \{1, \dots, K\}$). Furthermore, any ReLUs in the original parameterization whose activation threshold⁷ is outside \mathbb{B}_R^d can be implemented by an affine function on \mathbb{B}_R^d , which gives rise to the $\mathbf{c}^\top \mathbf{x} + c_0$ term in the implementation. If this new implementation is in “reduced form”, i.e., the collection $\{(\mathbf{u}_j, t_j)\}_{j=1}^J$ are distinct, then we have that $|f_{\boldsymbol{\theta}}|_V = \sum_{j=1}^J |a_j|$.*

The bounded variation function class is defined w.r.t. the unweighted variation norm.

Definition F.2. For the compact region $\Omega = \mathbb{B}_R^d$, we define the bounded variation function class as

$$V_C(\Omega) := \left\{ f: \Omega \rightarrow \mathbb{R} \mid f = \int_{\mathbb{S}^{d-1} \times [-R, R]} \phi(\mathbf{u}^\top \mathbf{x} - t) d\nu(\mathbf{u}, t) + \mathbf{c}^\top \mathbf{x} + b, |f|_V \leq C \right\}. \quad (48)$$

F.2 Metric Entropy and Variation Spaces

Metric entropy quantifies the compactness of a set A in a metric space (X, ρ_X) . Below we introduce the definition of covering numbers and metric entropy.

Definition F.3 (Covering Number and Entropy). Let A be a compact subset of a metric space (X, ρ_X) . For $t > 0$, the *covering number* $N(A, t, \rho_X)$ is the minimum number of closed balls of radius t needed to cover A :

$$N(t, A, \rho_X) := \min \left\{ N \in \mathbb{N} : \exists x_1, \dots, x_N \in X \text{ s.t. } A \subset \bigcup_{i=1}^N \mathbb{B}(x_i, t) \right\}, \quad (49)$$

where $\mathbb{B}(x_i, t) = \{y \in X : \rho_X(y, x_i) \leq t\}$. The *metric entropy* of A at scale t is defined as:

$$H_t(A)_X := \log N(t, A, \rho_X). \quad (50)$$

The metric entropy of the bounded variation function class has been studied in previous works. More specifically, we will directly use the one below in future analysis.

⁷The activation threshold of a neuron $\phi(\mathbf{w}^\top \mathbf{x} - b)$ is the hyperplane $\{\mathbf{x} \in \mathbb{R}^d : \mathbf{w}^\top \mathbf{x} = b\}$.

Proposition F.4 (Parhi and Nowak 2023, Appendix D). *The metric entropy of $V_C(\mathbb{B}_R^d)$ (see Definition F.2) with respect to the $L^\infty(\mathbb{B}_R^d)$ -distance $\|\cdot\|_\infty$ satisfies*

$$\log N(t, V_C(\mathbb{B}_R^d), \|\cdot\|_\infty) \lesssim_d \left(\frac{C}{t}\right)^{\frac{2d}{d+3}}. \quad (51)$$

where \lesssim_d hides constants (which could depend on d) and logarithmic factors.

F.3 Generalization Gap of Unweighted Variation Function Class

As a middle step towards bounding the generalization gap of the weighted variation function class, we first bound the generalization gap of the unweighted variation function class according to a metric entropy analysis.

Lemma F.5. *Let $\mathcal{F}_{M,C} = \{f \in V_C(\mathbb{B}_R^d) \mid \|f\|_\infty \leq M\}$ with $M \geq D$ where D refers to Theorem 3.5. Then with probability at least $1 - \delta$:*

$$\sup_{f \in \mathcal{F}_{M,C}} |R(f) - \hat{R}_n(f)| \lesssim_d C^{\frac{d}{2d+3}} M^{\frac{3(d+2)}{2d+3}} n^{-\frac{d+3}{4d+6}}. \quad (52)$$

Proof. According to Proposition F.4, one just needs $N(t)$ balls to cover \mathcal{F} in $\|\cdot\|_\infty$ with radius $t > 0$ such that where

$$\log N(t) \lesssim_d \left(\frac{C}{t}\right)^{\frac{2d}{d+3}}.$$

Then for any $f, g \in \mathcal{F}_{M,C}$ and any (\mathbf{x}, y) ,

$$|(f(\mathbf{x}) - y)^2 - (g(\mathbf{x}) - y)^2| = |f(\mathbf{x}) - g(\mathbf{x})| |f(\mathbf{x}) + g(\mathbf{x}) - 2y| \leq 4M \|f - g\|_\infty.$$

Hence replacing f by a centre f_i within t changes both the empirical and true risks by at most $4Mt$.

For any fixed centre \bar{f} in the covering, Hoeffding's inequality implies that with probability at least $\geq 1 - \delta$, we have

$$|R(\bar{f}) - \hat{R}(\bar{f})| \leq 4M^2 \sqrt{\frac{\log(2/\delta)}{n}} \quad (53)$$

because each squared error lies in $[0, 4M^2]$. Then we take all the centers with union bound to deduce that with probability at least $1 - \delta/2$, for any center \bar{f} in the set of covering index, we have

$$\begin{aligned} |R(\bar{f}) - \hat{R}(\bar{f})| &\leq 4M^2 \sqrt{\frac{\log(4N(t)/\delta)}{n}} \\ &\lesssim_d M^2 \cdot \left(\frac{C}{t}\right)^{\frac{d}{d+3}} n^{-\frac{1}{2}}. \end{aligned} \quad (54)$$

According to the definition of covering sets, for any $f \in \mathcal{F}_{M,C}$, we have that $\|f - \bar{f}\|_\infty \leq t$ for some center \bar{f} . Then we have

$$\begin{aligned} &|R(f) - \hat{R}(f)| \\ &\leq |R(\bar{f}) - \hat{R}(\bar{f})| + O(Mt) \\ &\leq M^2 \cdot \left(\frac{C}{t}\right)^{\frac{d}{d+3}} n^{-\frac{1}{2}} + O(Mt). \end{aligned} \quad (55)$$

After tuning t to be the optimal choice, we deduce that (52). \square

F.4 Concentration Property of Ball-Uniform Distribution

In the following analysis, we will handle the interior and boundary of the unit ball separately. In this part, we define the annulus of a ball rigorously and provide a high-probability bound on the number of samples falling in the annulus.

Definition F.6. Let \mathbb{B}_1^d be the unit ball. The ε -annulus is a subset of \mathbb{B}_1^d defined as

$$\mathbb{A}_\varepsilon^d := \{\mathbf{x} \in \mathbb{B}_1^d \mid \|\mathbf{x}\|_2 \geq 1 - \varepsilon\}$$

and the closure of its complement is called ε -strict interior and denoted by \mathbb{I}_ε^d .

Lemma F.7 (High-Probability Upper Bound on Annulus). *Let $d \in \mathbb{N}$ and $\varepsilon \in (0, 1)$. Let*

$$\mathbf{x}_1, \dots, \mathbf{x}_n \sim \text{Uniform}(\mathbb{B}_1^d).$$

Define $n_A := |\{i \mid \mathbf{x}_i \in \mathbb{A}_\varepsilon^d\}|$ and $p = \mathbb{P}(\mathbf{X} \in \mathbb{A}_\varepsilon^d) = 1 - (1 - \varepsilon)^d = \Theta(\varepsilon)$. Then for any $\delta \in (0, 1)$, with probability at least $1 - \delta$,

$$\frac{n_A}{n} \leq p + \sqrt{\frac{3p \log(1/\delta)}{n}}. \quad (56)$$

Proof. For each $i = 1, \dots, n$, consider a Bernorlli random variable

$$U = \mathbf{1}\{\mathbf{X} \in \mathbb{A}_\varepsilon^d\},$$

so that $\mathbb{E}[U] = p$ and regards U_i as a sample. Then we make take $n_A = \sum_{i=1}^n U_i$. By the multiplicative Chernoff bound for the upper tail of a sum of independent Bernoulli variables,

$$\mathbb{P}(n_A > (1 + \gamma)np) \leq \exp\left(-\frac{\gamma^2}{3}np\right), \quad \forall \gamma > 0.$$

Set the right-hand side equal to δ and solve for γ :

$$\exp\left(-\frac{\gamma^2}{3}np\right) = \delta \implies -\frac{\gamma^2}{3}np = \ln \delta \implies \gamma = \sqrt{\frac{3 \ln(1/\delta)}{np}}.$$

If $\gamma > 1$, note that trivially $n_A/n \leq 1 \leq p + \sqrt{\frac{3p \ln(1/\delta)}{n}}$, so the claimed bound holds in all cases. Otherwise, plugging this choice of γ into the Chernoff bound gives

$$\mathbb{P}\left(n_A \leq np(1 + \gamma)\right) \geq 1 - \delta,$$

i.e. with probability at least $1 - \delta$,

$$n_A \leq np + \sqrt{3np \ln(1/\delta)},$$

and dividing by n yields the stated inequality. \square

F.5 Upper Bound of Generalization Gap of Stable Minima

Let $f = f_{\theta}$ be a stable solution of the loss function $\mathcal{L}(\theta)$, trained by gradient descent with learning rate η . Then we have

$$\begin{aligned} \frac{2}{\eta} &\geq \lambda_{\max}(\nabla_{\theta}^2 \mathcal{L}(\theta)) \geq \mathbf{v}^{\top} \nabla_{\theta}^2 \mathcal{L}(\theta) \mathbf{v} \\ &= \underbrace{\lambda_{\max} \left(\frac{1}{n} \sum_{i=1}^n (\nabla_{\theta} f_{\theta}(\mathbf{x}_i)) (\nabla_{\theta} f_{\theta}(\mathbf{x}_i))^{\top} \right)}_{\text{(Term A)}} \\ &\quad + \underbrace{\frac{1}{n} \sum_{i=1}^n (f_{\theta}(\mathbf{x}_i) - y_i) \mathbf{v}^{\top} \nabla_{\theta}^2 f_{\theta}(\mathbf{x}_i) \mathbf{v}}_{\text{(Term B)}}. \end{aligned} \quad (57)$$

For (Term A), we have

$$\lambda_{\max} \left(\frac{1}{n} \sum_{i=1}^n (\nabla_{\theta} f_{\theta}(\mathbf{x}_i)) (\nabla_{\theta} f_{\theta}(\mathbf{x}_i))^{\top} \right) \geq 1 + 2|f_{\theta}|_{V_g}. \quad (58)$$

For (Term B), we have

$$|(\text{Term B})| \leq \sqrt{\frac{1}{n} \sum_{i=1}^n (f_{\theta}(\mathbf{x}_i) - y_i)^2} \cdot \sqrt{\frac{1}{n} \sum_{i=1}^n (\mathbf{v}^{\top} \nabla_{\theta}^2 f_{\theta}(\mathbf{x}_i) \mathbf{v})^2} \leq 4\sqrt{2\mathcal{L}(\theta)}. \quad (59)$$

Let $M = \max\{\|f\|_{\infty}, D\}$. Then we have

$$\sqrt{2\mathcal{L}(\theta)} = \sqrt{\frac{1}{n} \sum_{i=1}^n (f_{\theta}(\mathbf{x}_i) - y_i)^2} \leq 2M.$$

Combining these inequalities together, we may deduce that

$$|f_{\theta}|_{V_g} \leq \frac{1}{\eta} - \frac{1}{2} + 4M. \quad (60)$$

With all the preparations, we are ready to prove the generalization gap upper bound for stable minima.

Theorem F.8. (Restate the first part of Theorem 3.5) Let \mathcal{P} denote the joint distribution of (\mathbf{x}, y) . Assume that \mathcal{P} is supported on $\mathbb{B}_1^d \times [-D, D]$ for some $D > 0$ and that the marginal distribution of \mathbf{x} is $\text{Uniform}(\mathbb{B}_1^d)$. Fix a dataset $\mathcal{D} = \{(\mathbf{x}_i, y_i)\}_{i=1}^n$, where each (\mathbf{x}_i, y_i) is drawn i.i.d. from \mathcal{P} , and \mathcal{D} yields the empirical weight function g defined in (4). Then, with probability at least $1 - \delta$, we have that for the plug-in risk estimator $\hat{R}(f) := \frac{1}{n} \sum_{i=1}^n (f(\mathbf{x}_i) - y_i)^2$,

$$\sup_{\substack{f \in V_g(\mathbb{B}_1^d) \\ |f|_{V_g} \leq A, \|f\|_{L^{\infty}} \leq M}} \text{GeneralizationGap}(f; \hat{R}) := |R(f) - \hat{R}(f)| \lesssim_d A^{\frac{d}{d^2+4d+3}} M^2 n^{-\frac{1}{2d+4}},$$

where M is assumed > 1 for clean statement and \lesssim_d hides constants (which could depend on d) and logarithmic factors in n and $(1/\delta)$. In particular, Theorem 3.2 and (60) directly deduce that that

$$\left\{ f \in \mathcal{F}_{\text{stable}}(\eta) \mid \|f\|_{L^{\infty}(\mathbb{B}_1^d)} \leq M \right\} \subseteq \left\{ f \in V_g(\mathbb{B}_1^d) \mid |f|_{V_g} \leq \frac{1}{\eta} - \frac{1}{2} + 4M, \|f\|_{L^{\infty}(\mathbb{B}_1^d)} \leq M \right\}. \quad (61)$$

Therefore, we may conclude that

$$\begin{aligned} \sup_{f_{\boldsymbol{\theta}} \in \mathcal{F}_{\text{stable}}(\eta)} \text{GeneralizationGap}(f_{\boldsymbol{\theta}}; \hat{R}) &:= |R(f_{\boldsymbol{\theta}}) - \hat{R}(f_{\boldsymbol{\theta}})| \\ &\lesssim_d \left(\frac{1}{\eta} - \frac{1}{2} + 4M \right)^{\frac{d}{d^2+4d+3}} M^2 n^{-\frac{1}{2d+4}}, \end{aligned} \quad (62)$$

where $M := \max \left\{ D, \|f_{\boldsymbol{\theta}}\|_{L^\infty(\mathbb{B}_1^d)}, 1 \right\}$.

Proof. For any fixed $\varepsilon < 1/4$, we may decompose \mathbb{B}_1^d into ε -annulus and ε -strict interior

$$\mathbb{B}_1^d = \mathbb{A}_\varepsilon^d \cup \mathbb{I}_\varepsilon^d.$$

According to the law of total expectation, the population risk is decomposed into

$$\mathbb{E}_{(\mathbf{x}, y) \sim \mathcal{P}} \left[(f(\mathbf{x}) - y)^2 \right] = \mathbb{P}(\mathbf{x} \in \mathbb{A}_\varepsilon^d) \cdot \mathbb{E}_{\mathbb{A}} \left[(f(\mathbf{x}) - y)^2 \right] + \mathbb{P}(\mathbf{x} \in \mathbb{I}_\varepsilon^d) \cdot \mathbb{E}_{\mathbb{I}} \left[(f(\mathbf{x}) - y)^2 \right], \quad (63)$$

where $\mathbb{E}_{\mathbb{A}}$ means that $\{\mathbf{x}, y\}$ is a new sample from the data distribution conditioned on $\mathbf{x} \in \mathbb{A}_\varepsilon^d$ and $\mathbb{E}_{\mathbb{I}}$ means that (\mathbf{x}, y) is a new sample from the data distribution conditioned on $\mathbf{x} \in \mathbb{I}_\varepsilon^d$.

Similarly, we also have this decomposition for empirical risk

$$\begin{aligned} \frac{1}{n} \sum_{i=1}^n (f(\mathbf{x}_i) - y_i)^2 &= \frac{1}{n} \left(\sum_{i \in I} (f(\mathbf{x}_i) - y_i)^2 + \sum_{j \in A} (f(\mathbf{x}_j) - y_j)^2 \right) \\ &= \frac{n_I}{n} \frac{1}{n_I} \sum_{i \in I} (f(\mathbf{x}_i) - y_i)^2 + \frac{n_A}{n} \frac{1}{n_A} \sum_{j \in A} (f(\mathbf{x}_j) - y_j)^2, \end{aligned} \quad (64)$$

where I is the set of data points with $\mathbf{x}_i \in \mathbb{I}_\varepsilon^d$ and A is the set of data points with $\mathbf{x}_i \in \mathbb{A}_\varepsilon^d$. Then the generalization gap can be decomposed into

$$|R(f) - \hat{R}(f)| \leq \mathbb{P}(\mathbf{x} \in \mathbb{A}_\varepsilon^d) \cdot \mathbb{E}_{\mathbb{A}} \left[(f_{\boldsymbol{\theta}}(\mathbf{x}) - y)^2 \right] + \frac{n_A}{n} \frac{1}{n_A} \sum_{j \in A} (f(\mathbf{x}_j) - y_j)^2 + \quad (65)$$

$$+ \left| \mathbb{P}(\mathbf{x} \in \mathbb{I}_\varepsilon^d) - \frac{n_I}{n} \right| \frac{1}{n_I} \sum_{i \in I} (f(\mathbf{x}_i) - y_i)^2 \quad (66)$$

$$+ \mathbb{P}(\mathbf{x} \in \mathbb{I}_\varepsilon^d) \cdot \left| \mathbb{E}_{\mathbb{I}} \left[(f(\mathbf{x}) - y)^2 \right] - \frac{1}{n_I} \sum_{i \in I} (f(\mathbf{x}_i) - y_i)^2 \right|. \quad (67)$$

Using the property that the marginal distribution of \mathbf{x} is $\text{Uniform}(\mathbb{B}_1^d)$ and its concentration property (see Lemma F.7), with probability at least $1 - \delta/2$:

$$(65) \lesssim_d O(M^2 \varepsilon), \quad (68)$$

where \lesssim_d hides the constants that could depend on d and logarithmic factors of $1/\delta$.

For the term (66), with probability $1 - \delta/3$

$$\begin{cases} \left| \mathbb{P}(\mathbf{x} \in \mathbb{I}_\varepsilon^d) - \frac{n_I}{n} \right| &\lesssim \sqrt{\frac{\varepsilon \log(3/\delta)}{n}}, \quad (\text{Lemma F.7}) \\ \frac{1}{n_I} \sum_{i \in I} (f(\mathbf{x}_i) - y_i)^2 &\leq 4M^2 \end{cases} \quad (69)$$

so we may also conclude that

$$(66) \lesssim M^2 \sqrt{\frac{\varepsilon \log(3/\delta)}{n}} \quad (70)$$

For the part of the interior (67), the scalar $\mathbb{P}(\mathbf{x} \in \mathbb{I}_\varepsilon^d)$ is less than 1 with high-probability. Therefore, we just need to deal with the term

$$\mathbb{E}_{\mathbb{I}} \left[(f(\mathbf{x}) - y)^2 \right] - \frac{1}{n_I} \sum_{i \in I} (f(\mathbf{x}_i) - y_i)^2. \quad (71)$$

Since both the distribution and sample points only support in \mathbb{I}_ε^d , we may consider f by its restrictions in \mathbb{I}_ε^d , which are denoted by f^ε . Furthermore, according to the definition, we have

$$\begin{aligned} f(\mathbf{x}) &= \int_{\mathbb{S}^{d-1} \times [-1, 1]} \phi(\mathbf{u}^\top \mathbf{x} - t) d\nu(\mathbf{u}, t) + \mathbf{c}^\top \mathbf{x} + b \\ &= \int_{\mathbb{S}^{d-1} \times [-1+\varepsilon, 1-\varepsilon]} \phi(\mathbf{u}^\top \mathbf{x} - t) d\nu(\mathbf{u}, t) + \underbrace{\int_{\mathbb{S}^{d-1} \times [-1, -1+\varepsilon] \cup (1-\varepsilon, 1]} \phi(\mathbf{u}^\top \mathbf{x} - t) d\nu(\mathbf{u}, t)}_{\text{Annulus ReLU}} \\ &\quad + \mathbf{c}^\top \mathbf{x} + b \end{aligned} \quad (72)$$

where the Annulus ReLU term is totally linear in the strictly interior i.e. there exists \mathbf{c}', b' such that

$$\mathbf{c}'^\top \mathbf{x} + b' = \int_{\mathbb{S}^{d-1} \times [-1, -1+\varepsilon] \cup (1-\varepsilon, 1]} \phi(\mathbf{u}^\top \mathbf{x} - t) d\nu(\mathbf{u}, t), \quad \forall \mathbf{x} \in \mathbb{I}_\varepsilon^d. \quad (73)$$

Therefore, we may write

$$f(\mathbf{x}) = f^\varepsilon(\mathbf{x}) = \int_{\mathbb{S}^{d-1} \times [-1+\varepsilon, 1-\varepsilon]} \phi(\mathbf{u}^\top \mathbf{x} - t) d\nu(\mathbf{u}, t) + (\mathbf{c} + \mathbf{c}')^\top \mathbf{x} + \mathbf{b} + \mathbf{b}', \quad \mathbf{x} \in \mathbb{I}_\varepsilon^d. \quad (74)$$

The core of the argument is to rigorously bound the interior generalization gap. Recall that a stable minima $f \in \mathcal{F}_{\text{stable}}(\eta)$ satisfies $|f|_{V_g} \leq A$ with respect to the empirical weight function g . To analyze the complexity of its restriction f^ε on the core \mathbb{I}_ε^d , we need a lower bound on $g_{\min}^\varepsilon := \inf_{|t| \leq 1-\varepsilon} g(\mathbf{u}, t)$. This quantity is a random variable.

From empirical process we discussed in Section E.2, especially Theorem E.5, we know that with probability at least $1 - \delta/3$,

$$\sup_{\mathbf{u}, t} |g(\mathbf{u}, t) - g_P(\mathbf{u}, t)| \lesssim_d \sqrt{\frac{d + \log(6/\delta)}{n}} =: \epsilon_n. \quad (75)$$

This implies a lower bound on the empirical minimum weight in the core with probability at least $1 - \delta/3$,

$$g_{\min}^\varepsilon = \inf_{|t| \leq 1-\varepsilon} g(\mathbf{u}, t) \geq \underbrace{\inf_{|t| \leq 1-\varepsilon} g_P(\mathbf{u}, t)}_{g_{P, \min}^\varepsilon} - \epsilon_n = g_{P, \min}^\varepsilon - \epsilon_n. \quad (76)$$

Here, $g_{P, \min}^\varepsilon \asymp \varepsilon^{d+2}$ is the minimum of the population weight function in the core.

For the bound $|f^\varepsilon|_V \leq A/g_{\min}^\varepsilon \leq A/(g_{P, \min}^\varepsilon - \epsilon_n)$ to be meaningful with high probability, we must operate in a regime where $g_{\min}^\varepsilon \geq \epsilon_n$. We enforce a stricter **validity condition** for our proof

$$g_{\min}^\varepsilon \geq 2\epsilon_n \implies \varepsilon^{d+2} \gtrsim_d n^{-\frac{1}{2}}. \quad (77)$$

Therefore, we may choose

$$\varepsilon \asymp \left(A^{\frac{d}{d^2+4d+3}} \cdot \sqrt{\frac{d + \log(6/\delta)}{n}} \right)^{\frac{1}{d+2}} \quad (78)$$

Under this condition, we have $g_{\min}^\varepsilon \geq g_{P,\min}^\varepsilon - \varepsilon_n \geq g_{P,\min}^\varepsilon/2 \asymp \varepsilon^{d+2}$. Thus, for any stable solution f , its restriction f^ε has a controlled unweighted variation norm with high probability:

$$|f^\varepsilon|_{\mathbb{V}(\mathbb{B}_{1-\varepsilon}^d)} \leq \frac{A}{g_{\min}^\varepsilon} \leq \frac{A}{g_{P,\min}^\varepsilon/2} \asymp \frac{A}{\varepsilon^{d+2}} =: C_\varepsilon.$$

We can now apply the generalization bound from Lemma F.5 to the class $\mathbb{V}_{C_\varepsilon}(\mathbb{B}_{1-\varepsilon}^d)$ by plugging in (78), with probability $1 - \delta/3$,

$$\text{Interior Gap (67)} \lesssim_d (C_\varepsilon)^{\frac{d}{2d+3}} M^{\frac{3(d+2)}{2d+3}} n^{-\frac{d+3}{4d+6}} \quad (79)$$

$$= \left(A^{1-\frac{d}{d^2+4d+3}} \sqrt{\frac{n}{d + \log(6/\delta)}} \right)^{\frac{d}{2d+3}} M^{\frac{3(d+2)}{2d+3}} n^{-\frac{d+3}{4d+6}} \quad (80)$$

$$\lesssim_d A^{\frac{d}{d^2+4d+3}} M^{\frac{3(d+2)}{2d+3}} n^{-\frac{3}{4d+6}} \quad (81)$$

where \lesssim_d hides the constants that could depend on d and logarithmic factors of $1/\delta$.

Now we combine the upper bounds (68), (70) and (81) to deduce an upper bound of the generalization gap. With probability $1 - \delta$, we have

$$|R(f) - \hat{R}(f)| \lesssim_d A^{\frac{d}{d^2+4d+3}} M^2 n^{-\frac{1}{2d+4}} + A^{\frac{d}{d^2+4d+3}} M^{\frac{3(d+2)}{2d+3}} n^{-\frac{3}{4d+6}}. \quad (82)$$

Since $n^{-\frac{1}{2d+4}} > n^{-\frac{3}{4d+6}}$ and $M^2 > M^{\frac{3(d+2)}{2d+3}}$ with the assumption $M \geq 1$, we conclude that

$$|R(f) - \hat{R}(f)| \lesssim_d \left(\frac{1}{\eta} - \frac{1}{2} + 4M \right)^{\frac{d}{d^2+4d+3}} M^2 n^{-\frac{1}{2d+4}}, \quad (83)$$

which finishes the proof. \square

Remark F.9. For the generalization gap lower bound (second part of Theorem 3.5), we defer the proof to Appendix I as it relies on a construction that is used to prove Theorem 3.7 from Appendix H.

G Proof of Theorem 3.6: Estimation Error Rate for Stable Minima

G.1 Computation of Local Gaussian Complexity

It is known from Wainwright 2019 that a tight analysis of MSE results from *local gaussian complexity*. We begin with the following proposition that connects the local gaussian complexity to the critical radius.

Proposition G.1 (Wainwright 2019, Chapter 13). *Let \mathcal{F} be a convex model class that contains the constant function 1. Fix design points $\mathbf{x}_1, \dots, \mathbf{x}_n$ in the region of interest and denote the empirical norm*

$$\|f\|_n^2 := \frac{1}{n} \sum_{i=1}^n f(\mathbf{x}_i)^2.$$

For any radius $r > 0$ write

$$\mathcal{F}(r) := \{f \in \mathcal{F} : \|f\|_n \leq r\}, \quad \widehat{\mathcal{G}}_n(r, \mathcal{F}) := \sup_{f \in \mathcal{F}(r)} \frac{1}{n} \sum_{i=1}^n \varepsilon_i f(\mathbf{x}_i),$$

where $\varepsilon_1, \dots, \varepsilon_n \stackrel{i.i.d.}{\sim} \mathcal{N}(0, \sigma^2)$ and $\mathcal{G}_n(r, \mathcal{F}) := \mathbb{E} \widehat{\mathcal{G}}_n(r, \mathcal{F})$.

If δ satisfies the integral inequality

$$\frac{16}{\sqrt{n}} \int_0^r \sqrt{\log N(t, \partial\mathcal{F}, \|\cdot\|_n)} dt \leq \frac{r}{4}, \quad (84)$$

where $\partial\mathcal{F} := \{f_1 - f_2 : f_1, f_2 \in \mathcal{F}\}$, then the local empirical Gaussian complexity obeys

$$\frac{\mathcal{G}_n(r, \mathcal{F})}{r} \leq \frac{r}{2\sigma}. \quad (85)$$

Moreover, with probability at least $1 - \delta$ one has

$$\widehat{\mathcal{G}}_n(r, \mathcal{F}) \leq \frac{r^2}{2\sigma} + r \frac{\sqrt{\log(1/\delta)}}{\sqrt{n}} \quad (\delta > 0). \quad (86)$$

As a result, we can derive an upper bound for the local empirical Gaussian complexity of the variation function class through a careful analysis of the critical radius.

Lemma G.2. *Let $\mathcal{F}_{B,C}(\mathbb{B}_R^d) = \{f \in \mathcal{V}_C(\mathbb{B}_R^d) \mid \|f\|_{L^\infty(\mathbb{B}_R^d)} \leq B\}$. Then with probability at least $1 - \delta$, we have*

$$\frac{1}{n} \sum_{i=1}^n \varepsilon_i (f_1(\mathbf{x}_i) - f_2(\mathbf{x}_i)) \lesssim_d C^{\frac{2d}{2d+3}} n^{-\frac{d+3}{2d+3}} + C^{\frac{d}{2d+3}} n^{-\frac{3d+6}{4d+6}} \sqrt{\log(1/\delta)}, \quad (87)$$

for any two $f_1, f_2 \in \mathcal{F}_{B,C}$.

Proof. As $\partial\mathcal{F}_{B,C} = 2\mathcal{F}_{B,C} \subset \mathcal{F}_{2B,2C}$, bounding the entropy of $\mathcal{F}_{2B,2C}$ suffices. Using $\|f\|_n \leq \|f\|_{L^\infty(\mathbb{B}_1^d)}$ and referring to Proposition F.4, we have, up to logarithmic factors,

$$\log N(t, \mathcal{F}_{2B,2C}, \|\cdot\|_n) \lesssim_d \left(\frac{C}{t}\right)^{\frac{2d}{d+3}}.$$

Plugging this entropy bound into the left side of (84) and integrating,

$$\frac{16}{\sqrt{n}} \int_0^r \left(\frac{C}{t}\right)^{\frac{d}{d+3}} dt \lesssim_d \frac{C^{\frac{d}{d+3}}}{\sqrt{n}} \int_0^r t^{-\frac{d}{d+3}} dt = \frac{C^{\frac{d}{d+3}} r^{\frac{3}{d+3}}}{\sqrt{n}}.$$

Hence inequality (84) is met provided

$$\frac{C^{\frac{d}{d+3}} r^{\frac{3}{d+3}}}{\sqrt{n}} \lesssim_d \frac{r}{4}, \quad \iff \quad r^{\frac{d}{d+3}} \gtrsim_d C^{\frac{d}{d+3}} n^{-1/2}.$$

Solving for r^2 (and keeping only dominant terms) yields

$$r_n^2 \lesssim_d C^{\frac{2d}{2d+3}} n^{-\frac{d+3}{2d+3}}.$$

With this choice of r_n , Proposition G.1 guarantees

$$\mathcal{G}_n(\mathcal{F}_{B,C}(r_n)) \lesssim_d r_n,$$

and the high-probability version (86) holds verbatim. \square

G.2 Proof of the Estimation Error Upper Bound

Given the local gaussian complexity upper bound, together with the assumption of solutions being “optimized”, we can prove the following MSE upper bound.

Theorem G.3 (Restate Theorem 3.6). *Fix a step size $\eta > 0$ and noise level $\sigma > 0$. Given a ground truth function $f_0 \in \mathcal{V}_g(\mathbb{B}_1^d)$ such that $\|f_0\|_{L^\infty} \leq B$ and $|f_0|_{\mathcal{V}_g} \leq \tilde{O}\left(\frac{1}{\eta} - \frac{1}{2} + 2\sigma\right)$, suppose that we are given a data set $y_i = f_0(\mathbf{x}_i) + \varepsilon_i$, where \mathbf{x}_i are i.i.d. $\text{Uniform}(\mathbb{B}_1^d)$ and ε_i are i.i.d. $\mathcal{N}(0, \sigma^2)$. Then, with probability at least $1 - \delta$, we have that*

$$\frac{1}{n} \sum_{i=1}^n (f_\theta(\mathbf{x}_i) - f_0(\mathbf{x}_i))^2 \lesssim_d \left(\frac{1}{\eta} - \frac{1}{2} + 2\sigma\right)^{\frac{d}{(2d^2+6d+3)(d+2)}} B^2 \left(\frac{\sigma^2}{n}\right)^{\frac{1}{2d+4}}, \quad (88)$$

for any $f_\theta \in \mathcal{F}_{\text{stable}}(\eta)$ that is optimized, i.e., $(f_\theta(\mathbf{x}_i) - y_i)^2 \leq (f_0(\mathbf{x}_i) - y_i)^2$, for $i = 1, \dots, n$. Here, \lesssim_d hides constants (that could depend on d) and logarithmic factors in n and $(1/\delta)$.

Proof of Theorem 3.6. The empirical Mean Squared Error (MSE) we want to bound is $\text{MSE}(f_\theta, f_0) = \frac{1}{n} \sum_{i=1}^n (f_\theta(\mathbf{x}_i) - f_0(\mathbf{x}_i))^2$.

First, we establish bounds on the regularity of $f_\theta(\mathbf{x}) - f_0(\mathbf{x})$. The condition that f_θ is “optimized” means $(f_\theta(\mathbf{x}_i) - y_i)^2 \leq (f_0(\mathbf{x}_i) - y_i)^2$ for all i . Summing over i and dividing by n , we have $\frac{1}{n} \sum_{i=1}^n (f_\theta(\mathbf{x}_i) - y_i)^2 \leq \frac{1}{n} \sum_{i=1}^n (f_0(\mathbf{x}_i) - y_i)^2 = \frac{1}{n} \sum_{i=1}^n \varepsilon_i^2$. Since $\varepsilon_i \sim \mathcal{N}(0, \sigma^2)$, $\mathbb{E}[\frac{1}{n} \sum_{i=1}^n \varepsilon_i^2] = \sigma^2$. Standard concentration inequalities (e.g., for sums of $\chi^2(1)$ scaled variables) show that $\frac{1}{n} \sum_{i=1}^n \varepsilon_i^2 \lesssim \sigma^2$ with high probability (hiding logarithmic factors in $1/\delta$, which are absorbed into \lesssim_d). Thus, $2\mathcal{L}(\theta) \lesssim \sigma^2$. For $f_\theta \in \mathcal{F}_{\text{stable}}(\eta)$, by Corollary 3.3 (with $R = 1$ for \mathbb{B}_1^d , so $R + 1 = 2$), we have

$$|f_\theta|_{\mathcal{V}_g} \leq \frac{1}{\eta} - \frac{1}{2} + 2\sqrt{2\mathcal{L}(\theta)} \leq \frac{1}{\eta} - \frac{1}{2} + 2\sigma. \quad (89)$$

Let $C := \frac{1}{\eta} - \frac{1}{2} + 2\sigma$. The theorem assumes $|f_0|_{\mathcal{V}_g} \leq C$. Thus, we have $|f_0|_{\mathcal{V}_g} \lesssim C$. The difference $f_\theta(\mathbf{x}) - f_0(\mathbf{x})$ then satisfies

$$|f_\theta - f_0|_{\mathcal{V}_g} \leq |f_\theta|_{\mathcal{V}_g} + |f_0|_{\mathcal{V}_g} \leq 2C. \quad (90)$$

Also, $\|f_\theta - f_0\|_{L^\infty(\mathbb{B}_1^d)} \leq \|f_\theta\|_{L^\infty(\mathbb{B}_1^d)} + \|f_0\|_{L^\infty(\mathbb{B}_1^d)} \leq B + B = 2B$.

The optimized condition $(f_\theta(\mathbf{x}_i) - y_i)^2 \leq (f_0(\mathbf{x}_i) - y_i)^2$ implies $((f_\theta(\mathbf{x}_i) - f_0(\mathbf{x}_i)) - \varepsilon_i)^2 \leq \varepsilon_i^2$. Expanding this gives $(f_\theta(\mathbf{x}_i) - f_0(\mathbf{x}_i))^2 - 2(f_\theta(\mathbf{x}_i) - f_0(\mathbf{x}_i))\varepsilon_i + \varepsilon_i^2 \leq \varepsilon_i^2$, which simplifies to

$$(f_\theta(\mathbf{x}_i) - f_0(\mathbf{x}_i))^2 \leq 2(f_\theta(\mathbf{x}_i) - f_0(\mathbf{x}_i))\varepsilon_i. \quad (91)$$

This inequality is crucial and holds for each data point.

We decompose the MSE based on the location of data points. Let $\mathbb{A}_\varepsilon^d := \{\mathbf{x} \in \mathbb{B}_1^d : \|\mathbf{x}\|_2 \geq 1 - \varepsilon\}$ be the annulus and $\mathbb{B}_{1-\varepsilon}^d$ be the inner core. Let $S_A := \{i : \mathbf{x}_i \in \mathbb{A}_\varepsilon^d\}$ and $S_I := \{i : \mathbf{x}_i \in \mathbb{B}_{1-\varepsilon}^d\}$. The total empirical MSE is

$$\begin{aligned} \text{MSE}(f_\theta, f_0) &= \frac{1}{n} \sum_{i \in S_A} (f_\theta(\mathbf{x}_i) - f_0(\mathbf{x}_i))^2 + \frac{1}{n} \sum_{i \in S_I} (f_\theta(\mathbf{x}_i) - f_0(\mathbf{x}_i))^2 \\ &\leq \frac{n_A}{n} \left(\frac{1}{n_A} \sum_{i \in S_A} (f_\theta(\mathbf{x}_i) - f_0(\mathbf{x}_i))^2 \right) + \frac{n_I}{n} \left(\frac{1}{n_I} \sum_{i \in S_I} (f_\theta(\mathbf{x}_i) - f_0(\mathbf{x}_i))^2 \right) \\ &\leq \underbrace{\frac{n_A}{n} \left(\frac{1}{n_A} \sum_{i \in S_A} (f_\theta(\mathbf{x}_i) - f_0(\mathbf{x}_i))^2 \right)}_{\text{MSE}_S} + \underbrace{\frac{1}{n_I} \sum_{i \in S_I} (f_\theta(\mathbf{x}_i) - f_0(\mathbf{x}_i))^2}_{\text{MSE}_I} \end{aligned} \quad (92)$$

The contribution from the shell, $\text{MSE}_{\mathcal{S}}$, is bounded using the L^∞ norm of $f_\theta - f_0$ and the concentration of points in the shell. Let $n_A := |S_A|$. By Lemma F.7, $n_A/n \lesssim \varepsilon$ with high probability.

$$\text{MSE}_{\mathcal{S}} \leq \frac{n_A}{n} \|f_\theta - f_0\|_{L^\infty}^2 \leq \frac{n_A}{n} (2B)^2 \lesssim_d B^2 \varepsilon. \quad (93)$$

For the inner core's contribution, $\text{MSE}_{\mathcal{I}}$, we use Equation (91):

$$\text{MSE}_{\mathcal{I}} = \frac{1}{n} \sum_{i \in S_I} (f_\theta(\mathbf{x}_i) - f_0(\mathbf{x}_i))^2 \leq \frac{2}{n} \sum_{i \in S_I} (f_\theta(\mathbf{x}_i) - f_0(\mathbf{x}_i)) \varepsilon_i. \quad (94)$$

Let $n_I := |S_I|$. The empirical process term is $2 \frac{n_I}{n} \left(\frac{1}{n_I} \sum_{i \in S_I} (f_\theta(\mathbf{x}_i) - f_0(\mathbf{x}_i)) \varepsilon_i \right)$. The function $f_\theta - f_0$ restricted to $\mathbb{B}_{1-\varepsilon}^d$ has an unweighted variation norm. As shown in Appendix E, for $\mathbf{x} \in \text{Uniform}(\mathbb{B}_1^d)$, the population weight function $g_P(\mathbf{u}, t) \asymp (1 - |t|)^{d+2}$. For activation hyperplanes relevant to $\mathbb{B}_{1-\varepsilon}^d$ (i.e., $|t| \leq 1 - \varepsilon$), $g_P(\mathbf{u}, t) \gtrsim \varepsilon^{d+2}$. Thus, the unweighted variation of $f_\theta - f_0$ on $\mathbb{B}_{1-\varepsilon}^d$ is

$$|f_\theta - f_0|_{V(\mathbb{B}_{1-\varepsilon}^d)} \lesssim |f_\theta - f_0|_{V_{g_P}} / \varepsilon^{d+2} \lesssim C / \varepsilon^{d+2}. \quad (95)$$

We apply Lemma G.2 to bound $\frac{1}{n_I} \sum_{i \in S_I} (f_\theta(\mathbf{x}_i) - f_0(\mathbf{x}_i)) \varepsilon_i$. The function $h(\mathbf{x}) = f_\theta(\mathbf{x}) - f_0(\mathbf{x})$ has unweighted variation $\lesssim C / \varepsilon^{d+2}$ and L^∞ norm $\leq 2B$. Therefore, we have that

$$\text{MSE}_{\mathcal{I}} \lesssim \left(\frac{C}{\varepsilon^{d+2}} \right)^{\frac{2d}{2d+3}} \left(\frac{\sigma^2}{n} \right)^{\frac{d+3}{2d+3}}. \quad (96)$$

Combining the bounds for $\text{MSE}_{\mathcal{S}}$ and $\text{MSE}_{\mathcal{I}}$:

$$\text{MSE}(f_\theta, f_0) \lesssim B^2 \varepsilon + C^{\frac{2d}{2d+3}} \varepsilon^{-(d+2)\frac{2d}{2d+3}} \left(\frac{\sigma^2}{n} \right)^{\frac{d+3}{2d+3}}. \quad (97)$$

Similarly to the proof of Theorem 3.5 in Appendix F.5, we require that

$$\frac{1}{\inf_{|t| \leq 1-\varepsilon} g_P(\mathbf{u}, t)} \asymp \varepsilon^{d+2} \gtrsim_d \sqrt{\frac{1}{n}}. \quad (98)$$

to filling the gap between the empirical weighted function g and the population g_P with high probability, because with high probability,

$$\sup_{\mathbf{u}, t} |g(\mathbf{u}, t) - g_P(\mathbf{u}, t)| \lesssim_d \sqrt{\frac{1}{n}} \quad (99)$$

where \lesssim_d hides constants (which could depend on d) and logarithmic factors, as stated by Theorem E.5 in Section E.2. Therefore, we may choose

$$\varepsilon \asymp \left(C^{\frac{2d}{2d^2+6d+3}} \cdot \frac{\sigma^2}{n} \right)^{\frac{1}{2d+4}}, \quad (100)$$

and plug it into (97) to have

$$\text{MSE}(f_\theta, f_0) \lesssim_d \left(\frac{1}{\eta} - \frac{1}{2} + 2\sigma \right)^{\frac{d}{(2d^2+6d+3)(d+2)}} \left(B^2 \left(\frac{\sigma^2}{n} \right)^{\frac{1}{2d+4}} + \left(\frac{\sigma^2}{n} \right)^{\frac{3}{2d+3}} \right). \quad (101)$$

Since $\frac{1}{2d+4} < \frac{3}{2d+3}$, we conclude that

$$\text{MSE}(f_\theta, f_0) \lesssim_d \left(\frac{1}{\eta} - \frac{1}{2} + 2\sigma \right)^{\frac{d}{(2d^2+6d+3)(d+2)}} B^2 \left(\frac{\sigma^2}{n} \right)^{\frac{1}{2d+4}},$$

which completes the proof. \square

H Proof of Theorem 3.7: Minimax Lower Bound

H.1 Preliminaries: Minimax Risk and Fano's Lemma

Minimax lower bounds are fundamental tools in statistical theory for characterizing the intrinsic difficulty of an estimation problem over a class of functions or parameters. They provide a benchmark against which the performance of any estimator can be compared.

Definition H.1 (Minimax Risk). Let \mathcal{F} be a class of functions $f : \mathcal{X} \rightarrow \mathcal{Y}$. Suppose we observe data $\mathcal{D}_n = \{(\mathbf{x}_i, y_i)\}_{i=1}^n$, where y_i are typically noisy observations related to $f(\mathbf{x}_i)$. Let $\hat{f} = \hat{f}(\mathcal{D}_n)$ be an estimator of f , constructed based on the data \mathcal{D}_n . Given a loss function $L(f, \hat{f})$ that quantifies the discrepancy between f and \hat{f} (e.g., $L(f, \hat{f}) = \|f - \hat{f}\|_{L^2(\mathcal{X})}^2$), the risk of an estimator \hat{f} for a specific $f \in \mathcal{F}$ is its expected loss:

$$R(f, \hat{f}) = \mathbb{E}_{\mathcal{D}_n} [L(f, \hat{f})], \quad (102)$$

where the expectation is taken over the distribution of the data \mathcal{D}_n given f . The *maximum risk* of the estimator \hat{f} over the class \mathcal{F} is

$$\sup_{f \in \mathcal{F}} R(f, \hat{f}). \quad (103)$$

This quantity measures the worst-case performance of the estimator \hat{f} over all possible functions in \mathcal{F} . The *minimax risk* for estimating functions in \mathcal{F} is defined as

$$\mathcal{R}_n(\mathcal{F}) = \inf_{\hat{f}} \sup_{f \in \mathcal{F}} R(f, \hat{f}), \quad (104)$$

where the infimum is taken over all possible estimators \hat{f} . The minimax risk represents the best possible worst-case performance achievable by any estimator. It is a fundamental property of the function class \mathcal{F} , the sample size n , the data-generating process, and the chosen loss function, indicating the inherent statistical difficulty of the estimation problem. A lower bound on the minimax risk demonstrates that no estimator can achieve a better rate of convergence than this bound.

H.2 The Multivariate Case

In this section, we assume that $d > 1$ and all the norms and semi-norms are restricted to the unit ball \mathbb{B}_1^d . Let $\mathbf{u} \in \mathbb{S}^{d-1}$ be a unit vector. Let $\varepsilon \in \mathbb{R}_+$ be a constant with $\varepsilon \leq 1/2$. Consider the ReLU atom:

$$\varphi_{\mathbf{u}, \varepsilon^2}(\mathbf{x}) = \phi(\mathbf{u}^\top \mathbf{x} - (1 - \varepsilon^2)). \quad (105)$$

Lemma H.2. *The L^2 -norm of $\varphi_{\mathbf{u}, \varepsilon^2}$ over \mathbb{B}_1^d is given by*

$$\|\varphi_{\mathbf{u}, \varepsilon^2}\|_{L^2(\mathbb{B}_1^d)} \underset{c_7(d)}{\overset{c_8(d)}{\asymp}} \varepsilon^{\frac{d+5}{2}}, \quad (106)$$

where $c_7(d)$ and $c_8(d)$ are constants depends on d (the concrete definition is (113)). Recall that $\underset{c_7(d)}{\overset{c_8(d)}{\asymp}}$ means

$$c_7(d) \varepsilon^{\frac{d+5}{2}} \leq \|\varphi_{\mathbf{u}, \varepsilon^2}\|_{L^2(\mathbb{B}_1^d)} \leq c_8(d) \varepsilon^{\frac{d+5}{2}}.$$

Proof. The squared L^2 norm of $\varphi_{\mathbf{u}, \varepsilon^2}$ over the unit ball \mathbb{B}_1^d is defined as:

$$\|\varphi_{\mathbf{u}, \varepsilon^2}\|_{L^2(\mathbb{B}_1^d)}^2 = \int_{\mathbb{B}_1^d} |\varphi_{\varepsilon^2}(\mathbf{x})|^2 d\mathbf{x}$$

Substituting the definition of $\varphi_{\varepsilon^2}(\mathbf{w}, \mathbf{x})$ and using the property of the ReLU function that $\phi(z) = z$ for $z > 0$ and $\phi(z) = 0$ for $z \leq 0$, we get:

$$\begin{aligned} \|\varphi_{\mathbf{u}, \varepsilon^2}\|_{L^2(\mathbb{B}_1^d)}^2 &= \int_{\mathbb{B}_1^d} [\phi(\mathbf{u}^\top \mathbf{x} - (1 - \varepsilon^2))]^2 d\mathbf{x} \\ &= \int_{\{\mathbf{x} \in \mathbb{B}_1^d : \mathbf{u}^\top \mathbf{x} > 1 - \varepsilon^2\}} (\mathbf{u}^\top \mathbf{x} - (1 - \varepsilon^2))^2 d\mathbf{x} \end{aligned} \quad (107)$$

To simplify the integral, we perform a rotation of the coordinate system such that \mathbf{w} aligns with the d -th standard basis vector $e_d = (0, \dots, 0, 1)$. In these new coordinates, $\mathbf{u}^\top \mathbf{x} = X_d$. The unit ball remains the unit ball under rotation. The integral becomes:

$$I = \|\varphi_{\mathbf{u}, \varepsilon^2}\|_{L^2(\mathbb{B}_1^d)}^2 = \int_{\{X \in \mathbb{B}_1^d : X_d > 1 - \varepsilon^2\}} (X_d - (1 - \varepsilon^2))^2 dX$$

We can write the volume element dX as $dX' dX_d$, where $X' \in \mathbb{R}^{d-1}$ represents the first $d-1$ coordinates. The condition $X \in \mathbb{B}_1^d$ translates to $\|X'\|_2^2 + X_d^2 \leq 1$. The integral can be written as an iterated integral:

$$I = \int_{1 - \varepsilon^2}^1 \left(\int_{\|X'\|_2^2 \leq 1 - X_d^2} (X_d - (1 - \varepsilon^2))^2 dX' \right) dX_d$$

The inner integral is over a $(d-1)$ -dimensional ball in \mathbb{R}^{d-1} with radius $R = \sqrt{1 - X_d^2}$. The integrand $(X_d - (1 - \varepsilon^2))^2$ is constant with respect to X' . Therefore, the inner integral evaluates to:

$$(X_d - (1 - \varepsilon^2))^2 \cdot \text{Vol}_{d-1}(R)$$

where $\text{Vol}_{d-1}(R)$ is the volume of the $(d-1)$ -dimensional ball of radius R . This volume is given by $V_{d-1} R^{d-1}$, with $V_{d-1} = \frac{\pi^{(d-1)/2}}{\Gamma(\frac{d+1}{2})}$. So, the inner integral is $(X_d - (1 - \varepsilon^2))^2 V_{d-1} (1 - X_d^2)^{(d-1)/2}$, and the outer integral becomes:

$$I = V_{d-1} \int_{1 - \varepsilon^2}^1 (X_d - (1 - \varepsilon^2))^2 (1 - X_d^2)^{\frac{d-1}{2}} dX_d \quad (108)$$

Let $X_d = 1 - \delta$ performing a change of variable. Then $dX_d = -d\delta$. The integration limits change

$$\begin{aligned} I &= V_{d-1} \int_{\varepsilon^2}^0 ((1 - \delta) - (1 - \varepsilon^2))^2 (1 - (1 - \delta)^2)^{\frac{d-1}{2}} (-d\delta) \\ &= V_{d-1} \int_0^{\varepsilon^2} (\varepsilon^2 - \delta)^2 (1 - (1 - 2\delta + \delta^2))^{\frac{d-1}{2}} d\delta \\ &= V_{d-1} \int_0^{\varepsilon^2} (\varepsilon^2 - \delta)^2 (2\delta - \delta^2)^{\frac{d-1}{2}} d\delta \end{aligned} \quad (109)$$

Since we assumed $\varepsilon^2 < \frac{1}{4}$, for the integration range $[0, \varepsilon^2]$, we may write $2\delta - \delta^2 = (2 - \delta)\delta \asymp_{7/4}^2 2\delta$.

$$\left(\frac{7}{4}\right)^{\frac{d-1}{2}} \delta^{\frac{d-1}{2}} \leq (2\delta - \delta^2)^{\frac{d-1}{2}} \leq 2^{\frac{d-1}{2}} \delta^{\frac{d-1}{2}}$$

The integral is approximated by:

$$V_{d-1} \left(\frac{7}{4}\right)^{\frac{d-1}{2}} \int_0^{\varepsilon^2} (\varepsilon^2 - \delta)^2 \delta^{\frac{d-1}{2}} d\delta \leq I \leq V_{d-1} 2^{\frac{d-1}{2}} \int_0^{\varepsilon^2} (\varepsilon^2 - \delta)^2 \delta^{\frac{d-1}{2}} d\delta \quad (110)$$

Consider another change of variable: $\delta = \varepsilon^2 s$. Then $d\delta = \varepsilon^2 ds$. The limits change

$$\begin{aligned}
\int_0^{\varepsilon^2} (\varepsilon^2 - \delta)^2 \delta^{\frac{d-1}{2}} d\delta &= \int_0^1 (\varepsilon^2 - \varepsilon^2 s)^2 (\varepsilon^2 s)^{\frac{d-1}{2}} (\varepsilon^2 ds) \\
&= \int_0^1 (\varepsilon^2)^2 (1-s)^2 (\varepsilon^2)^{(d-1)/2} s^{\frac{d-1}{2}} \varepsilon^2 ds \\
&= (\varepsilon^2)^{2+\frac{d-1}{2}+1} \int_0^1 (1-s)^2 s^{\frac{d-1}{2}} ds \\
&= \varepsilon^{d+5} \int_0^1 (1-s)^2 s^{\frac{d-1}{2}} ds \\
&= \underbrace{\left(\int_0^1 (1-s)^2 s^{\frac{d-1}{2}} ds \right)}_{\text{constant}} \varepsilon^{d+5}
\end{aligned} \tag{111}$$

The L^2 norm is the square root of I is given by

$$c_7(d) \varepsilon^{\frac{d+5}{2}} \leq \|\varphi_{\mathbf{u}, \varepsilon^2}\|_{L^2(\mathbb{B}_1^d)} = \sqrt{I} \leq c_8(d) \varepsilon^{\frac{d+5}{2}} \tag{112}$$

where $c_7(d)$ and $c_8(d)$ are constants defined by

$$\begin{aligned}
c_7(d) &= \sqrt{V_{d-1} \left(\frac{7}{4}\right)^{\frac{d-1}{2}} \left(\int_0^1 (1-s)^2 s^{\frac{d-1}{2}} ds\right)} \\
c_8(d) &= \sqrt{V_{d-1} 2^{\frac{d-1}{2}} \left(\int_0^1 (1-s)^2 s^{\frac{d-1}{2}} ds\right)}
\end{aligned} \tag{113}$$

This completes the proof. \square

Lemma H.3. *Let $\varphi_{\mathbf{u}, \varepsilon^2}$ be a ReLU atom defined in (105). Then*

$$|\varphi_{\mathbf{u}, \varepsilon^2}|_{V_g} = \varepsilon^{2d+4}. \tag{114}$$

Proof. We decode the definition (see Example 3.1) and compute directly the weighted function $g(\mathbf{u}, 1 - \varepsilon^2) = (\varepsilon^2)^{d+2} = \varepsilon^{2d+4}$. \square

Let \mathbb{S}^{d-1} be the unit sphere in \mathbb{R}^d . For $0 < \varepsilon < 1$ and $\mathbf{w} \in \mathbb{S}^{d-1}$, define the spherical cap $C(\mathbf{u}, \varepsilon^2)$ as

$$C(\mathbf{u}, \varepsilon^2) = \{\mathbf{x} \in \mathbb{S}^{d-1} : \mathbf{u}^\top \mathbf{x} \geq 1 - \varepsilon^2\}. \tag{115}$$

Lemma H.4. *Let $N_{max}(\varepsilon, d)$ denote the maximum number of points $\mathbf{u}_1, \dots, \mathbf{u}_N \in \mathbb{S}^{d-1}$ such that the caps $C(\mathbf{u}_i, \varepsilon^2)$ are mutually disjoint. Then, as $\varepsilon \rightarrow 0$,*

$$N_{max}(\varepsilon, d) \asymp \varepsilon^{-(d-1)}$$

where the implicit constants depend only on the dimension d .

Proof. The spherical cap $C(\mathbf{u}, \varepsilon^2)$ has an angular radius $\vartheta = \arccos(1 - \varepsilon^2)$, satisfying $\vartheta = \Theta(\varepsilon)$ for small ε . The condition that caps $C(\mathbf{u}_i, \varepsilon^2)$ and $C(\mathbf{u}_j, \varepsilon^2)$ are disjoint requires the angular separation ϕ_{ij} between their centers \mathbf{w}_i and \mathbf{w}_j to be at least 2θ . Thus, $N_{max}(\varepsilon, d)$ is the maximum size $M(\mathbb{S}^{d-1}, 2\theta)$ of a 2θ -separated set (packing number) on \mathbb{S}^{d-1} .

The upper bound $N_{max}(\varepsilon, d) = O(\varepsilon^{-(d-1)})$ follows from a surface area argument: N disjoint caps $C(\mathbf{u}_i, \varepsilon^2)$, each with surface area $\Theta(\vartheta^{d-1}) = \Theta(\varepsilon^{d-1})$, must fit within the total surface area of \mathbb{S}^{d-1} .

For the lower bound, we relate the packing number $M(\mathbb{S}^{d-1}, \alpha)$ to the covering number $N(\mathbb{S}^{d-1}, \alpha)$, the minimum number of caps of angular radius α needed to cover \mathbb{S}^{d-1} . It is a standard result that these quantities are closely related, for instance, $M(\mathbb{S}^{d-1}, \alpha) \geq N(\mathbb{S}^{d-1}, \alpha)$ can be shown via a greedy packing argument [Vershynin, 2018, see discussions in Chapter 4]. Furthermore, the asymptotic behavior of the covering number is known to be $N(\mathbb{S}^{d-1}, \alpha) \asymp \alpha^{-(d-1)}$ for small α [Vershynin, 2018, Corollary 4.2.14]. Setting the minimum separation $\alpha = 2\vartheta = \Theta(\varepsilon)$, we obtain the lower bound:

$$N_{max}(\varepsilon, d) = M(\mathbb{S}^{d-1}, 2\vartheta) \geq N(\mathbb{S}^{d-1}, 2\vartheta) \asymp (2\vartheta)^{-(d-1)} = \Omega(\varepsilon^{-(d-1)}),$$

where the implicit constants depend only on the dimension d . Combining the upper and lower bounds, we conclude that $N_{max}(\varepsilon, d) \asymp \varepsilon^{-(d-1)}$. \square

Construction H.5. We construct a suitable packing set in $\mathcal{F} = \{f \in V_g(\mathbb{B}_1^d) : \|f\|_{L^\infty} \leq 1, |f|_{V_g} \leq 1\}$ based on a weighted ReLU atoms. Let $\varphi_{\mathbf{u}, \varepsilon^2}$ be the ReLU atom defined in (105), and according to Lemma H.2 and Lemma H.3:

$$\Phi_{\mathbf{u}, \varepsilon^2} := \varepsilon^{-2} \varphi_{\mathbf{u}, \varepsilon^2} \implies \begin{cases} \|\Phi_{\mathbf{u}, \varepsilon^2}\|_{L^\infty(\mathbb{B}_1^d)} = 1, \\ \|\Phi_{\mathbf{u}, \varepsilon^2}\|_{L^2(\mathbb{B}_1^d)} \asymp \varepsilon^{\frac{d+1}{2}}, \\ |\Phi_{\mathbf{u}, \varepsilon^2}|_{V_g} = \varepsilon^{2d+2}. \end{cases} \quad (116)$$

According to Lemma H.2, there exists $N = c_N(d)\varepsilon^{-d+1}$ spherical caps $\mathbf{u}_1, \dots, \mathbf{u}_N$ such that the caps $C(\mathbf{u}_i, \varepsilon^2)$ are mutually disjoint, for some constant $c_N(d) \leq 1$ that may depend on the dimension d . For convenience, we simply denote $\Phi_i = \Phi_{\mathbf{u}_i, \varepsilon^2}$. Therefore, we have $|N \Phi_i|_{V_g} = c_N(d) \varepsilon^{d+3} < 1$ referring to (116). For each $\xi = (\xi_1, \dots, \xi_N) \in \{-1, 1\}^N$, define

$$f_\xi(\mathbf{x}) = \sum_{i=1}^N \xi_i \Phi_i(\mathbf{x}).$$

According to the conventions, each f_ξ belongs to \mathcal{F} . Since the supports of the ridge functions are disjoint, for any $\xi, \xi' \in \{-1, 1\}^N$ we have

$$\|f_\xi - f_{\xi'}\|_{L^2(\mathbb{B}_1^d)}^2 = \sum_{i \in S} \|2\Phi_i\|_{L^2(\mathbb{B}_1^d)}^2 \asymp \varepsilon^{\frac{d+1}{2}} d_H(\xi, \xi'),$$

where $d_H(\xi, \xi')$ denotes the Hamming distance between ξ and ξ' , and S is the set of indices where $\xi_i \neq \xi'_i$. By the Varshamov–Gilbert lemma, there exists a subset $\Xi \subset \{-1, 1\}^N$ with

$$\log |\Xi| = K \asymp \varepsilon^{-d+1}.$$

for some constant, and such that for any distinct $\xi, \xi' \in \Xi$, the Hamming distance d_H

$$d_H(\xi, \xi') \gtrsim K.$$

Thus, for any distinct $\xi, \xi' \in \Xi$, we obtain

$$\|f_\xi - f_{\xi'}\|_{L^2(\mathbb{B}_1^d)} \gtrsim \varepsilon^{\frac{d+1}{2}} \sqrt{K} \asymp \varepsilon^{\frac{d+1}{2}} \varepsilon^{-\frac{d+1}{2}} = \varepsilon.$$

Proposition H.6 (Minimax Lower Bound via Fano's Lemma). *Consider the problem of estimating a function $f \in \mathcal{F} = \{f \in V_g(\mathbb{B}_1^d) : \|f\|_{L^\infty} \leq 1, |f|_{V_g} \leq 1\}$ with*

$$y_i = f(\mathbf{x}_i) + \varepsilon_i, \quad i = 1, \dots, n$$

where $\{\varepsilon_i\}_{i=1}^n$ are i.i.d. $\mathcal{N}(0, \sigma^2)$ random variables and $\{\mathbf{x}_i\}_{i=1}^n \subset \mathbb{B}_1^d$ are i.i.d. uniform random variables on \mathbb{B}_1^d . The lower bound of the minimax non-parametric risk is given by

$$\inf_{\hat{f}} \sup_{f \in \mathcal{F}} \mathbb{E} \|\hat{f} - f\|_{L^2(\mathbb{B}_1^d)}^2 \gtrsim \left(\frac{\sigma^2}{n}\right)^{\frac{2}{d+1}}.$$

Proof. We use the standard Fano's lemma argument. By our Construction (105), we have a packing set $\{f_\xi : \xi \in \Xi\}$ in \mathcal{F} with the following properties:

1. The L^2 -distance between any two distinct functions is at least δ , where $\delta \asymp \varepsilon$.
2. The size of the packing set satisfies $\log |\Xi| \gtrsim K \asymp \varepsilon^{-(d-1)}$.

For Gaussian noise with variance σ^2 , the Kullback–Leibler divergence between the distributions induced by two functions f_ξ and $f_{\xi'}$ is

$$\text{KL}(P_\xi \| P_{\xi'}) = \frac{n}{2\sigma^2} \|f_\xi - f_{\xi'}\|_{L^2(\mathbb{B}_1^d)}^2 = \frac{n \delta^2}{2\sigma^2}.$$

In order to use Fano's lemma J.1 effectively, we need to satisfy the requirement (140), where in this context is

$$\frac{n \delta^2}{2\sigma^2} \lesssim \log |\Theta|$$

for some small constant $\alpha > 0$, then the minimax risk is bounded from below by a constant multiple of δ^2 .

Substituting $\delta \asymp \varepsilon$ and $\log |\Xi| \gtrsim \varepsilon^{-(d-1)}$, the condition becomes

$$\frac{n \varepsilon^2}{\sigma^2} \lesssim \varepsilon^{-(d-1)},$$

or equivalently,

$$n \lesssim \frac{\sigma^2}{\varepsilon^{d+1}}.$$

Solving for ε , we have

$$\varepsilon^{d+1} \asymp \frac{\sigma^2}{n} \implies \varepsilon \asymp \left(\frac{\sigma^2}{n}\right)^{\frac{1}{d+1}}.$$

Then, the separation becomes

$$\delta \asymp \varepsilon \asymp \left(\frac{\sigma^2}{n}\right)^{\frac{1}{d+1}}.$$

Therefore, Fano's lemma J.1 (particularly (139)) yields

$$\inf_{\hat{f}} \sup_{f \in \mathcal{F}} \mathbb{E} \|\hat{f} - f\|_{L^2(\mathbb{B}_1^d)}^2 \gtrsim \delta^2 \asymp \left(\frac{\sigma^2}{n}\right)^{\frac{2}{d+1}},$$

which is the desired result. □

Corollary H.7. Let $\{f \in V_g(\mathbb{B}_1^d) : \|f\|_{L^\infty} \leq B, |f|_{V_g} \leq C\}$. Then

$$\inf_{\hat{f}} \sup_{f \in \mathcal{F}} \mathbb{E} \|\hat{f} - f\|_{L^2}^2 \gtrsim \min(B, C)^2 \left(\frac{\sigma^2}{n}\right)^{\frac{2}{d+1}}.$$

Proof. We just need to replace f_ξ in Construction 105 by $\min(B, C)f_\xi$ and adapt it to the the proof of Proposition H.6. \square

H.3 Why Classical Bump-Type Constructions Are Ineffective

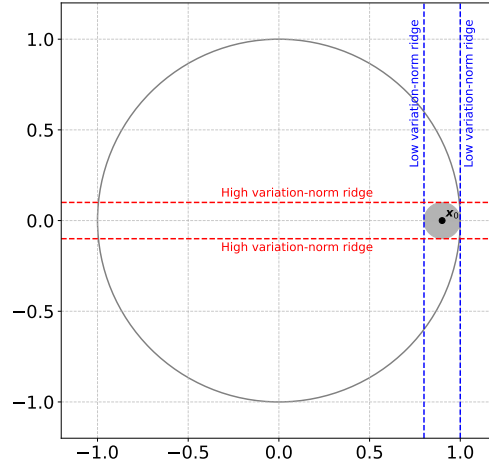


Figure 11: **Isotropic Locality is Costly:** An isotropic bump function, by definition, must be localized (decay rapidly) in all directions around its center. Suppose we place such a bump centered at a point \mathbf{x}_0 near the boundary in direction \mathbf{u}_0 (i.e., $\mathbf{u}_0^\top \mathbf{x}_0 \approx 1 - \varepsilon^2$, here $\mathbf{u}_0 = (1, 0)$). To achieve localization in directions *orthogonal* to \mathbf{u}_0 , one would need to combine ReLU activations whose ridges are oriented appropriately. More critically, to achieve localization in the direction *parallel* to \mathbf{u}_0 (i.e., to ensure the bump decays as we move radially inward from \mathbf{x}_0), we would need ReLU activations whose ridges $\{\mathbf{x} : \mathbf{u}_0^\top \mathbf{x} = t\}$ have $t < 1 - \varepsilon^2$ and are potentially much closer to the origin (i.e., t is significantly smaller than 1).

The minimax lower bound construction in this paper crucially hinges on exploiting the properties of the data-dependent weighted variation norm, denoted as $|\cdot|_{V_g}$, where the weight function is $g(\mathbf{u}, t)$. A key characteristic of $g(\mathbf{u}, t)$ (when data is, for instance, uniform on the unit ball \mathbb{B}_1^d) is that $g(\mathbf{u}, t) \asymp (1 - |t|)^{d+2}$. This implies that $g(\mathbf{u}, t)$ becomes very small as $|t| \rightarrow 1$, i.e., for activations near the boundary of the domain. This property allows for the construction of functions with significant magnitudes near the boundary using a relatively small variation norm. Therefore, any effective construction for the lower bound must create functions that are highly localized near this boundary.

For these ReLU activations whose ridges are not very close to the boundary (i.e., t is not close to 1), the weight function $g(\mathbf{u}_0, t)$ will *not* be small. Consequently, constructing a sharply localized bump isotropically would require a substantial sum of weighted coefficients in the V_g norm to cancel out the function in regions away from its intended support while maintaining a significant peak. This large variation norm would make such functions "too regular" or "too expensive" to serve as effective elements in a packing set for Fano's Lemma, especially when aiming to show a rate degradation due to dimensionality.

In essence, isotropic bump functions do not efficiently leverage the anisotropic nature of the ReLU activation and the specific properties of the $g(\mathbf{u}, t)$ weighting. The construction used in this paper, which employs ReLU atoms active only on thin spherical caps near the boundary (an anisotropic construction), is far more effective. It allows for localization and significant function magnitude primarily by choosing the activation threshold t to be very close to 1 (making $g(\mathbf{u}, t)$ small), rather than by intricate cancellations of many neurons with large weighted coefficients. This is why such anisotropic, boundary-localized constructions are essential for revealing the curse of dimensionality in this setting.

H.4 The Univariate Case

The minimax lower bound construction detailed above, which leverages a packing argument with boundary-localized ReLU neurons exploiting the multiplicity of available directions on \mathbb{S}^{d-1} , is particularly effective in establishing the curse of dimensionality for $d > 1$. However, the geometric foundation of this approach, specifically the ability to pack an exponential number of disjoint spherical caps, does not directly translate to the univariate case ($d = 1$) where the notion of distinct directional activation regions fundamentally changes. Consequently, the lower bound for $d = 1$ necessitates a separate construction or modification of the argument. Fortunately, in the one-dimensional setting, the distinction between isotropic and anisotropic function characteristics, which posed challenges for classical approaches in higher dimensions under the specific data-dependent weighted norm, becomes moot. This simplification allows us to directly employ classical bump function constructions, suitably adapted to the function class, to establish the minimax rates in one dimension.

According to Theorem 3.4, we have

$$|f|_{V_g} = \|g \cdot \mathcal{R}(-\Delta)^{\frac{d+1}{2}} f\|_{\mathcal{M}} \quad (117)$$

When $d = 1$ and f is smooth, (117) is simplified to be

$$|f|_{V_g} = \|f'' \cdot g\|_{\mathcal{M}} = \int_{-1}^1 |f''(x)|g(x) dx = \int_{-1}^1 |f''(x)|(1 - |x|)^3 dx \quad (118)$$

and so is the unweighted variation seminorm

$$|f|_V = \|f''\|_{\mathcal{M}} = \int_{-1}^1 |f''(x)| dx =: \text{TV}^2(f) \quad (119)$$

which is also known as the second-order total variation seminorm. Therefore, the function class of stable minima in univariate case is characterized into

$$\mathcal{F}_{B,C} := \{f: [-1, 1] \rightarrow \mathbb{R} \mid \|f\|_{L^\infty} \leq B, \|f'' \cdot (1 - |\cdot|)^3\|_{\mathcal{M}} \leq C\}. \quad (120)$$

Using this characterization, it is more convenient to smooth bump functions to construct a minimax risk lower bound for stable minima class.

Construction H.8. Consider a smooth compact support function:

$$\Phi(x) = \begin{cases} c \exp(-\frac{1}{1-x^2}) & |x| < 1 \\ 0 & \text{otherwise} \end{cases}. \quad (121)$$

By adjusting the constant c , we may assume

$$\text{TV}^2(\Phi) := \int_{-1}^1 |\Phi''(t)| dt = 1 \quad (122)$$

and let D be a constant such that $\|\Phi(x)\|_{L^2} = \sqrt{2}D$. We can construct a translated and scaled version:

$$\Phi_{a,b}(x) = \Phi\left(\frac{2x - (a+b)}{b-a}\right) \quad \text{for } a < b. \quad (123)$$

and in particular, $\Phi_{a,b}$ has the following properties by directly computations:

$$\begin{cases} \text{supp}(\Phi_{a,b}) &= (a, b), \\ \text{TV}^2(\Phi_{a,b}) &= \frac{1}{b-a}, \\ \|\Phi_{a,b}\|_{L^2([-1,1])} &= \sqrt{b-a}D. \end{cases} \quad (124)$$

Proposition H.9. *Consider the problem of estimating a function $f \in \mathcal{F}_{1,1}$ with*

$$y_i = f(x_i) + \varepsilon_i, \quad i = 1, \dots, n$$

where $\{\varepsilon_i\}_{i=1}^n$ are i.i.d. $\mathcal{N}(0, \sigma^2)$ random variables and $\{x_i\}_{i=1}^n \subset [-1, 1]$ are i.i.d. uniform random variables on $[-1, 1]$. The lower bound of the minimax non-parametric risk is given by

$$\inf_{\hat{f}} \sup_{f \in \mathcal{F}_{1,1}} \mathbb{E} \|f - \hat{f}\|_{L^2([-1,1])}^2 \gtrsim \left(\frac{\sigma^2}{n}\right)^{\frac{1}{2}}$$

Proof. For any $\varepsilon > 0$, we may construct a family. Let $a_k = 1 - \varepsilon + k\varepsilon^2$, $k = 0, \dots, \lfloor \frac{1}{\varepsilon} \rfloor$. We denote $K = \lfloor \frac{1}{\varepsilon} \rfloor$. For each $k = 1, \dots, K$, we define $\Phi_k := \Phi_{a_{k-1}, a_k}$. Since $a_k - a_{k-1} = \varepsilon^2$, we have the following properties

- $\|\Phi_k\|_{L^2} = D \cdot \varepsilon$;
- $\text{TV}^2(\Phi_k) \asymp \frac{1}{\varepsilon^2} \implies \int_{-1}^1 |f''(t)|g(t) dx \lesssim \varepsilon$ because $g(t) < \varepsilon^3$, $\forall t \in [a_{k-1}, a_k]$.

Let $\{\Phi_1, \dots, \Phi_K\}$, $K \asymp \lfloor \frac{1}{\varepsilon} \rfloor$ be such a family of function classes, and any K -terms combination $\{\Phi_1, \dots, \Phi_K\}$ is in $\mathcal{F}_{1,1}$. Then we let

$$\phi : \{\pm 1\}^K \rightarrow \mathcal{F}_{1,1}, \quad \xi = (a_k)_{k=1}^K \mapsto \sum_{k=1}^K a_k \Phi_k =: f_\xi. \quad (125)$$

For any two indexes ξ_1, ξ_2 in $\{\pm 1\}^K$, we have that

$$\|f_{\xi_1} - f_{\xi_2}\|_{L^2} = \varepsilon \sqrt{d_H(\xi_1, \xi_2)}. \quad (126)$$

where d_H is the Hamming distance. Then, using Varshamov-Gilbert's lemma (Lemma J.2), the pruned cube of $\{f_1, \dots, f_M\}$ has a size $M \geq 2^{K/8}$, and each has the property that if $i \neq j$,

$$\|f_i - f_j\|_{L^2([-1,1])} \geq D \cdot \sqrt{\frac{K}{8}} \cdot \varepsilon \asymp \sqrt{\varepsilon},$$

and thus for any $i \neq j$

$$\text{KL}(P_{f_i} \| P_{f_j}) = \frac{n\varepsilon}{2\sigma^2}$$

On the other hand, to satisfy the Fano inequality (140):

$$\frac{n\varepsilon}{2\sigma^2} = \text{KL}(P_{f_i} \| P_{f_j}) \lesssim \log M \asymp \frac{1}{\varepsilon}$$

we let

$$\varepsilon \asymp \left(\frac{\sigma^2}{n}\right)^{\frac{1}{2}}.$$

and thus Fano's lemma (Lemma J.1, particularly (139)) implies that

$$\inf_{\hat{f}} \sup_{f \in \mathcal{F}_{1,1}} \mathbb{E} \|f - \hat{f}\|_{L^2([-1,1])}^2 \gtrsim \left(\frac{\sigma^2}{n}\right)^{\frac{1}{2}}.$$

Note that by rescale the functions □

Corollary H.10. *For general case $\mathcal{F}_{B,C}$, we can scale the construction functions by $\min(B, C)$ to deduce the result:*

$$\inf_{\hat{f}} \sup_{f \in \mathcal{F}_{B,C}} \mathbb{E} \|f - \hat{f}\|_{L^2([-1,1])}^2 \gtrsim \min(B, C)^2 \left(\frac{\sigma^2}{n}\right)^{\frac{1}{2}} \quad (127)$$

I Lower Bound on Generalization Gap

In this section, we derive a lower bound for the generalization gap. The core of our argument rests on an indistinguishability lemma. This lemma demonstrates that with high probability, there exist functions within a specially constructed class that are difficult to differentiate based on a finite sample set, yet remain significantly distinct in the L^2 sense.

We begin by adopting the notations and function constructions as detailed in Construction H.5. Specifically, we consider the family of functions $\{f_\xi\}_{\xi \in \Xi}$ built from ReLU atoms, where Ξ is the pruned cube in Varshamov-Gilbert lemma (Lemma J.2). For any pair of distinct sign vectors $\xi, \xi' \in \Xi$ and a given dataset $\mathcal{D}_n = \{\mathbf{x}_j\}_{j=1}^n$ (where each $\mathbf{x}_j \sim \text{Uniform}(\mathbb{B}_1^d)$ i.i.d.), we define the event $A_{\xi, \xi'}$ as the scenario where f_ξ and $f_{\xi'}$ produce identical outputs on all points in \mathcal{D}_n :

$$A_{\xi, \xi'} := \{f_\xi(\mathbf{x}_j) = f_{\xi'}(\mathbf{x}_j) \text{ for all } j = 1, \dots, n\}. \quad (128)$$

The following lemma quantifies the likelihood of such an event and the inherent separation of the functions.

Lemma I.1 (Indistinguishability under i.i.d. uniform sampling). *For any distinct $\xi, \xi' \in \Xi$, let $A_{\xi, \xi'}$ be the event $\{f_\xi(\mathbf{x}_j) = f_{\xi'}(\mathbf{x}_j) \text{ for all } j = 1, \dots, n\}$ for a dataset $\mathcal{D}_n = \{\mathbf{x}_j, y_j\}_{j=1}^n$ with $\mathbf{x}_j \sim \text{Uniform}(\mathbb{B}_1^d)$ i.i.d.*

There exists a constant κ_d such that

$$\mathbb{P} \left(\bigcup_{\xi \neq \xi' \in \Xi} A_{\xi, \xi'} \right) \geq 1 - \exp(-\kappa_d n^{(d-1)/(d+1)}) \quad (129)$$

Furthermore, for any distinct $\xi, \xi' \in \Xi$, their squared L^2 -distance satisfies

$$\|f_\xi - f_{\xi'}\|_{L^2(\mathbb{B}_1^d)}^2 \gtrsim_d \left(\frac{1}{n}\right)^{\frac{2}{d+1}}. \quad (130)$$

Proof. Let $c > 0$ be a constant whose value will be chosen appropriately later. We define ε in terms of c and n as:

$$\varepsilon = \left(\frac{c}{n}\right)^{1/(d+1)}. \quad (131)$$

The properties of the functions f_ξ and the parameters K (number of atoms) and q (disagreement probability for a single sample) are derived from this ε based on Construction H.5. We may write $K = c_k \varepsilon^{-d-1}$ for some constant $c_k < 1/2$.

Now, we turn to the probability of collision. Let $D_{\xi, \xi'} := \{\mathbf{x} \in \mathbb{B}_1^d : f_\xi(\mathbf{x}) \neq f_{\xi'}(\mathbf{x})\}$ be the disagreement region. The probability $q = \mathbb{P}(X_j \in D_{\xi, \xi'})$ scales as $q \lesssim_d \varepsilon^2$. We can write this more formally as $q = c_q c_k \varepsilon^2$ for some positive constant c_q that depends on dimension d and fixed geometric factors from the construction (but not on c or n), for ε in the relevant range. The probability of the event $A_{\xi, \xi'}$ (collision on all n samples) for a specific pair is $\mathbb{P}(A_{\xi, \xi'}) = (1 - q)^n$. For q to be sufficiently small⁸, we have $(1 - q)^n \geq \exp(-2nq)$ is a suitable lower bound.

The union bound argument relies on the inequality:

$$\mathbb{P}\left(\bigcup_{\xi \neq \xi' \in \Xi} A_{\xi, \xi'}\right) \geq 1 - \exp(K \ln 2 - 2nq). \quad (132)$$

Let $X_{\text{exp}} = K \ln 2 - 2nq$. We need to show we can choose c such that $X_{\text{exp}} \leq -1$ for large n . Substituting $\varepsilon = (c/n)^{1/(d+1)}$:

$$\begin{aligned} K \ln 2 &= c_k (\ln 2) \varepsilon^{-(d-1)} = c_k (\ln 2) \left(\frac{c}{n}\right)^{-(d-1)/(d+1)} \\ &= c_k (\ln 2) c^{-(d-1)/(d+1)} n^{(d-1)/(d+1)}. \\ 2nq &= 2n(c_q \varepsilon^2) = 2nc_q \left(\frac{c}{n}\right)^{2/(d+1)} \\ &= 2c_q c_k c^{2/(d+1)} n^{1-2/(d+1)} = 2c_q c_k c^{2/(d+1)} n^{(d-1)/(d+1)}. \end{aligned}$$

Thus, the exponent X_{exp} can be expressed as:

$$X_{\text{exp}} = \left[c_k (\ln 2) c^{-(d-1)/(d+1)} - 2c_q c_k c^{2/(d+1)} \right] \cdot n^{(d-1)/(d+1)}. \quad (133)$$

Let $f_c(c) = c_k (\ln 2) c^{-(d-1)/(d+1)} - 2c_q c_k c^{2/(d+1)}$. The constants c_k and c_q are positive and depend only on d . Our goal is to choose the constant c (which is independent of n) such that $f_c(c)$ becomes a fixed negative constant. The term $c^{-(d-1)/(d+1)}$ decreases as c increases (since $d \geq 2 \implies -(d-1)/(d+1) < 0$). The term $c^{2/(d+1)}$ increases as c increases (since $2/(d+1) > 0$). Therefore, $f_c(c)$ can be made negative if the second part, $-2c_q c_k c^{2/(d+1)}$, dominates the first part. This requires:

$$2c_k c_q c^{2/(d+1)} > c_k (\ln 2) c^{-(d-1)/(d+1)} \implies 2c_q c > \ln 2. \quad (134)$$

So, we must choose c such that $c > \frac{\ln 2}{2c_q}$. Let $c_{\text{crit}}(d) = \frac{c_k \ln 2}{2c_q}$. This $c_{\text{crit}}(d)$ is a positive constant determined by d -dependent geometric factors. We now fix our choice of c to be a specific constant $c^* = c^*(d)$ such that $c^* > c_{\text{crit}}(d)$. For example, we can set $c^* = 2 \cdot c_{\text{crit}}(d)$. This c^* is a fixed positive constant, independent of n . With this fixed c^* , the term $f_c(c^*) = c_k (\ln 2) (c^*)^{-(d-1)/(d+1)} - 2c_q c_k (c^*)^{2/(d+1)}$ evaluates to some fixed negative constant. Let $f_c(c^*) = -\kappa_d$, where $\kappa_d > 0$ is a positive constant (dependent on d). Now, the exponent X_{exp} is written to be

$$X_{\text{exp}} = -\kappa_d n^{(d-1)/(d+1)}. \quad (135)$$

Therefore

$$\mathbb{P}\left(\bigcup_{\xi \neq \xi' \in \Xi} A_{\xi, \xi'}\right) \geq 1 - \exp(-\kappa_d n^{(d-1)/(d+1)}) \quad (136)$$

□

⁸It requires that $n^{2/(d+1)} \geq 2c_k c_q c^{2/(d+1)}$, i.e. $n \geq (2c_k c_q)^{(d+1)/2} c$, where the constant term $2c_k c_q$ is smaller than one, because the volume coefficient of high-dimensional ball decrease to zero, when $d \rightarrow \infty$. We will see c is a very mild constant. In this case, this assumption is a very mild assumption.

This lemma can be interpreted as a noiseless version of Fano's Lemma. It establishes the difficulty in distinguishing functions based on limited data even when the labels are not noisy.

Corollary I.2 (Stronger Version of Minimax Lower Bound). *Consider the problem of estimating a function $f \in \mathcal{F} = \{f \in \mathcal{V}_g(\mathbb{B}_1^d) : \|f\|_{L^\infty(\mathbb{B}_1^d)} \leq 1, |f|_{\mathcal{V}_g} \leq 1\}$ with*

$$y_i = f(\mathbf{x}_i)$$

where $\{\mathbf{x}_i\}_{i=1}^n \subset \mathbb{B}_1^d$ are i.i.d. uniform random variables on \mathbb{B}_1^d . The lower bound of the minimax nonparametric risk is given by

$$\inf_{\hat{f}} \sup_{f \in \mathcal{F}} \mathbb{E} \|\hat{f} - f\|_{L^2(\mathbb{B}_1^d)}^2 \gtrsim_d \left(\frac{1}{n}\right)^{\frac{2}{d+1}}.$$

Proof. Let $\mathcal{F}_{\text{pack}}$ be the packing set in Construction H.5 and Lemma I.1. Then we have

$$\inf_{\hat{f}} \sup_{f \in \mathcal{F}} \mathbb{E} \|\hat{f} - f\|_{L^2(\mathbb{B}_1^d)}^2 \geq \inf_{\hat{f}} \sup_{f \in \mathcal{F}_{\text{pack}}} \mathbb{E} \|\hat{f} - f\|_{L^2(\mathbb{B}_1^d)}^2$$

Here the randomness comes from the dataset sampling and with high probability as stated in (129), there exists two $f_\xi, f_{\xi'} \in \mathcal{F}_{\text{pack}}$ such that the dataset \mathcal{D} of size n cannot distinguish them, since $f_\xi(\mathbf{x}_i) = f_{\xi'}(\mathbf{x}_i)$ for all $\mathbf{x}_i \in \mathcal{D}$. Therefore any estimator will yield square error $\Theta((1/n)^{2/(d+2)})$ according to (130) in the worst case that $f = f_\xi$ and $\hat{f} = f_{\xi'}$. \square

Now, leveraging this indistinguishability lemma, we establish a lower bound on the expected generalization gap. Before proceeding to the theorem, we clarify some notation. Let $f : \mathbb{B}_1^d \rightarrow [-1, 1]$ be a function. We define a joint distribution \mathcal{P}_f over $\mathbb{B}_1^d \times [-1, 1]$ such that the conditional distribution of Y given $\mathbf{X} = \mathbf{x}$ is a point mass at $f(\mathbf{x})$:

$$\mathcal{P}_f(Y = y' \mid \mathbf{X} = \mathbf{x}) = \delta_{(\mathbf{x}, f(\mathbf{x}))}. \quad (137)$$

For any dataset $\mathcal{D}_n = \{(\mathbf{x}_j, y_j)\}_{j=1}^n$, we denote the empirical risk (Mean Squared Error) of a function g as $\tilde{R}(g; \mathcal{D}_n)$ is the empirical risk estimation based on the dataset \mathcal{D}_n . The corresponding population risk is $R_{\mathcal{P}_f}(h) = \mathbb{E}_{(\mathbf{X}, Y) \sim \mathcal{P}_f} [(f(\mathbf{X}) - h(\mathbf{X}))^2] = \|f - h\|_{L^2(\mathbb{B}_1^d)}^2$.

Theorem I.3. *Let \mathcal{P} denote any joint distribution of (\mathbf{x}, y) where the marginal distribution of \mathbf{x} is Uniform(\mathbb{B}_1^d) and y satisfies the $\mathbb{P}_{\mathcal{P}}[-1 \leq y \leq 1] = 1$. Let $\mathcal{D}_n = \{(\mathbf{x}_j, y_j)\}_{j=1}^n$ be a dataset of n i.i.d. samples from \mathcal{P} , and that \tilde{R} is any risk estimator that takes any f and \mathcal{D}_n as input, then outputs a scalar that aims at estimating the risk $R_{\mathcal{P}}(f) := \mathbb{E}_{(\mathbf{x}, y) \sim \mathcal{P}} [(f(\mathbf{x}) - y)^2]$. Moreover, assume η is sufficiently small such that $\mathcal{F}_{\text{pack}}$ from Construction H.5 satisfies that $\mathcal{F}_{\text{pack}} \subset \mathcal{F}_{\text{stable}}(\eta)$. Then*

$$\inf_{\tilde{R}} \sup_{\mathcal{P}} \mathbb{E} \left[\sup_{f \in \mathcal{F}_{\text{stable}}(\eta)} \left| R_{\mathcal{P}}(f) - \tilde{R}(f; \mathcal{D}_n) \right| \right] \gtrsim_d n^{-\frac{2}{d+1}}. \quad (138)$$

Proof. Let the $\mathbb{E}[\cdot]$ be the short-hand for the expectation over the random training dataset \mathcal{D}_n .

$$\begin{aligned}
& \inf_{\tilde{R}} \sup_{\mathcal{P}} \mathbb{E} \left[\sup_{f \in \mathcal{F}_{\text{stable}}(\eta)} \left| R_{\mathcal{P}}(f) - \tilde{R}(f; \mathcal{D}_n) \right| \right] \\
& \geq \inf_{\tilde{R}} \sup_{\substack{\mathcal{P} = \text{Unif}(\mathbb{B}_1^d) \times f_0 \\ f_0 \in \mathcal{F}_{\text{pack}}}} \mathbb{E} \left[\sup_{f \in \mathcal{F}_{\text{stable}}(\eta)} \left| R_{\mathcal{P}}(f) - \tilde{R}(f; \mathcal{D}_n) \right| \right] \\
& \geq \inf_{\tilde{R}} \sup_{\substack{\mathcal{P} = \text{Unif}(\mathbb{B}_1^d) \times f_0 \\ f_0 \in \mathcal{F}_{\text{pack}}}} \frac{1}{2} \mathbb{E} \left[R_{\mathcal{P}}(\hat{f}_{\text{ERM}}(\tilde{R}(\cdot, \mathcal{D}_n))) - R_{\mathcal{P}}(f_0) \right] \\
& \geq \inf_{\hat{f}} \sup_{\substack{\mathcal{P} = \text{Unif}(\mathbb{B}_1^d) \times f_0 \\ f_0 \in \mathcal{F}_{\text{pack}}}} \frac{1}{2} \mathbb{E} \left[R_{\mathcal{P}}(\hat{f}(\mathcal{D}_n)) - R_{\mathcal{P}}(f_0) \right] \\
& = \frac{1}{2} \inf_{\hat{f}} \sup_{\substack{\mathcal{P} = \text{Unif}(\mathbb{B}_1^d) \times f_0 \\ f_0 \in \mathcal{F}_{\text{pack}}}} \mathbb{E} \left[\|\hat{f}(\mathcal{D}_n) - f_0\|_{L^2(\mathbb{B}_1^d)}^2 \right]
\end{aligned}$$

(Corollary I.2) $\longrightarrow \gtrsim_d n^{-\frac{2}{d+1}}$.

The first inequality restricts \mathcal{P} further to deterministic labels with labeling functions in $\mathcal{F}_{\text{pack}}$. Check that any function in $\mathcal{F}_{\text{pack}}$ is bounded between $[-1, 1]$. The second inequality uses the fact that $f_0 \in \mathcal{F}_{\text{stable}}(\eta)$, and the following decomposition

$$\begin{aligned}
& R_{\mathcal{P}}(\hat{f}_{\text{ERM}}(\tilde{R})) - R_{\mathcal{P}}(f_0) \\
& = R_{\mathcal{P}}(\hat{f}_{\text{ERM}}(\tilde{R})) - \tilde{R}(\hat{f}_{\text{ERM}}; \mathcal{D}_n) + \tilde{R}(\hat{f}_{\text{ERM}}; \mathcal{D}_n) - \tilde{R}(f_0; \mathcal{D}_n) + \tilde{R}(f_0; \mathcal{D}_n) - R_{\mathcal{P}}(f_0) \\
& \leq \left| R_{\mathcal{P}}(\hat{f}_{\text{ERM}}(\tilde{R})) - \tilde{R}(\hat{f}_{\text{ERM}}; \mathcal{D}_n) \right| + \left| \tilde{R}(f_0; \mathcal{D}_n) - R_{\mathcal{P}}(f_0) \right| \\
& \leq 2 \sup_{f \in \mathcal{F}_{\text{stable}}(\eta)} \left| R_{\mathcal{P}}(f) - \tilde{R}(f; \mathcal{D}_n) \right|,
\end{aligned}$$

where we used $\tilde{R}(\hat{f}_{\text{ERM}}; \mathcal{D}_n) - \tilde{R}(f_0; \mathcal{D}_n) \leq 0$ from the definition of \hat{f}_{ERM}

$$\hat{f}_{\text{ERM}}(\tilde{R}(\cdot, \mathcal{D}_n)) := \underset{f \in \mathcal{F}_{\text{stable}}(\eta)}{\text{argmin}} \tilde{R}(f; \mathcal{D}_n).$$

The third inequality enlarges the set of ERM estimators to any function of the data \hat{f} that output. The subsequent identity uses the fact that $R_{\mathcal{P}}(f_0) = 0$. \square

This completes the proof for the lower bound on generalization gap stated in Theorem 3.5.

J Technical Lemmas

Fano's Lemma provides a powerful method for establishing such minimax lower bounds by relating the estimation problem to a hypothesis testing problem. It leverages information-theoretic concepts, particularly the Kullback-Leibler (KL) divergence.

Lemma J.1 (Fano's Lemma (Statistical Estimation Context)). *Consider a finite set of functions (or parameters) $\{f_1, f_2, \dots, f_M\} \subset \mathcal{F}$, with $M \geq 2$. Let P_{f_j} denote the probability distribution of the observed data \mathcal{D}_n when the true underlying function is f_j . Suppose that for any estimator \hat{f} , the loss function $L(f_j, \hat{f})$ satisfies $L(f_j, \hat{f}) \geq s^2/2 > 0$ if \hat{f} is not close to f_j (e.g., if we make a wrong decision in a multi-hypothesis test where closeness is defined by a metric $d(f_j, f_k) \geq s$). More specifically, for*

function estimation with squared L^2 -norm loss, if we have a packing set $\{f_1, \dots, f_M\} \subset \mathcal{F}$ such that $\|f_j - f_k\|_{L^2}^2 \geq s^2$ for all $j \neq k$, then the minimax risk is bounded as:

$$\inf_{\hat{f}} \sup_{f \in \mathcal{F}} \mathbb{E} \|\hat{f} - f\|_{L^2}^2 \geq \frac{s^2}{4} \left(1 - \frac{\max_{j \neq k} \text{KL}(P_{f_j} \| P_{f_k}) + \log 2}{\log M} \right), \quad (139)$$

provided the term in the parenthesis is positive. $\text{KL}(P_{f_j} \| P_{f_k})$ denotes the Kullback-Leibler divergence between the distributions P_{f_j} and P_{f_k} . For this bound to be non-trivial (e.g., $\gtrsim s^2$), we typically require that the number of well-separated functions M is large enough such that

$$\log \frac{M}{2} > \max_{j \neq k} \text{KL}(P_{f_j} \| P_{f_k}). \quad (140)$$

One can refer to [Wasserman \[2020, Theorem 12, Corollary 13\]](#) or [Tsybakov \[2009, Chapter 2\]](#) for more details.

Our application of Fano's Lemma (for proving [Proposition H.6](#)) involves:

1. Constructing a suitable finite subset of functions $\{f_1, \dots, f_M\}$ within the class \mathcal{F} such that they are well-separated in the metric defined by the loss function (e.g., pairwise L^2 -distance s). This is often achieved using techniques like the Varshamov-Gilbert lemma ([Lemma J.2](#)) for constructing packings.
2. Bounding the KL divergence (or another information measure like χ^2 -divergence) between the probability distributions generated by pairs of these functions. For n i.i.d. observations with additive Gaussian noise $\mathcal{N}(0, \sigma^2)$, and if using the empirical L^2 norm $\|\cdot\|_{L^2(\mathbb{P}_n)}$ based on fixed data points \mathbf{x}_i , this divergence is often related to $\frac{1}{2\sigma^2} \sum_{i=1}^n (f_j(\mathbf{x}_i) - f_k(\mathbf{x}_i))^2$. More generally, for population norms, it's often $\frac{n\|f_j - f_k\|_{L^2}^2}{2\sigma^2}$.
3. Choosing M and s (or the parameters defining the packing) to maximize the lower bound, typically by ensuring that the KL divergence term does not dominate $\log M$.

Lemma J.2 (Varshamov–Gilbert Lemma). *Let*

$$\Xi = \{\xi = (\xi_1, \dots, \xi_N) : \xi_j \in \{0, 1\}\}.$$

Suppose $N \geq 8$. Then there exist

$$\xi^0, \xi^1, \dots, \xi^M \in \Xi$$

such that

1. $\xi_0 = (0, \dots, 0)$,
2. $M \geq 2^{N/8}$,
3. for all $0 \leq j < k \leq M$, the Hamming distance satisfies

$$d_H(\xi^j, \xi^k) \geq \frac{N}{8}.$$

We call $\{\xi^0, \xi^1, \dots, \xi^M\}$ a pruned hypercube.

One can refer to [Tsybakov \[2009, Lemma 2.9\]](#) and [Wasserman \[2020, Lemma 15\]](#) for more details.